

**FABRICATION AND CHARACTERIZATION OF RICE HUSK PYROLYZED
BIOCHAR REINFORCED POLYPROPYLENE COMPOSITE**

by

Tareq Hossain

Student No: 1014112503

A thesis submitted to the Department of
Materials and Metallurgical Engineering in partial fulfillment of
the requirements for the degree of

MASTER OF SCIENCE IN MATERIALS SCIENCE



Department of Materials and Metallurgical Engineering

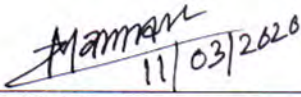
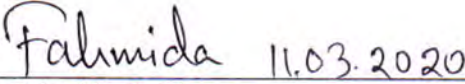
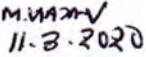
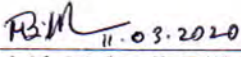
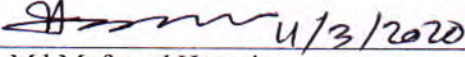
BANGLADESH UNIVERSITY OF ENGINEERING AND TECHNOLOGY

Dhaka-1000, Bangladesh

MARCH 2020

The thesis titled “FABRICATION AND CHARACTERIZATION OF RICE HUSK PYROLYZED BIOCHAR REINFORCED POLYPROPYLENE COMPOSITE” submitted by Tareq Hossain, Student No: 1014112503, Session: October 2014, has been accepted as satisfactory in partial fulfillment of the requirements for the degree of Master of Science in Materials Science on 11 MARCH 2020.

BOARD OF EXAMINERS

1. 
11/03/2020
Dr. Md. Moniruzzaman
Professor
Department of Materials and Metallurgical Engineering,
BUET, Dhaka-1000. Chairman
(Supervisor)
2. 
11.03.2020
Dr. Fahmida Gulshan
Professor and Head
Department of Materials and Metallurgical Engineering,
BUET, Dhaka-1000. Member
(Ex-officio)
3. 
11.3.2020
Dr. Mahbub Hasan
Professor
Department of Materials and Metallurgical Engineering,
BUET, Dhaka-1000. Member
4. 
11.03.2020
Dr. Md. Muktedir Billah
Assistant Professor
Department of Materials and Metallurgical Engineering,
BUET, Dhaka-1000. Member
5. 
4/3/2020
Dr. Md Mufazzal Hossain
Professor
Department of Chemistry,
University of Dhaka, Dhaka-1000. Member
(External)

DECLARATION

This is to certify that this research work has been carried out by the author under the supervision of Dr. Md. Moniruzzaman, Professor, Department of Materials and Metallurgical Engineering, BUET, Dhaka and it is the outcome of accomplishment of the thesis on **–Fabrication and Characterization of Rice Husk Pyrolyzed Biochar Reinforced Polypropylene Composite.**” It is also declared that this thesis or any part of it has not been submitted elsewhere for the award of any degree or diploma.

MARCH 2020

Tareq Hossain
Student No: 1014112503

Dedicated to my Parents & Teachers

Acknowledgement

First and foremost, all praise is due to the Almighty Allah; the most Merciful and the most Beneficent for enabling me to complete this thesis work successfully.

Secondly, I express my utmost gratitude and profound indebtedness to my respected supervisor Dr. Md. Moniruzzaman, Professor, Department of Materials and Metallurgical Engineering, Bangladesh University of Engineering and Technology (BUET), Dhaka, for his constant supervision, continuous guidance, encouragement and valuable suggestion at every stage of my research work.

Here, I am grateful to CASR, BUET for approving necessary funding and providing documentation needed at various stages of my research project. I also wish to convey honest gratefulness to Materials and Metallurgical Engineering (MME) Department and Head of the Department for providing laboratory and instrument facilities needed for the project.

Also, I would like to express heartiest thanks to all in charge and staff of various laboratories of the MME Department for their technical assistance and support. I acknowledge with appreciation to Mr. Md. Abdullah Al Maksud (Instrument engineer), Mr. Md. Nazmul Haque (Assistant instrument engineer), Mr. Md. Ashiqur Rahman (Sr. technical officer), and Mr. Md. Harun Or Rashid (Sr. lab instructor) for their help to perform different tests of the thesis work.

Furthermore, I wish to express my deepest gratitude to Mr. Muhammad Shahriar Bashir, Principal Scientific Officer, Renewable Energy Technology Laboratory, Institute of Fuel Research & Development, BCSIR, Dhaka, for his kind help, technical advice, and permission to use his lab facilities to perform characterization tests of the fabricated composite samples.

Finally, I am thankful to my parents and friends for their support and invaluable suggestions. Especial thanks to my mother for her moral support and continuous encouragement that has enabled me to attain this level.

Abstract

Growing polymer consumption, depletion of metallic resources, and rising environmental concerns have resulted in an increased interest in bio-derived environment friendly polymeric composite materials. The utilization of biochar as a reinforcement in polymers can be viewed as a sustainable attempt that incorporates pyrolyzed biomass based value-added material and simultaneously aids environmental management through effective utilization of bio-wastes. On the other hand, polypropylene (PP), a semi-crystalline thermoplastic polymer has favorable properties like low cost, good mechanical strength, lightweight, easy processing, excellent chemical resistance, etc. However, some other properties such as inferior mechanical properties at alleviated temperatures, poor UV resistance, and poor surface adhesion, etc. limit its application. To overcome the limitations exhibited by polymeric composites, biochar reinforced polymer composites have attracted the attention of researchers all over the world because of their low cost, renewability, and improved thermochemical properties. In this thesis work, rice husk biochar (RHB) reinforcement polypropylene (PP) composite has been fabricated and characterized to evaluate its performance. Biochar was prepared from rice husk via slow pyrolysis at four different temperatures (400, 550, 700, and 850⁰C). Characterization of the RHB samples revealed high carbon, ash, and silicon contents. The RHB samples exhibited a porous structure and their thermal stability increased with increasing pyrolysis temperatures. The biochar samples were then hand ground and applied as particle reinforcement material for PP composite fabrication with two different loadings of 10 and 15 wt%. RHB was blended with PP by melt mixing technique followed by the hot press molding process. Pyrolysis temperature and wt% of RHB were found to be crucial factors affecting the compatibility, thermo-mechanical and electrical properties of the resulted composites. The tensile strength of the fabricated composites was found to be lower when compared with neat PP, but the flexural strength and hardness (shore D) were improved, where composite containing 15 wt% of RHB prepared at higher temperatures (700 and 850⁰C) exhibited better results. According to SEM results, the biochar particles were firmly embedded in the PP matrix due to their porous structure and the molten PP has penetrated a large number of pores of the biochar particles creating a mechanically interlocked system, which consequently improved the mechanical properties. Moreover, the incorporation of thermally stable biochar was found to have a positive impact on the thermal stability of the composites, where increasing the RHB pyrolysis temperature and higher RHB loading helped the fabricated composite to sustain higher thermal decomposition temperatures. However, the RHB incorporation into the PP matrix had a negligible effect on the melting temperature (T_m) of the developed composites. Finally, the increased loading of high-temperature RHB has potentially reduced the resistance and the impedance of the fabricated composites. Thus, except for a little deviation, the improvements of the composite properties were found to increase when the RHB content was increased (15 wt%) and the incorporated RHB had been pyrolyzed at higher temperatures (700 and 850⁰C). The minor deviation might be due to the lack of homogeneous mixture formation of light RHB powder into the PP matrix during composite fabrication.

Table of Contents

Title	i
Board of Examiners	ii
Declaration	iii
Dedication	iv
Acknowledgements	v
Abstract	vi
Table of Contents	vii
List of Tables	xii
List of Figures	xiii
List of Abbreviations	xvi
List of Notations	xvii
Chapter 1	1
Introduction	
1.1 Overview	2
1.2 Present State and Goal of the Work	4
Chapter 2	5
Literature Review	
2.1 Biochar	6
2.1.1 Properties of Biochar	6
2.1.1.1 Composition and Structure	7
2.1.1.2 pH and Zeta Potential	7
2.1.1.3 Surface Area and Porosity	7
2.1.1.4 Absorption Capability and Cation Exchange Capacity	7
2.1.2 Preparation Methods of Biochar	8
2.1.2.1 Slow Pyrolysis	9
2.1.2.2 Intermediate Pyrolysis	9
2.1.2.3 Fast Pyrolysis	9
2.1.2.4 Gasification	10
2.1.2.5 Hydrothermal Carbonization	10
2.1.2.6 Torrefaction	10
2.1.3 Factors Affecting Biochar Quality	10

2.1.3.1 Temperature	10
2.1.3.2 Heating Rate	11
2.1.3.3 Particle Size	11
2.1.3.4 Feedstock Composition	11
2.1.4 Applications of Biochar	12
2.1.4.1 Soil Improvement	12
2.1.4.2 Carbon Sequestration	12
2.1.4.3 Reduction of GHG Emissions	12
2.1.4.4 Waste Water Purification	13
2.1.4.5 Waste Utilization and Management	13
2.1.4.6 Composite and Engineering Materials Development	13
2.1.5 Rice Husk Derived Pyrolyzed Biochar	14
2.2 Polypropylene (PP)	15
2.2.1 Structure and Types of PP	17
2.2.1.1 Atactic PP	17
2.2.1.2 Syndiotactic PP	17
2.2.1.3 Isotactic PP	18
2.2.2 Properties of PP	18
2.2.3 Synthesis Methods of PP	19
2.2.4 Applications of PP	20
2.3 Fundamental Concept of Composites	20
2.3.1 Classifications of Composite Materials	22
2.3.1.1 On the Basis of Matrix Materials	22
2.3.1.2 On the Basis of Reinforcement Materials	23
2.3.2 Advantages and Disadvantages of Composite Materials	25
2.4 Fundamental Concept of Polymer Matrix	26
2.5 Fundamental Concept of Reinforcements for Polymer Matrix	28
2.6 Reinforcing Theories	28
2.6.1 Interfacial Adhesion Reinforcing Theory	29
2.6.2 Filler Inducing Crystallization Reinforcing Theory	29
2.6.3 Filler Frame Reinforcing Theory	30

2.6.4 Synergistic Reinforcing Effect Theory	30
2.7 Particle Reinforced Polymeric Composites	31
2.7.1 Biochar Reinforced Thermoplastic Polymer Composites	32
2.8 Review of Related Research Works	33
2.9 Viability of Rice Husk Pyrolyzed Biochar Reinforced PP Composite Fabrication	36
2.10 Likely Applications of Rice Husk Pyrolyzed Biochar Reinforced PP Composites	38
Chapter 3	39
Experimental Procedure	
3.1 Raw Materials	40
3.1.1 Rice Husk (Precursor of Biochar)	40
3.1.2 Virgin PP Resin	40
3.1.3 Other Accessories	41
3.2 Biochar Preparation	41
3.3 Composite Fabrication	44
3.3.1 Melt Blending	44
3.3.2 Hot Pressing	45
3.4 Characterization of RHB	46
3.4.1 Biochar Yields	47
3.4.2 Proximate Analysis and pH	47
3.4.3 Morphological Characterization	48
3.4.3.1 Optical Microscopy	48
3.4.3.2 Scanning Electron Microscopy (SEM)	48
3.4.4 Energy Dispersive X-Ray (EDX) Analysis	48
3.4.5 Fourier Transform Infrared Spectroscopy (FTIR)	49
3.4.6 Thermogravimetric Analysis (TGA)	49
3.4.7 Differential Scanning Calorimetry (DSC)	49
3.5 Characterization and Testing of RHB reinforced PP composite	50
3.5.1 Mechanical Properties Test	50
3.5.1.1 Tensile Test	50

3.5.1.2 Flexural Test	51
3.5.1.3 Hardness Test	52
3.5.2 Morphology and Structure	52
3.5.2.1 Scanning Electron Microscopy (SEM)	52
3.5.2.2 Energy Dispersive X-Ray (EDX) Analysis	53
3.5.2.3 X-Ray Diffraction (XRD)	53
3.5.3 Thermal Properties Test	54
3.5.3.1 Thermogravimetric Analysis (TGA)	54
3.5.3.2 Differential Scanning Calorimetry (DSC)	54
3.5.4 Impedance Analysis (IA)	55
Chapter 4	56
Results and Discussion	
4.1 Evaluation of RHB Characteristics	57
4.1.1 Biochar Yields and pH	57
4.1.2 Micrographs of RHB	58
4.1.2.1 Optical Micrograph	58
4.1.2.2 SEM Analysis	59
4.1.3 Proximate Analysis	62
4.1.4 SEM-EDX Analysis	63
4.1.5 FTIR Analysis	65
4.1.6 Analysis of Thermal Properties	68
4.1.6.1 Thermogravimetric Analysis	68
4.1.6.2 DSC Analysis	69
4.2 Characteristics and Properties of RHB Reinforced PP Composite	70
4.2.1 Mechanical Properties Analysis	70
4.2.1.1 Tensile Test	70
4.2.1.2 Flexural Test	72
4.2.1.3 Hardness Test	75
4.2.2 Morphological and Structural Analysis	77
4.2.2.1 EDX Analysis	77
4.2.2.2 SEM Analysis	78

4.2.2.3 XRD Analysis	84
4.2.3 Analysis of Thermal Properties	87
4.2.3.1 Thermogravimetric Analysis	87
4.2.3.2 DSC Analysis	89
4.2.4 Analysis of Electrical Properties	91
4.2.4.1 Resistance Measurement	91
4.2.4.2 Impedance Measurement	93
Chapter 5	95
Conclusion and Recommendations for Future Work	
5.1. Conclusion	96
5.2. Recommendations for Future Work	97
References	98
Appendix A	112

List of Tables

Table No.	Title	Page No.
Table 2.1:	Product yields and the operational conditions of different biochar production methods	9
Table 2.2:	Advantages and Disadvantages of PP	16
Table 2.3:	Mechanical and thermal properties of PP [86]	18
Table 2.4:	Gains and losses of composite materials	26
Table 2.5:	Remarkable studies on biochar reinforced polymeric composites	33
Table 3.1:	Properties of the PP resin used in this study (from Sabic website for SABIC PP 575P)	40
Table 3.2:	Name and constituents of the developed composites	44
Table 4.1:	Proximate analysis data for RHB samples produced at four different temperatures	62
Table 4.2:	Major elements of RHB prepared at different temperatures	65
Table 4.3:	Peak position of functional groups observed in the FTIR spectra of RHB samples	67
Table 4.4:	Tensile test results of RHB reinforced PP composites	71
Table 4.5:	Flexural test results of RHB reinforced PP composites	73
Table 4.6:	Shore hardness (D scale) test results of RHB reinforced PP composites	75
Table 4.7:	Resistance of PP and the developed RHB reinforced PP composites	91
Table 4.8:	Impedance of PP and the fabricated RHB reinforced PP composites	93

List of Figures

Figure No.	Title	Page No.
Figure 1.1:	Estimated rice husk generation in the recent five fiscal years a) around the world b) in Bangladesh	3
Figure 2.1:	Some biomass and their biochar [32]	6
Figure 2.2:	Pyrolysis process [33]	8
Figure 2.3:	Prospect of biochar applications [78]	14
Figure 2.4:	Different parts of paddy rice, loosen rice husk and rice hush derived biochar [79]	15
Figure 2.5:	Propylene and Polypropylene structure.	16
Figure 2.6:	Structure of aPP	17
Figure 2.7:	Structure of sPP	17
Figure 2.8:	Structure of iPP	18
Figure 2.9:	PP Synthesis process	19
Figure 2.10:	Schematic representation of composite applications in cars [97]	21
Figure 2.11:	Matrix based classification of composites [99]	23
Figure 2.12:	Classification of composites based reinforcement type [99]	23
Figure 2.13:	Types of Particle reinforced composites [103]	24
Figure 2.14:	Types of Particle reinforced composites [103]	25
Figure 2.15:	Structural composite types [103]	25
Figure 2.16:	Classification of polymer matrix	27
Figure 2.17:	Molecular Structure of Thermoplastic and Thermoset Polymers [90]	28
Figure 3.1:	Picture of rice husk a) as obtained from the mill, b) washed and dried	40
Figure 3.2:	Polypropylene (PP)- a) A sack of PP, b) Virgin PP granulates	41
Figure 3.3:	a) Oven, b) the pot inside which pyrolysis was performed, c) Muffle Furnace	41
Figure 3.4:	Slow pyrolysis of rice husk	42
Figure 3.5:	a) Dry RH before pyrolysis, b) rice husk biochar (RHB) c) Grinding of RHB	42
Figure 3.6:	RHB fine powder stored in labeled jars	43
Figure 3.7:	Flowchart of RHB powder preparation	43
Figure 3.8:	Internal mixer unit	44
Figure 3.9:	Composite sample after melt blending	45
Figure 3.10:	Hot press molding a) aluminium mold, b) Fontijne hydraulic hot press machine	45
Figure 3.11:	Hot pressed sheet of a) PP, b) RHB reinforced PP composite	46
Figure 3.12:	Flowchart of RHB reinforced PP composite preparation	46
Figure 3.13:	pH test- a) Solution preparation, b) pH measurement of RHB	47
Figure 3.14:	Optical microscope	48
Figure 3.15:	Cary 630 FTIR spectrometer	49

Figure 3.16:	Tensile test specimens a) specimen measurements, b) prepared specimens	50
Figure 3.17:	Flexural test specimens a) specimen measurements, b) prepared specimens	51
Figure 3.18:	Hardness test a) Shore D Durometer, b) test specimens	52
Figure 3.19:	ZEISS EVO 18 Research Scanning Electron Microscope	53
Figure 3.20:	The Emma (enhanced mini-materials analyser) X-Ray Diffractometer	53
Figure 3.21:	TGA Q50 Thermo-gravimetric Analyzer	54
Figure 3.22:	Differential scanning calorimeter (DSC131 EVO)	55
Figure 3.23:	Impedance analysis- a) Precision Impedance Analyzer, 6500B series, b) Test specimens	55
Figure 4.1:	Biochar yield at different pyrolysis temperatures	57
Figure 4.2:	pH of 1:5 wt% of RHB/water solution containing RHB pyrolyzed at four different temperatures	58
Figure 4.3:	Rice husk a) before pyrolysis, b) after pyrolysis (RHB)	58
Figure 4.4:	RHB after grinding a) $\times 40$, b) $\times 1000$	59
Figure 4.5:	SEM micrograph of RHB400	60
Figure 4.6:	SEM micrograph of RHB550	60
Figure 4.7:	SEM micrograph of RHB700	61
Figure 4.8:	SEM micrograph of RHB850	61
Figure 4.9:	EDX spectra of rice husk biochar samples- a) RHB400, b) RHB550, c) RHB700, and d) RHB850	63-64
Figure 4.10:	FTIR spectra of biochar samples- a) RHB400, b) RHB550, c) RHB700, and d) RHB850	66
Figure 4.11:	TGA with DTG curves of biochar samples- a) RHB400, b) RHB550, c) RHB700, and d) RHB850	68
Figure 4.12:	DSC curves of- a) RHB400, b) RHB550, c) RHB700, and d) RHB850	69
Figure 4.13:	Variation of tensile strength due to RHB addition	72
Figure 4.14:	Variation of flexural strength due to RHB addition	74
Figure 4.15:	Hardness (Shore D) of composites containing 10 wt% and 15 wt% of prepared RHB reinforcements at different temperatures	76
Figure 4.16:	EDX analysis of the composite- a) area of analysis, b) EDX spectra of the point representing RHB particle in the composite (Area 2), c) EDX spectra of the point representing PP matrix in the composite (Area 1)	77
Figure 4.17:	SEM micrograph of tensile fracture surface of PP	78
Figure 4.18:	SEM micrograph of tensile fracture surface of PP-10RHB-400	79
Figure 4.19:	SEM micrograph of tensile fracture surface of PP-15RHB-400	79
Figure 4.20:	SEM micrograph of tensile fracture surface of PP-10RHB-550	80
Figure 4.21:	SEM micrograph of tensile fracture surface of PP-15RHB-550	80
Figure 4.22:	SEM image of tensile fracture surface of composite containing	81

	RHB700	
Figure 4.23:	Image of circled area in figure 4.24 with $\times 5000$ magnification	81
Figure 4.24:	SEM image of tensile fracture surface of composite containing RHB850 at $\times 1000$ magnification	82
Figure 4.25:	SEM micrograph of tensile fracture surface of PP-10RHB-850 composite at $\times 5000$ magnification	83
Figure 4.26:	SEM micrograph of tensile fracture surface of PP-10RHB-850 composite at $\times 5000$ magnification	83
Figure 4.27:	XRD spectra of PP	84
Figure 4.28:	XRD spectra of RHB reinforced PP composite a) PP-10RHB-400, b) PP-15RHB-400, c) PP-10RHB-550, d) PP-15RHB-550, e) PP-10RHB-700, f) PP-15RHB-700, g) PP-10RHB-850, and f) PP-15RHB-850	85
Figure 4.29:	Comparison of the XRD spectra of 100PP and PP-15RHB-400	86
Figure 4.30:	TGA and DTG curves of PP	87
Figure 4.31:	TGA and DTG curves of RHB reinforced PP composite a) PP-10RHB-400, b) PP-15RHB-400, c) PP-10RHB-550, d) PP-15RHB-550, e) PP-10RHB-700, f) PP-15RHB-700, g) PP-10RHB-850, and f) PP-15RHB-850	88
Figure 4.32:	DSC curve of PP	89
Figure 4.33:	DSC curves of RHB reinforced PP composite a) PP-10RHB-400, b) PP-15RHB-400, c) PP-10RHB-550, d) PP-15RHB-550, e) PP-10RHB-700, f) PP-15RHB-700, g) PP-10RHB-850, and f) PP-15RHB-850	90
Figure 4.34:	Resistance of PP and composites containing 10 wt% of prepared RHB samples	92
Figure 4.35:	Resistance of PP and composites containing 15 wt% of four different RHB samples	92
Figure 4.36:	Impedance of PP and fabricated composites	94

List of Abbreviations

PP	Polypropylene
aPP	Atactic Polypropylene
sPP	Syndiotactic Polypropylene
iPP	Isotactic Polypropylene
BC	Biochar
RHB	Rice Husk Biochar
RH	Rice Husk
CEC	Cation Exchange Capacity
HTC	Hydrothermal Carbonization
ESP	Electrostatic Precipitator
GHG	Greenhouse Gas
MSW	Municipal Solid Waste
HDEP	High-Density Polyethylene
PAM	Polyazomethine
PVA	Polyvinyl Alcohol
ABS	Acrylonitrile Butadiene Styrene
SBR	Styrene-Butadiene Rubber
PTT	Poly (trimethylene terephthalate)
PVdF	Polyvinylidene fluoride
CNT	Carbon Nanotube
GB	Glass Beads
MMC	Metal Matrix Composite
CMC	Ceramic Matrix Composite
PMC	Polymer Matrix Composite
Wt%	Weight Percent
UV	Ultra Violet
VM	Volatile Matter
SEM	Scanning Electron Microscopy
EDX	Energy Dispersive X-Ray
XRD	X-Ray Diffraction
FTIR	Fourier Transform Infrared Spectroscopy
TGA	Thermo-gravimetric Analysis
DTG	Derivative Thermo-gravimetry
DSC	Differential Scanning Calorimetry
UTM	Universal Testing Machine
ASTM	American Society for Testing and Materials
IA	Impedance Analysis

List of Notations

β	Average Number of Branch Points Per Molecule
λ	Number of Branch Points Per 103 Carbons
A	Area
F	Load
L	Support Span Distance
b	Width of Beam
d	Depth of Beam
σ	Ultimate Tensile Strength
σ_f	Flexural Strength
T_{onset}	Onset Degradation Temperature
T_{max}	Temperatures at the Maximum Mass Loss Rates
T_m	Melting Temperature
R	Resistance
Z	Impedance
Ω	Ohm

CHAPTER 1
INTRODUCTION

1.1 Overview

Polypropylene (PP), a semi-transparent thermoplastic polymer synthesized by polymerization of propylene (propene) monomer, is a semi-crystalline, colorless and odorless solid that is non-toxic and not biodegradable in nature [1]. It is the highest produced thermoplastic resin after polyethylene because of its extensive use in various industrial products such as automobile parts, electrical insulator, furniture, product packaging, kitchen gadgets, etc. [2,3]. Some favorable properties like low cost, easy processing, excellent chemical resistance, etc. are the main reason for the popularity of this thermoplastic polymer. However, some other properties such as inferior mechanical property, low thermal stability, etc. limit its application [4]. To improve the overall properties researchers introduced PP composites by incorporating various inorganic and organic compounds as fillers and reinforcements in the PP matrix [2,5]. Glass fiber, carbon nanotube (CNT), graphene, talc, etc. are few popular fillers/reinforcements utilized for PP composite fabrications [6,7]. Nevertheless, due to cost mitigation efforts, interest in renewable sources utilization and environmental safety concerns organic biomass based fillers are used in PP composites which include jute, sugarcane bagasse, wood, etc. [8]. Though, composites of PP having biomass based natural fillers exhibit several improvements, drawbacks like moisture absorption, low thermal stability, etc. still exist [9]. Very recently, researchers introduced biochar as filler/reinforcement in various polymeric composite developments. Properties like the presence of activated carbon, broad surface area, thermal stability, higher carbon content, and porous structure make biochar very successful as reinforcement in polymeric composites [10]. Examples of biochar reinforced polymer composite include but are not limited to polypropylene with ultrafine bamboo biochar [1], polypropylene with pinewood waste biochar [2], polyester with rice husk biochar [11], starch with rice husk biochar [12], styrene-butadiene rubber with birch wood biochar [13], polypropylene with date palm waste biochar [14], polyamide with commercial biochar [15], epoxy with pine cone biochar/char [16], high-density polyethylene with rice husk biochar [17], and polyvinyl alcohol with hardwood biochar [18]. Incorporation of biochar in PP matrix produced composites with improved mechanical, thermal and electrical properties [1,2,14].

Biochar is a carbon-rich porous structured material obtained by the thermochemical conversion, well known as pyrolysis, of biomass in a closed receptacle with little or no oxygen presence [19]. Biomass consists of agricultural waste/residue, municipal solid waste (MSW) and forest residue, which is a renewable and sustainable source that has the potential for energy and other value-added product development [20]. Pyrolysis is one of the most widely used methods for biomass to value-added product conversion, where three valuable products namely biochar, bio-oil and syngas are produced [21]. Among three different pyrolysis processes (slow, intermediate, and fast) slow pyrolysis is considered as better for biochar production because of the higher char yield than that of the other pyrolysis processes [22]. Slow pyrolysis yields high-quality biochar that is very effective as a soil amendment, pollutant eliminator, sieve medium and filler/reinforcement [17,18,23]. In recent years, researchers paid much attention to reinforcing

polymer matrix with biochar for composite fabrication that exhibits superior properties. Biochar is more convenient than other filler materials as properties of the biochar can be modified by changing pyrolysis conditions and greater compatibility with the polymeric matrix can be achieved. Moreover, better thermal stability and electrical conductivity can also be obtained by the incorporation of biochar in the composite system [14,24]. Paddy rice is among the highest cultivated agricultural crop around the world and the cumulative growth of paddy rice production is observed in recent years [25,26]. The paddy rice cultivation produces a significant amount of biomass byproducts such as straw, rice bran, and rice husk. Generally, straw and bran are used as animal feeding. On the other hand, rice husk (RH) is a waste product that has limited uses. An average of 20 kg husk is produced during 100 kg milled rice is processed [28]. Considering this ratio, we can estimate the rice husk generation in the world from the world's average milled rice production. Figure 1.1 presents the estimated rice husk production in recent years [26,27]. This huge amount of rice husk is not effectively utilized, especially in developing countries, causing environmental and health issues [29]. High-quality biochar can be produced from rice husk via the pyrolysis process and it can be utilized as filler/reinforcement in polymeric composite development [17,30]. Though there are one or two studies investigating rice husk derived biochar (RHB) in polymeric composites [11,12,17], rice husk slow pyrolyzed biochar reinforced polypropylene binary composites are not studied yet.

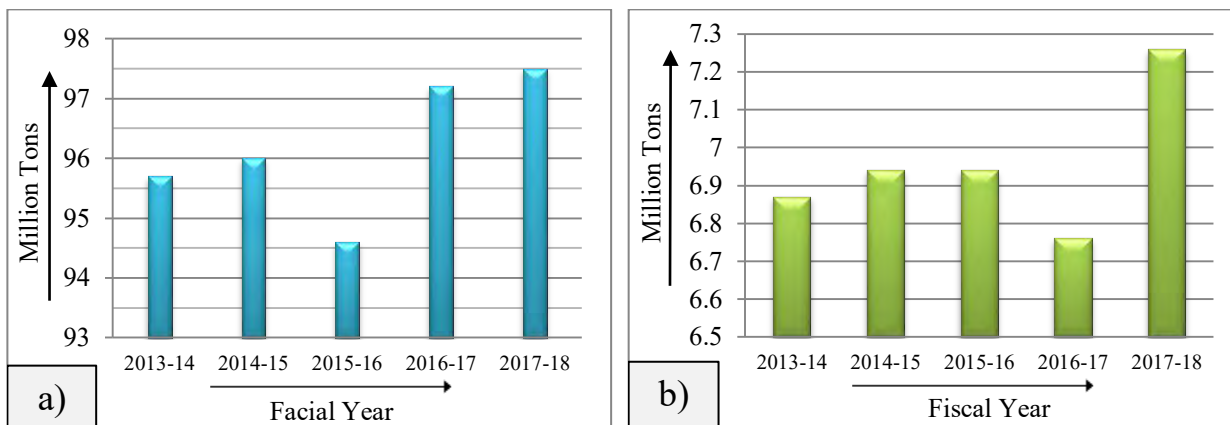


Figure 1.1: Estimated rice husk generation in the recent five fiscal years a) around the world b) in Bangladesh.

Poor management of waste biomass and reckless disposal of organic waste causes environmental pollution, which adversely affects human health and climate. As a result, waste biomass to value-added product conversion is necessary, which will ensure waste mitigation, pollution reduction and economic development [31]. Rice husk, a by-product of rice processing, can be converted into fuel and other value-added products, like biochar, via pyrolysis method and the obtained biochar can be utilized by reinforcing polymer matrix, such as polypropylene, for composite development that exhibits superior properties. The basic background of the project is that the excellent thermal stability and high carbon content of biochar [32] have the potentiality to

improve the thermal and electrical properties of PP composite. Moreover, rice husk biochar has high silica content and porous structure [32], which may lead to the enhancement of mechanical properties of the PP composite.

1.2 Present State and Goal of the Work

Previous studies have reported successful incorporation of various biomass-derived biochar particles in different polymer matrices and mentioned improvements in different properties. In some research work, rice husk derived biochar was also utilized for polymeric composite development, but there is no study exploring the viability of RHB reinforced PP composite. As a consequence, in this research, a comprehensive study on RHB reinforced PP composite fabrication and characterization of its mechanical, thermal and electrical properties have been performed.

The goal of this work is the fabrication of RHB reinforced PP composite and investigation of the effect of rice husk biochar addition on the properties of PP. As RHB is a potential reinforcement for polymeric composites and PP has good interaction with biochar fillers, so RHB reinforced PP composites are expected to possess superior mechanical, thermal and electrical properties. Keeping this in mind, the main objectives are:

- (i) Fabrication of new PP composites with improved properties by the incorporation of bio-derived material in the PP matrix.
- (ii) Mechanical properties enhancement by mitigation of poor interfacial adhesion and compatibility in the composite.
- (iii) Improvement of thermal stability and electrical properties of the composite.

Successful fabrication of the RHB reinforced PP composite will not only provide a high-quality material but also ensure the conversion of agricultural waste into value-added products and save the environment. The composite could potentially reduce the use of metal, wood, ceramic, and glass in industrial applications.

This thesis report is chronologically organized from the background studies to the final findings of the work. The above mentioned first chapter contains problem statements and prime target of the research. The next chapter bears a broad review of the relevant literatures, especially about biochar reinforced polymer composites, and also presents some general information about the materials utilized in this work. After that in chapter three, sampling plans and experimental techniques of the study have been described. Afterwards, in chapter four experimental data that was obtained during this study has been given and discussed. Finally, the concluding chapter presents the prime findings of the study with some future work statements.

CHAPTER 2
LITERATURE REVIEW

2.1 Biochar

Biochar is a stabilized, recalcitrant carbonaceous compound, produced when biomass is heated to temperatures usually between 300 and 1000⁰C, under low oxygen concentrations [34]. Biochar is part of a series of materials referred to as black carbons, which are all produced by chemical and/or thermal transformation of the original biomass material [35]. Any organic matter that is available and can be used as an energy source including residues and wastes from various agricultural activities, forest remnant, animal wastes, and livestock operation residues, various types of wood and wood wastes, organic wastes from municipalities and oceanic plants can be defined as biomass [20]. Biomass is a very promising source for char/biochar and other value-added materials [36]. Biochar is renewable and environment friendly [37]. The image of some biomass feedstock and obtained biochar is showed in Figure 2.1 [32].



Figure 2.1: Some biomass and their biochar [32]

The use of biochar as an agricultural amendment and for energy is not a new idea. Transforming biomass materials into biochar or black carbon has been documented back to the beginning of the modern era and there is archeological evidence of even older applications [38,39]. However, less attention has been given to the usage of biochar in engineering applications that is even more practical use of the material considering its favorable properties like low cost and eco-friendliness [35]. Therefore, the use of biochar in targeted engineering applications is encouraged.

2.1.1 Properties of Biochar

Ash, labile organic matter (volatile compounds and labile carbon), fixed or stable carbon, and moisture are the main components of biochar. The physicochemical condition of the carbon (C) in biochar gets altered by the thermal treatment process and produces aromatic structures which are highly resistant to microbial decomposition. As a result, the C compounds in biochar are stable for long periods of time. Thus, they are found to be effective for long-term C sequestration [40,41]. An overview of the prime characteristics of biochar is detailed in the next section.

2.1.1.1 Composition and Structure

During thermal treatment for biochar generation, labile organic matter of the biomass is almost destroyed, but the fixed C remains mostly intact. As higher temperatures are needed to burn off the more stable forms of C (i.e. cellulose and lignin), the final temperature of the thermal decomposition process determines the amount of labile C loss and fixed organic C content of the resultant biochar. At higher temperatures, the C content of the biochar increases while the H and O contents decrease, causing a higher degree of carbonization in the biochar [42]. Nitrogen (N) in the biochar generally decreases with increasing temperatures [43]. Pretreatment procedures also affect the elemental composition of biochars [44].

The skeletal structure of biochar consists mainly of C and minerals of different pore sizes [45]. Macro-pores are significant for hydrology, aeration, movement of roots, and bulk structure and micro-pores are liable for surface area and high absorptive capacity, while meso-pores are important for adsorption processes.

2.1.1.2 pH and Zeta Potential

The pH value of biochar usually increases with rising temperatures [43,44]. However, in some studies, the produced biochar was found to be neutral [46]. The surface of biochar is often negatively charged and is not likely to sorb negatively charged ions such as nitrate or phosphate [44].

2.1.1.3 Surface Area and Porosity

Generally, both surface area and porosity of the biochar increases with increasing temperatures [47]. Biochar generation at higher temperatures (above 900⁰C) causes the widening of the micro-pores due to the destruction of walls between adjacent pores that increase the surface area. As the surface area is an important characteristic of biochar, the temperature is clearly a significant factor for biochar production.

The porous structure of biochar is caused by numerous aromatic compounds and other functional groups that are produced from lignin-based biomasses. The pore size and pore pattern of the biochar depend on the temperature adopted during biochar formation and the composition of the feedstock biomass material. The morphology, pore distribution and pore size of the biochar can be examined by SEM (scanning electron microscopy).

2.1.1.4 Absorption Capability and Cation Exchange Capacity

Biochars contains aromatic C groups that are capable of adsorbing heavy metals or hazardous molecules. H, N, O, P, and S present in the aromatic rings of the biochar determine the electronegativity of the biochar product and influence the cation exchange capacity (CEC).

Researchers investigated the adsorption of cations onto biochar to better understand the heavy metal contaminants' remediation capacity of biochar [48].

2.1.2 Preparation Methods of Biochar

Thermochemical decomposition processes like pyrolysis, torrefaction, hydrothermal carbonization (HTC), and gasification are usually applicable to convert biomass into biochar, biofuel, and other bio-based gaseous products [49,50]. The thermal decomposition, at high temperatures and in the absence of oxygen, converts the organic matter of the biomass into biochar. In some processes, high pressure is also required. This process irreversibly changes the physical state and chemical composition of the organic matter. The structural building blocks of biomass (cellulose, hemicelluloses, lignin, and pectin) undergo cross-linking, fragmentation, and depolymerization at different temperatures during pyrolysis or other decomposition processes [51]. Biomass is primarily transformed into biochar, small quantities of condensable liquid (bio-oil), and non-condensable gas (syngas). Among the above mentioned thermal conversion methods pyrolysis is the most common and favorable process for biochar production. Several types of reactors or pyrolysis units have been developed for the process. These units operate on similar principles regarding O₂ availability but might differ in heating rates, highest temperature, residence times, and pressure. These differences mainly determine the proportions of the final products [49,50]. The basic pyrolysis process is depicted in Figure 2.2 [33].

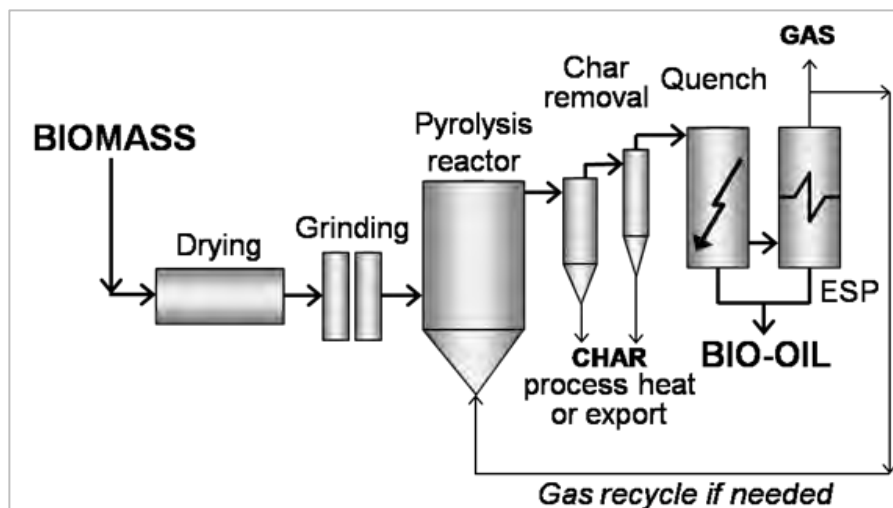


Figure 2.2: Pyrolysis process [33]

The yield of biochar, bio-oil, and syngas depends on the type of pyrolysis process utilized, and the pyrolysis conditions. Based on the heating rate, temperature, and residence time, pyrolysis can be classified into slow, intermediate and fast pyrolysis [49,52,53]. Table 2.1 presents the typical product yields (biochar, bio-oil, and syngas) and the operational conditions (residence time and process temperature) of different biochar production methods.

Table 2.1: Product yields and the operational conditions of different biochar production methods

Process	Yield (%)			Residence Time	Process Temperature (°C)	Ref.
	Biochar	Bio-oil	Syngas			
Slow Pyrolysis	35	30	35	Several Hours	350-800	[51,50]
Intermediate Pyrolysis	20	50	30	~1.5 min	~450	[52]
Fast Pyrolysis	12	75	13	~2s	500-1000	[53]
Gasification	10	5	85	10-20s	700-900	[54]
Hydrothermal Carbonization	50	-	-	1-12h	180-250	[55]
Torrefaction	-	-	-	10~60min	200-300	[56]

2.1.2.1 Slow Pyrolysis

Slow pyrolysis is a thermal decomposition process that distinct for its slow heating rate and long residence time [50]. In general, the heating rate ranges from 10 to 20⁰C per minute. Almost equal portions of gas, liquid, and solid products are produced in this process. The process is carried out at atmospheric pressure, with heat provided by external heaters, partial combustion of the feeds, or hot-gas recirculation [51]. Slow pyrolysis is favorable for biochar production due to its high char yields and easy operational conditions. Biochar yields are also affected by the particle sizes, along with lignin and ash content of the biomass during slow pyrolysis. These conditions promote biochar production by increasing cracking reactions that hinder the production of liquids or bio-oil [50].

2.1.2.2 Intermediate Pyrolysis

Intermediate pyrolysis is a thermal conversion process with comparatively higher heating rates and lower residence times (few minutes) than that of slow pyrolysis. Products are unevenly distributed among liquid, gas, and char. Intermediate pyrolysis exhibits lower biochar yields compared to slow pyrolysis [52].

2.1.2.3 Fast Pyrolysis

Fast pyrolysis is also a biomass conversion process that is distinguished by fast heating rates (~120⁰C/min⁻¹), short residence times (< 0.05 min), and high yields of liquid product (bio-oil) from biomass, together with fewer amounts of gas (syngas) and solid (biochar) [53]. This process offers high bio-oil (75%) yields compared to solid (12%) or gaseous (13%) products. The bio-oil produced can be used directly as an efficient energy carrier [49]. In addition to rapid heating during fast pyrolysis chemical reaction kinetics, phase transition phenomena, and mass-transfer processes play important roles in increasing bio-oil yields. A free-flowing dark brown liquid, possessing almost half the heating value of conventional fuel oil, with an acrid and smoky odor,

is generated through fast pyrolysis [49]. Bio-oil is the prime product of fast pyrolysis (75 wt% on dry feedstock basis), together with biochar and gases. Biochar obtained via fast pyrolysis contains recalcitrant conjugated aromatic structures [53]. However, due to low char yield and tougher operational conditions fast-pyrolysis process is not favored for biochar production.

2.1.2.4 Gasification

Gasification is a thermochemical conversion method that involves breaking down a carbon source, such as biomass into hydrogen (H_2), carbon dioxide (CO_2), carbon monoxide (CO), and a small number of other hydrocarbons such as methane (CH_4). During gasification, the organic materials (biomass) are reacted in an O_2 controlled environment at very high temperatures (700-900 $^{\circ}C$) without combustion [54]. The gasification product is 85% syngas and the gas mixture contains H_2 , CO_2 , CO , CH_4 , C_2H_2 , and N_2 . The solid product of gasification is biochar (10%), while the liquid product is tar (5%), mainly containing aromatic hydrocarbon compounds.

2.1.2.5 Hydrothermal Carbonization

Hydrothermal carbonization (HTC) is a thermochemical conversion process to convert organic feedstock such as biomass into carbon-rich products. Typical conditions for HTC are the presence of liquid water, higher temperatures (180-250 $^{\circ}C$), and high pressure (2-10 MPa). Though HTC offers high biochar yields (around 50%), the necessity of high pressure makes the process complicated and less favorable [55].

2.1.2.6 Torrefaction

Torrefaction, also known as mild pyrolysis, is a thermal process to convert biomass into a coal-like material, which has better fuel characteristics than the original biomass. During torrefaction, biomass is heated to a temperature between 200 and 300 $^{\circ}C$ in the absence of oxygen which is similar to slow pyrolysis but requires much lower temperature [56].

2.1.3 Factors Influencing Biochar Quality

Biochars produced by different conversion techniques usually have different properties because of the variation in operating conditions and post-operation treatments. Factors affecting the quality of biochar are discussed below.

2.1.3.1 Temperature

Pyrolysis temperature is the prime thermodynamic parameter that influences biochar properties. The characteristics and structure of the biochar are highly dependent on pyrolysis temperature [57,58]. The ash content, surface area, and pH of biochar produced from biomass increase with raising temperature [59], but the biochar yield decreases [60]. Biochars synthesized at low pyrolysis temperatures contain aliphatic and cellulose-type structures that give a more diversified

organic character to the material. This might be good for mineralization by bacteria and fungi that are important for aggregate formation and nutrient turnover process. Biochars prepared at higher temperatures are characterized by high surface area and micro-porous structure which have high adsorption capacity. On the other hand, lower temperature provides biochar with inferior adsorption capacity. The higher the operating or pyrolysis temperature, the higher the biochar surface area [58,59].

2.1.3.2 Heating Rate

The heating rate also affects the structure of biochar as well as the yields of biochar, syngas, and bio-oil [61]. Higher heating rates and optimum processing temperatures promote bio-oil production, whereas, slower heating rates with lower processing temperatures enhance the production of biochar. During biochar production from pine sawdust, a lower heating rate of $20^{\circ}\text{C s}^{-1}$ helped the natural porosity of the sawdust to be transferred to the biochar with almost no morphological changes. On the other hand, a higher heating rate of $500^{\circ}\text{C s}^{-1}$ destroyed the cell structure of the sawdust derived biochar by de-volatilization [57]. Researchers found that lower pyrolysis temperatures and low heating rates promote biochar production whereas; higher final pyrolysis temperatures, longer residence times, and lower heating rates favor the conversion of biomass into syngas (gaseous products). Contrariwise, Intermediate pyrolysis temperatures ($500\text{-}550^{\circ}\text{C}$), short vapor residence times, and high heating rates usually increase the yield of bio-oil (liquid products) [60].

2.1.3.3 Particle Size

The particle size of the biomass is also an important parameter that affects the distribution of the products during pyrolysis. Mass and heat transfer rates and the extent of secondary reactions within the particles are influenced by the particle size of the biomass. The raw materials particle size differs depending upon the type of the pyrolysis process and the type of feedstock used. Researchers found that larger particles (over 1.8 mm) have greater temperature gradients within, which leads to lower temperatures in the core than the surface of the particles. This is likely to increase in the char yields, and decrease the bio-oil and syngas yields [62]. Generally, particles with smaller sizes are preferred in the fast pyrolysis system because small particles heat up uniformly, thus the more volatile matter is released leading to higher bio-oil and syngas yields [63].

2.1.3.4 Feedstock Composition

Feedstock type and its composition have a significant influence on the physicochemical properties of biochar [64]. The composition of the resultant biochar after pyrolysis varies due to variations in feedstock materials. The proportions of inorganic and organic compounds entirely depend on the type of feedstock selected. Biomass feedstock such as animal manure contains high nutrients and can result in biochars with high nutrient content compared to plant feedstocks

that are mainly composed of hemicelluloses, cellulose, lignin, and some inorganic compounds [65]. Feedstock composition coupled with pyrolysis conditions potentially affects the physical properties related to the surface area, pore structure, adsorption properties, pH, CEC, and the chemical properties related to the organic carbon content of the biochar [64].

2.1.4 Applications of Biochar

Properties such as large surface area, porous structure, adsorption properties, and CEC make biochar suitable for various applications. The chemical and physical properties of biochar can vary significantly depending on the thermochemical conversion process and the feedstock utilized [64]. As a result, the performance of biochar in different applications can vary significantly with the production methods utilized and the composition of the feedstock material. Applications of biochar are described below.

2.1.4.1 Soil Improvement

The application of biochar in the soil is highly beneficial because of the numerous merits it provides. Biochar improves the biological and physical properties of soils such as water-holding capacity and soil-nutrient retention capability, which promote plant growth [66]. It has been found that biochar can (a) improve soil structure and pH, (b) improve fertilizer use efficiency, (c) decrease soil tensile strength, (d) decrease aluminum toxicity to plant roots and microbes, and (e) improve soil conditions for earthworm populations [50,67].

2.1.4.2 Carbon Sequestration

In the carbon sequestration process, carbon (C) is captured and stored to prevent it from being emitted into the atmosphere [50]. It is essential that the C is transferred to a passive carbon pool that is stable and inert, in order to reduce C emission. Biochar provides an easy transfer route from the active carbon pool to the passive pool. Transferring, even a small fraction of the C that cycles between the plants and atmosphere, to the much slower biochar cycle, will have a great impact on atmospheric CO₂ concentrations, as the annual uptake of CO₂ by plants from the atmosphere through photosynthesis is eight times greater than anthropogenic GHGs emissions. Biochar is chemically and biologically more stable than the original carbon, because of its molecular structure, and origins. It is tough for the sequestered carbon in the biochar to be released as CO₂, making this a good method for carbon sequestration [68]. The diversion of even 1% of the net annual uptake of C by plants into biochar would mitigate almost 10% of current anthropogenic C emissions [69].

2.1.4.3 Reduction of GHG Emissions

When biochar is applied to the soil, its recalcitrant nature enables it to stay in the soil for long periods of time, thus reduces CO₂ and CH₄ (GHG) emissions [68]. Moreover, biochar adsorbs

ammonia from the soil and acts as a buffer, thus potentially reduces NH_3 volatilization from agricultural fields [70].

2.1.4.4 Waste Water Purification

The application of biochar for the removal of heavy metal and organic contaminants from aqueous media is a promising technology for contaminated water and wastewater treatment. The presence of cellulose, lignin, hemicelluloses, lipids, proteins, and sugars in the biomass feedstocks contain a variety of functional groups that can be physically activated upon pyrolysis or by other thermochemical treatments during biochar preparation, to improve their ability to adsorb contaminants [71]. The type and concentration of surface functional groups play significant roles in the adsorption capacity of the biochar [72]. Mostly, the carbon-structured matrix of biochar, coupled with its large surface area, a high degree of porosity, and strong affinity for non-polar substances such as furans, dioxins, and other compounds, enables it to play a crucial role as a surface sorbent for controlling contaminants in the water [73].

2.1.4.5 Waste Utilization and Management

Management of MSW, agricultural and animal wastes can provide huge environmental challenges that eventually lead to the pollution of the environment [74]. The utilization of this waste, as well as other by-products, as feedstocks for biochar production, represents significant environmental management and economic achievement [75]. The landfilling of organic waste and the anaerobic digestion of animal waste can result in the release of huge amounts of N_2O and CH_4 . Therefore, using this waste organic matter for biochar production, and its applications, is an effective waste management strategy that helps to reduce GHG emissions and reduce waste-disposal costs associated with traditional waste management methods.

2.1.4.6 Composites and Engineering Materials Development

Biochar has potential application as filler and reinforcement in polymeric composite development which is capable of enhancing the physical and mechanical properties of the composites. The incorporation of biochar with polymer as a reinforcing agent may impart many benefits through improving both physical and chemical properties and also dimensional stability of the composite product [76]. While optimizing the properties of the polymer, the addition of biochar in polymer also helps to reduce the cost and to improve the processability of the composite material. Biochar has been explored for the composite applications such as sustainable reinforcement in polyazomethine (PAM), epoxy, polyvinyl alcohol (PVA), polypropylene (PP), styrene-butadiene rubber (ABS) and nitrile matrixes [77].

Biochar wood polymer composite is an example of biochar reinforced polymer composite development in recent years. Wood polymer composites are widely used in manufacturing furniture and construction materials. The large surface area, high carbon content and increased stability of biochar make it potential filler or reinforcement in wood polymer composites, by

lowering the moisture absorption of the composite. Furthermore, biochar is applied to wood polymer composites due to its high thermal stability which increases the thermal stability of the composite [10]. Properties such as low in cost, easy to obtain and renewability make biochar truly desired as reinforcement material in polymer composite production. A pictorial representation of different applications of biochar based on the specific properties as described above is presented in Figure 2.3 [78].

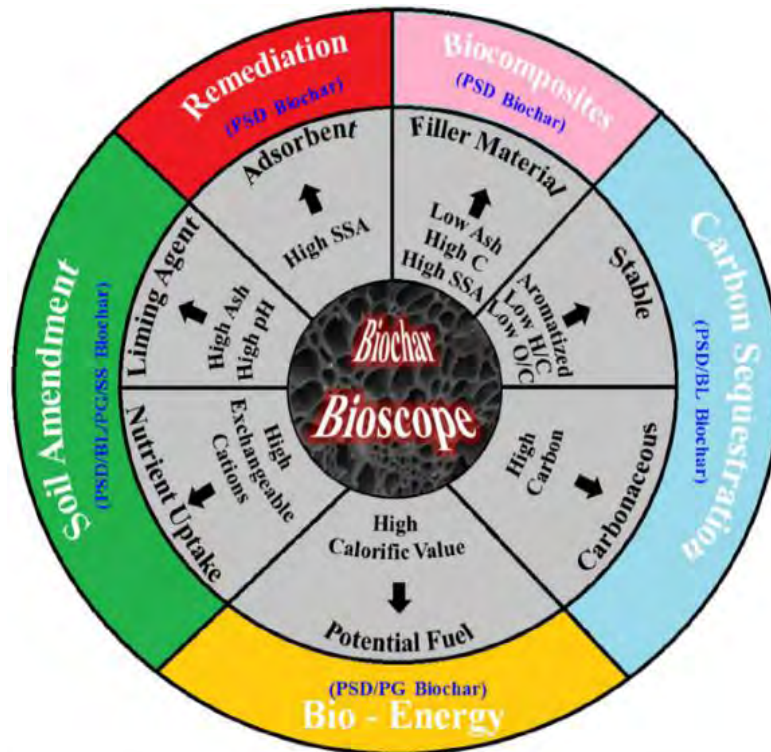


Figure 2.3: Prospect of biochar applications [78]

2.1.5 Rice Husk Derived Pyrolyzed Biochar

Biochar production from woody biomass is not always a feasible and sustainable option, especially in farming areas. However, biochar can be produced from any biomass and is a product of thermochemical decomposition processes such as gasification and pyrolysis. Therefore, rice husk could successfully be used for the production of energy, and biochar. The rice husk, also known as rice hull, is the coating on a rice grain. It is formed from hard materials, mainly lignin and silica, to protect the seed during the growing season. Each kg of milled white rice results in roughly 0.20 kg of rice husk as a by-product of rice production during milling [28]. Components of the rice grain, an image of loose rice husk and biochar are presented in Figure 2.4 [79].

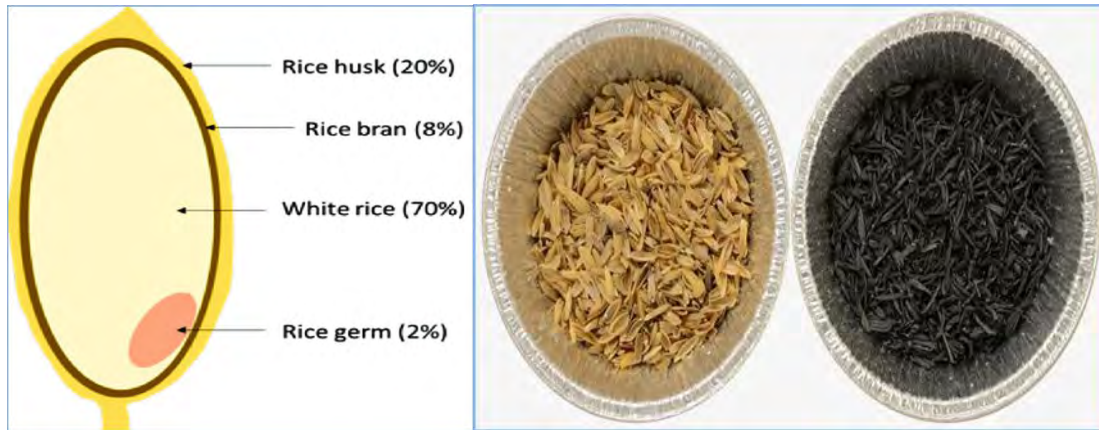


Figure 2.4: Different parts of paddy rice, loosen rice husk and rice hush derived biochar [79]

The supposedly high stability of carbonized residues could help to reduce GHG (greenhouse gas) emissions from rice-based systems and sequester carbon in the soil. This coupling of biochar and bioenergy generation in rice production systems would offer several advantages:

- Rice husk is a by-product of rice production. Therefore, bioenergy and char based on rice husk do not affect food security. Higher rice production would increase biochar output simultaneously.
- The complete removal of residues from the field leads to soil organic matter and soil quality degradation in most agricultural systems. However, studies in flooded rice-based systems have shown that soil quality is maintained over decades even if all husks are removed [78,88].
- Removal of husk from rice fields for biochar production directly decreases emissions of GHG and air pollution caused by field burning.
- The high cropping intensity, especially in irrigated rice systems, ensures a more constant husk supply for biochar production.

2.2 Polypropylene (PP)

Polypropylene (PP), a thermoplastic polymer, gained strong popularity very quickly since its discovery in 1954 due to its good temperature resistance and lowest density among the commodity plastics [80]. PP has excellent resistance to chemicals and can be processed via a variety of methods such as blow molding, injection molding, and extrusion, etc. PP is a polymer of propylene prepared catalytic polymerization. Polypropylene is a vinyl polymer in which every second carbon atom of the chain is attached to a methyl (-CH₃) group. The structure of propene and polypropylene is shown in Figure 2.5 [3,81]

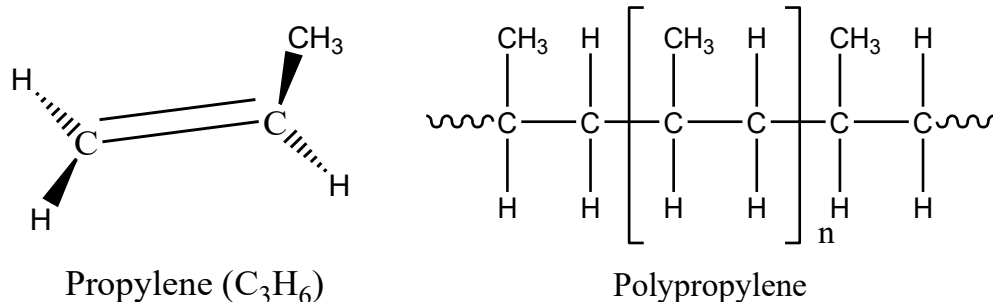


Figure 2.5: Propylene and Polypropylene structure.

The structure of PP is based on the chemical formula C_3H_6 and it is a downstream petrochemical product-driven from the olefin monomer propene or propylene. There are three major sources of propylene: from steam cracking of naphtha, gasoline refining process and propane dehydrogenation technology [82]. The polymer is produced by a monomer connection process called addition polymerization. In this process, heat, high-energy radiation and initiator or catalyst are added to combine monomers together. Thus, propylene molecules are polymerized into very long polymer chains. There are four different routes to enhance the polymerization of any polymer: suspension polymerization, solution polymerization, gas-phase polymerization, and bulk polymerization. However, properties of PP vary depending on the process conditions, molecular weight and molecular weight distribution [83]. Chemical resistance of PP can be described as follows: excellent resistance to dilute and concentrated acids, bases and alcohols, good resistance to aldehydes, ketones, aliphatic hydrocarbons, esters and limited resistance to aromatic and halogenated hydrocarbons and oxidizing agents [3,81]. The overview of PP is presented in Table 2.2.

Table 2.2: Advantages and Disadvantages of PP

Advantages of PP	Disadvantages of PP
Excellent processability	Low-temperature impact strength is poor
Good Impact resistance at room temperature	Attacked by chlorinated solvents and aromatics
High strength to weight ratio	Poor resistance to UV
Suitable for corrosion resistance	Flammable, but retarded grades available
Good chemical resistance	Difficult to bond
Good stiffness	Poor paint adhesion
Food contact acceptable	Embrittles below $-20^{\circ}C$

Polypropylene is the most widely used polymer among polyolefins due to three main reasons. Firstly, favorable properties of PP such as low density, high melt temperature and chemical inertness with low-cost making PP optimum for different applications. Secondly, Polypropylene is one of those rather versatile polymers out there, meaning that diversity in structural designs

and mechanical properties are achievable. Thirdly, different morphological structures of PP are possible by blending PP with other polymers. Moreover, incorporation of reinforcing agents and fillers with PP yields new composites with superior characteristics. Special and reinforced polypropylene grades include elastomer-modified PP, elastomer modified filled PP, glass fiber-reinforced PP, particle reinforced PP, filled PP, esthetic filled PP, and flame-retardant PP [84].

2.2.1 Structure and Types of PP

Generally, PP has a semi-crystalline structure and the degree of crystallinity could vary, depending on the stereo-chemical structure, and crystallization conditions. Crystallinity arises from the stereo-regularity in the molecular structure. However, irregularities such as branching or tail addition during polymerization limit the degree of crystallinity in the polymer [85]. There are three types of PP:

2.2.1.1 Atactic PP (aPP):

Atactic PP is completely amorphous with $-CH_3$ (methyl) groups that are randomly placed on the main chain. It does not have a melting temperature; rather it just softens upon heating until it flows like a very viscous liquid [83]. Figure 2.6 presents the structure of aPP polymer.

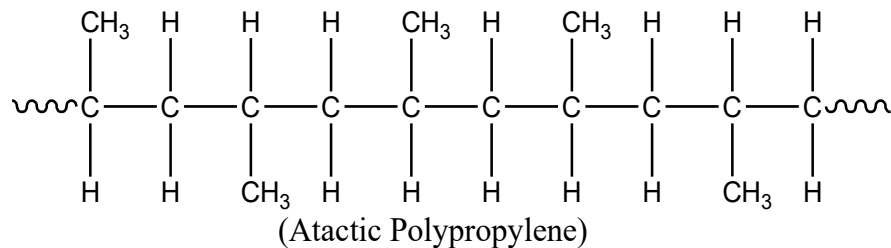


Figure 2.6: Structure of aPP.

2.2.1.2 Syndiotactic PP (sPP):

Syndiotactic PP is a semi-crystalline polymer with $-CH_3$ groups alternatively oriented and positioned along the main chain. The polymer is more homogeneous than aPP [83]. The structure of sPP polymer is presented below in Figure 2.7.

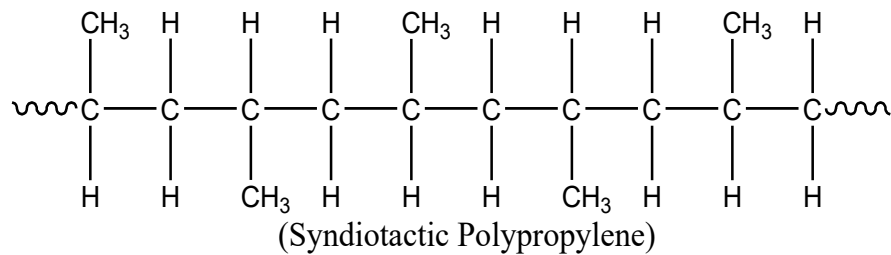


Figure 2.7: Structure of sPP.

2.2.1.3 Isotactic PP (iPP):

Isotactic PP is also semi-crystalline polymer but with the highest degree of crystallinity. The -CH₃ groups are all oriented on one side of the main chain, which makes the polymer very homogeneous and stable [3,81]. In most applications, iPP is used. Figure 2.8 presents the structure of aPP polymer.

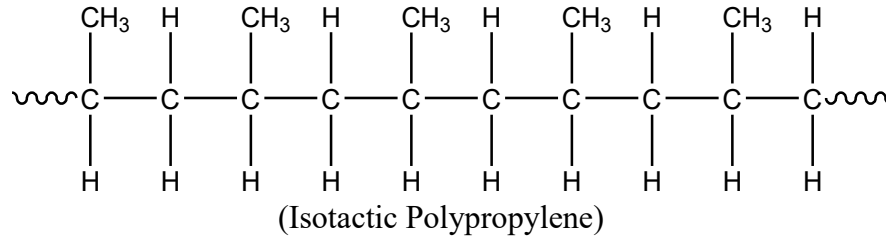


Figure 2.8: Structure of iPP.

2.2.2 Properties of PP

PP with a highly crystalline structure has a high level of stiffness and a higher melting point compared to other commercial thermoplastic polymers. Table 2.3 below shows some important mechanical and thermal properties of PP [86].

Table 2.3: Mechanical and thermal properties of PP [86]

Properties of PP	Value	Unit
Density	0.91-0.94	g/cm ³
Specific volume	30.4-30.8	cm ³ /lb
Tensile strength	3200-5000	Psi (Pound/sq. in.)
Flexural strength	7000	Psi (Pound/sq. in.)
Elongation	3-700	%
Water absorption (24h)	0.01	%
Rockwell hardness	95	R-scale
Thermal expansion	5.8-10	10-5 in./in.°C
Melting point, T _m	160-166	°C
Softening point, T _g	140-150	°C
Max. working temperature	150	°C
Glass transition temperature	-10	°C
Electric resistivity	10 ⁷ -10 ⁹	Ohm m

Properties of PP are strongly dependent on their crystallinity. The Hardness resulted from the -CH₃ groups in its molecular chain structure. PP is a lightweight polymer with a density of 0.90

g/cm³ that makes it suitable in many industrial applications. However, PP is not suitable for applications at temperatures below 0°C [82]. It is experimentally proven that PP has excellent and desirable mechanical, physical, and thermal properties at room temperature [3,81]. It has a low density and relatively good resistance to impacts [84]. The typical crystallinity of PP is between 40 and 60%. PP is a low-cost thermoplastic polymer with excellent properties like flame resistance, transparency, high heat distortion temperature, dimensional stability and recyclability making it ideal for a wide range of applications [82]. PP is a free-color material with excellent mechanical properties. Chemical resistance of PP can be described as follows: high resistance to dilute and concentrated alcohols, acids, and bases, moderate resistance to esters, aliphatic hydrocarbons, aldehydes, ketones and poor resistance to aromatic and halogenated hydrocarbons and oxidizing agents [3,81].

2.2.3 Synthesis of PP

In 1954, Giulio Natta first discovered PP and commercial production began in 1957. PP is a petrochemical product of the olefin monomer propylene. The PP polymer is produced by a monomer connection process called addition polymerization. High heat, coupled with initiator or catalyst is needed in this process to combine monomers together. Thus, propylene monomers are polymerized into very long polymer macro-molecules or chains. PP can be synthesized from the propylene monomer by Ziegler-Natta polymerization or by metallocene catalysis polymerization [3,81]. PP production from propylene is shown in Figure 2.9.

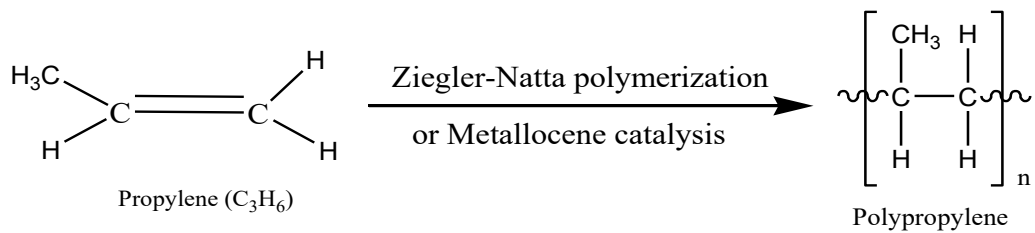


Figure 2.9: PP Synthesis process.

Researchers found that branching of linear Ziegler–Natta PP is possible by creating chains based on the molecular weight distribution. Introducing branching into a linear PP results in a product with high molecular weight, high melt temperature and improvement in properties like modulus and tensile strength, rigidity and heat resistance [82]. To identify the polymer structure and properties, branching parameter β , which is the average number of branch points per molecule, and λ which is the number of branch points per 10³ carbons, are calculated [3,81]. For the branching process, a post-reactor is used. The branching efficiency is associated with the temperature and chemical composition of the reaction. The relation between branching parameters and the molecular weight is significant to design polymers with unique properties for different applications [87,89].

2.2.4 Applications of PP

PP is the second most used thermoplastic polymer in the world, due to high availability, moderate cost, ease of manufacturing, and favorable properties. It is made from the combination of propylene monomers and used in a wide variety of applications [83]. Common applications of PP include:

- **Packaging Applications:** Good barrier properties, high strength, good surface finish, and low cost make PP ideal for both flexible and rigid packaging applications.
- **Consumer Goods:** PP is used to make in several household products and consumer goods applications including housewares, translucent parts, appliances, furniture, toys, luggage, etc.
- **Automotive Applications:** Due to the low cost, outstanding mechanical properties, and moldability, PP is widely used in automotive industries. Main applications include bumpers, battery cases and trays, instrumental panels, fender liners, interior trim, and door trims.
- **Fibers and Fabrics:** PP ropes and twines are very strong and moisture resistant highly favorable for marine applications. PP fiber is used in a wide variety of applications including slit-film, tape, strapping, staple fibers, spun bond and continuous filament, etc. A large volume of the PP utilized in the market is in the fibers and fabric form.
- **Medical Applications:** Due to its high chemical and bacterial resistance PP is suitable for use in various medical applications. Moreover, the medical-grade PP exhibits good resistance to steam sterilization. Disposable syringes are the most common medical application of polypropylene. Other applications include diagnostic devices, medical vials, intravenous bottles, Petri dishes, pill containers, specimen bottles, pans, food trays, etc.
- **Industrial Applications:** PP sheets are widely used in the industrial sector to produce acid and chemical tanks, pipes, sheets, RTP (returnable transport packaging), etc. because of its properties like high tensile strength, lightweight and corrosion resistance.
- **Composites and engineering materials development:** PP is very suitable for reinforcing and filling. Thus, PP is extensively used for Composites and engineering materials synthesis.

2.3 Fundamental Concept of Composites

Composites are miscellaneous materials prepared from two or more different materials with varying physical and chemical properties, and the final product exhibits the combined properties of the constituent materials [90,91]. Usually, the mixing is done physically, but sometimes chemical reactions aid the process and within the structure of the composite constituent materials remain distinguishable on a macro level. When one or more of the constituent materials used to fabricate the composite are derived from biological origins, the resulting composite is then defined as bio-composite [92]. Simple composites are made of only two different materials, one

is the matrix and the other is reinforcement. Though, the application of a binary matrix and several reinforcing agents is becoming more popular to develop superior composites [93]. The reinforcing agents (fibers or particles) in a composite are added to increase the desired properties of the composite, while the main job of the matrix (polymer, ceramic or metal) is to hold the whole thing together [94].

Polymeric composites are popular and widely used forms of composites. Generally, polymer composites consist of a polymer resin (acting as the matrix) and one or more reinforcements are added to serve specific objectives or requirements. For example, composites for automotive and aerospace applications require special properties such as high mechanical strength and lightweight. Traditionally synthetic fibers like glass or carbon fibers have been used to reinforce composites and are able to serve such requirements. However, with the growing global environmental concerns, the very slow biodegradability of synthetic fiber-reinforced composites is a crucial disadvantage. Therefore researchers are finding other viable approaches to enhance or accelerate the biodegradability of polymeric composites [95]. For this reason, natural ingredients from organic sources provide good prospective as reinforcements in thermoplastics, thermosets, and elastomers. Major advantages of using natural reinforcements (fibers, flakes, and particulates) in composites are low cost, renewability, lightweight, being nonhazardous and more importantly they can accelerate biodegradability of the polymeric composites [92,96]. Figure 2.10 is the graphical illustration of the current applications of polymeric composites in automotive industries [97].

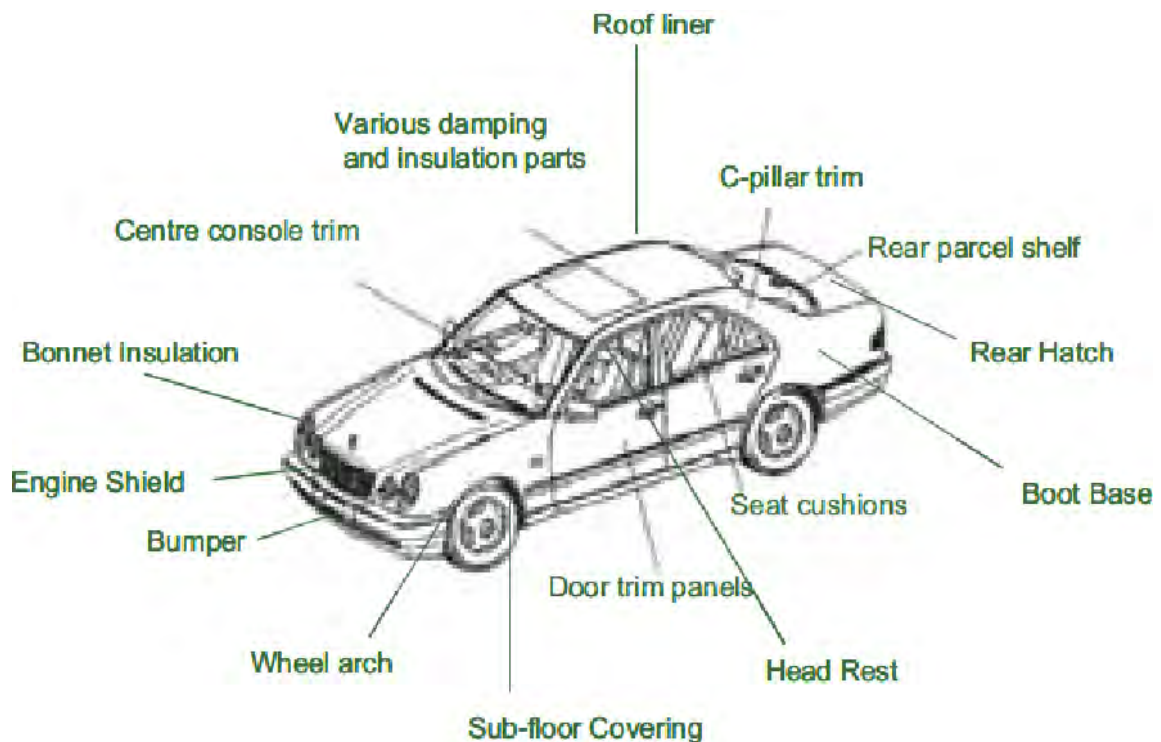


Figure 2.10: Schematic representation of composite applications in cars [97]

In Germany, most of the car manufacturing industries (i.e. Volkswagen Audi Group, BMW, Mercedes, Opel, and Daimler-Chrysler, etc.) are now using natural fiber and particle reinforced composites for interiors, door linings and paneling [97,98].

2.3.1 Classifications of Composite Materials

The overall properties of a composite system are determined by both the matrix and the reinforcements. So it is convenient to classify composite materials according to the type of matrix and the characteristics of reinforcements [91].

2.3.1.1 On the Basis of Matrix Materials

On the basis of the matrix, composites can be classified into three major types [99]. They are as follows:

- **Metal matrix composites (MMCs):** These types of composites are made by reinforcing materials (usually ceramics or metals) into a metallic matrix. MMCs pose advantageous properties such as high stiffness, high strength even at elevated temperatures, excellent abrasion resistance, high thermal conductivity, high thermal stability, high wear resistance, etc.
- **Ceramic matrix composites (CMCs):** These types of composites are fabricated by reinforcing ceramic fibers into a ceramic matrix. Thus, CMCs are ceramic fiber reinforced ceramic material and the main reason behind developing such materials is to overcome the limitation of the conventional ceramic materials like alumina, aluminium nitride, silicon carbide, silicon nitride, zirconia, etc. Improved properties of CMCs include excellent corrosion resistance even at high temperatures, higher mechanical strength even at high temperatures, high stiffness, high toughness, decreased density, high thermal shock resistance, etc.
- **Polymer matrix composites (PMCs):** These types of composites contain fibers or particles as reinforcements embedded in a polymeric resin matrix [99]. PMCs are the most popular and widely used composites in the world due to their low cost and simple fabrication methods [91]. Polymers without reinforcements have limitations such as inferior mechanical properties, low thermal stability, short lifetime or durability. PMCs have the potentiality to overcome such limitations. Superior properties of PMCs include low cost, good abrasion resistance, high specific stiffness, high tensile strength, high fracture resistance, good corrosion resistance, good fatigue resistance, etc. [91]. Figure 2.11 illustrates the classification scheme for composite materials on the base of the matrix [99].

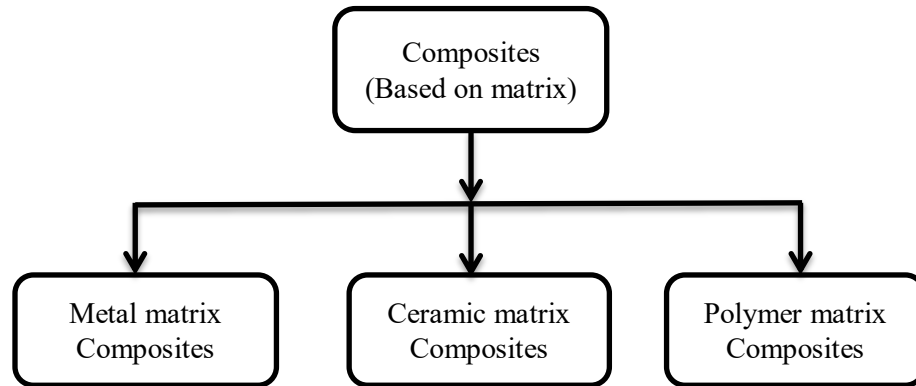


Figure 2.11: Matrix based classification of composites [99]

However, depending on the degradability composite matrices can be divided into two more types as biodegradable matrix and non-biodegradable matrix [100]. Composites made from natural biodegradable matrices are referred to as green composites [91].

2.3.1.2 On the Basis of Reinforcement Materials

The classification of composites according to the types of reinforcements are particle reinforced composites (also known as particulate composites), fiber reinforced composites (also known as fibers composites), and structural composites (also known as laminate composites) [99]. The classification of composites on the base of the reinforcement materials is presented in Figure 2.12.

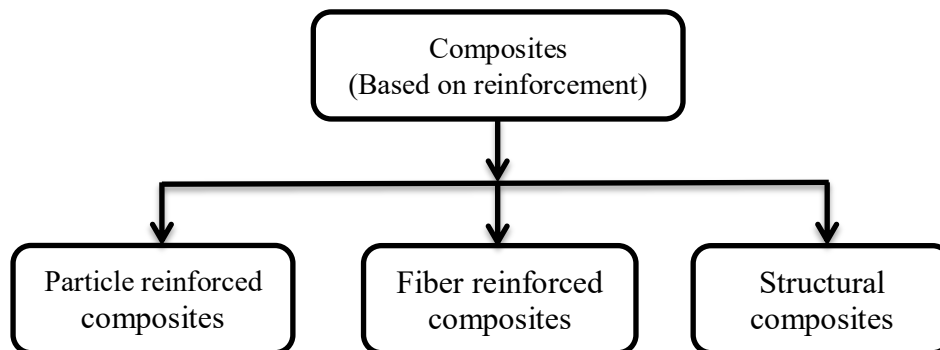


Figure 2.12: Classification of composites based reinforcement type [99]

- **Particle reinforced composites:** These types of composites consist of a matrix reinforced by particles. The particles are used to decrease the ductility and increase the modulus of the matrix [101]. Particles can have virtually any shape, size or geometry. However, for effective reinforcement, the particles should be minimum and evenly distributed throughout the matrix. Generally, the particulate phase of the particle reinforced composite is stiffer and harder than the matrix. These reinforcing particles tend to restrain movement of the matrix phase around each particle and the matrix transfers some of the applied stress to the particles, thus the composite

becomes harder and stiffer. The degree of reinforcement depends on strong bonding at the matrix–particle interface, which is related directly to the improvement of mechanical behavior [102]. There are two types of particle reinforced composite, that are illustrated in Figure 2.13 [103].

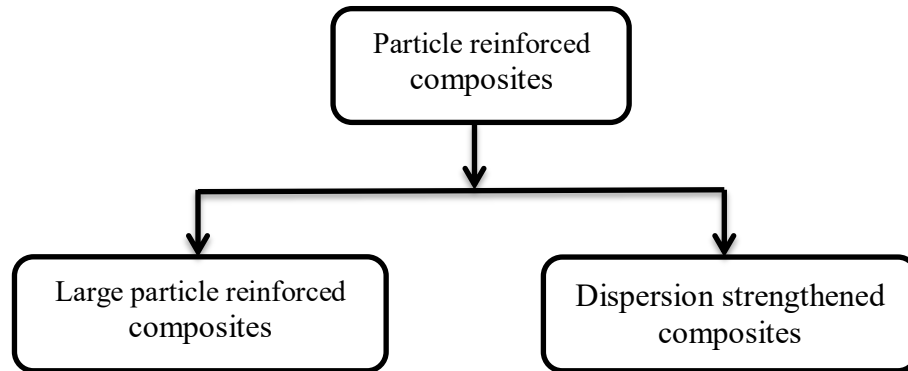


Figure 2.13: Types of Particle reinforced composites [103]

In large particle reinforced composites, the term large is used to define that the interactions are not at the molecular or atomic level; rather overall interaction mechanism is used [102]. An example of large particle reinforced composite is concrete, where sand and gravel are the particle reinforcement and cement is the matrix.

On the other and, much smaller particles are used in dispersion-strengthened composites [102]. In this type of composite interactions between particle and matrix occur at the atomic or molecular level, resulting in improvements in mechanical and other properties. Ultrafine bamboo char reinforced PP composite is an ideal example of the dispersion-strengthened composite [1].

- **Fiber reinforced composites:** Fibers are applied as reinforcement in a fiber reinforced composites. Fibers are a class of hair-like material that are continuous filaments or are in discrete elongated pieces, similar to pieces of thread. They can be used as a component of composites materials. Fiber reinforced composites exhibit improved mechanical properties, especially tensile strength, stiffness and fracture toughness, etc. Moreover, the application of natural fiber makes the composite eco-friendly, lightweight, strong, renewable, cheap and biodegradable [104]. However, Internal delamination damages in a fiber-reinforced composite are difficult to detect and nearly impossible to repair by conventional methods [105].

Fiber reinforced composites can be of two types, they are continuous and discontinuous fiber reinforced composites as illustrated in Figure 2.14. Continuous type of composite contains long continuous fibers as reinforcements. On the other hand, in discontinuous composites, a matrix is reinforced by a dispersed phase form by discontinuous short fibers.

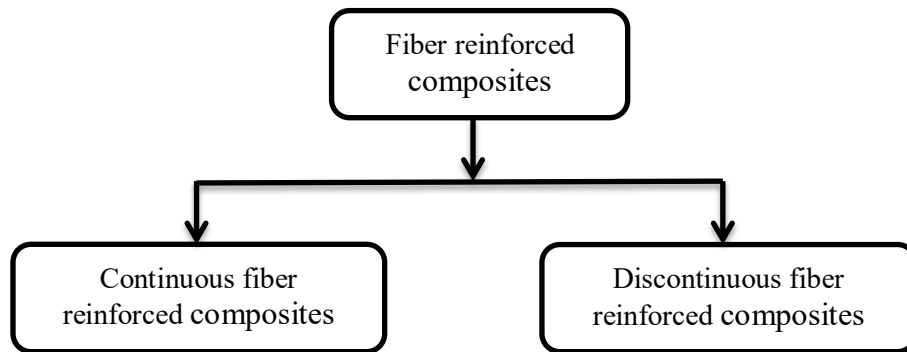


Figure 2.14: Types of Particle reinforced composites [103]

• **Structural composites:** Structural composites are an especial composite type containing both the homogeneous and the composite materials. Geometrical shapes play a vital rule in structural composites. The properties of such composites depend on both the constituent materials and the geometrical design of the structural elements [106]. Figure 2.15 presents the most common types of structural composites [103].

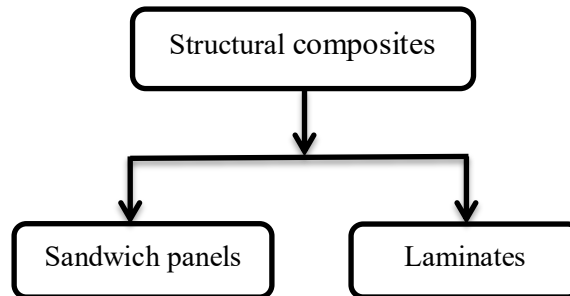


Figure 2.15: Structural composite types [103]

Sandwich panel composite contains two outer sheets that are adhesively bonded to a thicker core. The outer sheets are made of relatively strong and stiff materials (i.e., reinforced plastics, aluminum alloys, titanium, steel, etc.) and the core materials are usually lightweight and have a low modulus of elasticity (i.e., polyurethanes, epoxy, balsa wood, etc.).

2.3.2 Advantages and Disadvantages of Composite Materials

During the last few decades, compared to metals and other synthetic materials, the use of composite materials in the number of applications has increased very rapidly. Composites, Polymeric composites have influenced every aspect of modern civilization and simplified human lives. Today, various types of composites are available for the household to aerospace applications and can be easily seen in everyday applications [107]. Different kinds of materials such as natural and artificial fibers, organic and inorganic particles, elastomers, plastic compounds, ceramics, and metals can be used for composites, and these materials are being tailored frequently to meet the desired industrial applications. Composites have even replaced

glass-based materials and traditional metals for a number of applications due to their low cost, ease of processing, and availability [108]. However, due to rising environmental awareness, health concerns, and depletion of petroleum resources, recent years have seen a dramatic shift in the development of novel materials derived from bio-based renewable resources [109]. Polysaccharides, such as starch, chitin/chitosan, cellulose, alginate, and carbohydrate polymers, and animal protein-based biopolymers, such as gelatin, wool, silk, and collagen, are some well-known examples of bio-renewable resource-based environment friendly polymeric materials that can be used for environment friendly bio-composites synthesis. Moreover, bio-based materials procured from different natural resources, such as natural fibers, biochar, wood flour, etc. could be used as reinforcements for bio-based composite development [10,110]. Diverse efforts are being made to incorporate bio-based materials such as natural fibers/agriculture residue in matrices to make the final product completely/partially biodegradable and eco-friendly [111]. Properties such as good specific strength, low density, ease of preparation, high toughness, good thermal properties, no health risk, reduced tool wear, and enhanced energy recovery have made composite materials very popular choice among the designers, fabricators, equipment manufacturers, and consumers [94,95]. However, composites have some drawbacks. The pros and cons of composite materials have been illustrated in Table 2.4 below.

Table 2.4: Gains and losses of composite materials

Advantages	Disadvantages
High strength to weight ratios	Difficulty in adhesion
Improved strength and stiffness	Not biodegradable (most cases)
Ease of fabrication	Possible weakness of transverse properties
Modified electrical properties	Weak matrix resulting in low toughness
Good thermal stability	Cost of fabrication
Good corrosion resistance	Difficulty with damage recovery

2.4 Fundamental Concept of Polymer Matrix

The matrix serves two vital functions in a composite. Firstly, it holds the reinforcement phase in place and secondly, under an applied force it deforms and distributes the stress among the constituent materials [94]. To do this, the matrix must transmit the applied load to the reinforcement phase and change shape as required. Matrix also protects the constituents from the environment and abrasion with each other. Furthermore, the matrix helps to maintain the distribution of reinforcements as well as the distribution of load evenly among the reinforcements. It enhances some of the properties of the resulting material. It also provides a better finish to the final product [95].

Polymer resins as a matrix in composites are very popular due to its easy fabrication and good room temperature properties. Composites developed by reinforcing polymer resins with fibers or particles exhibit improved tensile strength and stiffness, good corrosion resistance, low cost, high durability [97]. However, the limited temperature range of using, low transverse strength,

residual stress between matrix and reinforcement, and poor adhesion are some of the limitations associated with polymer matrix composites. Matrix adhesion to reinforcements coupled with sufficient matrix shear strength has the potentiality to minimize such limitations [102]. Polymer matrices can be of two major types as illustrated in Figure 2.16.

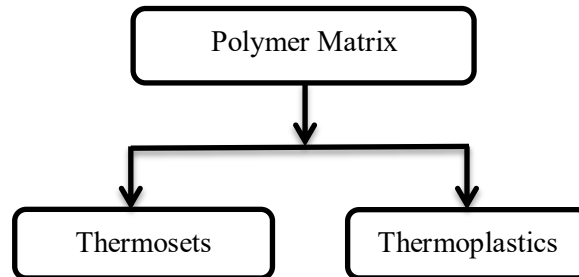


Figure 2.16: Classification of polymer matrix.

- **Thermosets:** Thermoset polymers contain a network of atoms (e.g. carbon) covalently bonded to form a rigid solid structure. Sometimes nitrogen, oxygen, and sulfur atoms are also covalently bonded to aid the thermoset structure formation. Prior curing thermosets are viscous or soft solid and after curing the polymer irreversible changes to a hard and rigid solid [112]. During curing, extensive covalent crosslinks are formed between adjacent polymer chains; which bonds the chains together to resist the chain motions at high temperatures. Curing of thermoset polymer is done by a chemical reaction in the presence of heat or radiation, or sometimes both needed. Thermosets may be heated and shaped before curing. However, after curing they become permanently stiff and solid and cannot be reshaped again. Thermosets are generally stronger and more brittle than thermoplastics due to their three-dimensional network of bonds and can be used in high-temperature applications [113]. Widely used thermoset polymers are epoxies, polyester, phenolic polyamides, etc.

- **Thermoplastics:** Thermoplastic is a type of polymer that can be reformed by the application of heat and pressure to different shapes for several times without significant change of its properties [114]. Thermoplastic polymers can be heated to viscous liquid form and when cooled below a certain temperature it freezes to a glassy state. This type of plastic polymers has a high molecular weight chain like long macro-molecules and the molecules are linked to each other with different types of weak bonds such as Van der Waals force in polyethylene (PE), hydrogen bond in polyvinyl alcohol (PVA), aromatic rings stacking in polystyrene, etc. Due to the chain type long molecules and week bonding between the molecules thermoplastics are usually ductile, tough, damage tolerant, and moldable [115].

Thermoplastics are very effective for composite development. Properties such as ease of processing, low cost, good mechanical strength, high resistance to damage and chemical attack make thermoplastics a very potential matrix for composite fabrication. Polyethylene, polypropylene, polyvinyl chloride, polystyrene, nylon, polyamide, etc. are the most common

thermoplastics with a wide range of applications. Thermoplastics are better than thermosets for composite fabrication as thermoplastics do not need curing process, it can be reshaped simply by heating, and it has advantageous properties that are mentioned above [116]. The schematic representation of the structure of thermoplastics and thermosets is given in Figure 2.17.

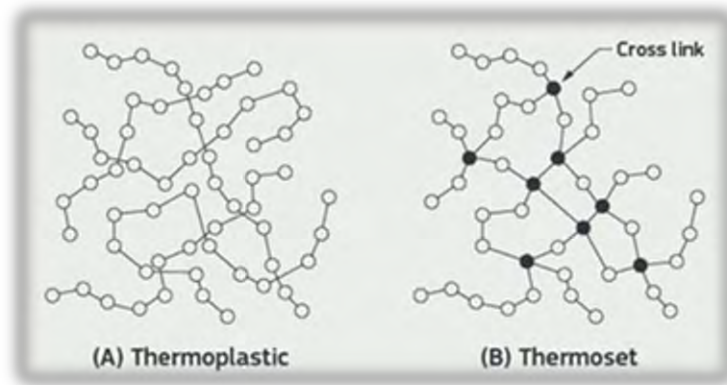


Figure 2.17: Molecular Structure of Thermoplastic and Thermoset Polymers [90]

2.5 Fundamental Concept of Reinforcements for Polymer Matrix

Reinforcements, also known as fillers, are used to modify the properties of matrix material and develop a composite with superior properties. Composites with reinforcements usually exhibit superior properties compared to the properties of the neat polymer. Carbon black, glass and carbon fiber, CNT, natural and synthetic fibers, metallic and natural particulates, etc. are some common examples of reinforcements used in reinforced thermoplastic polymers such as PP, acrylonitrile butadiene styrene (ABS), polystyrene, polyvinyl chloride, etc. [100-105]. Reinforcements usually have superior mechanical, thermal and/or electrical properties than that of the polymer resin. Reinforcing compounds tend to restrain movement of the polymeric matrix around them and the matrix transfers some of the applied stress to the reinforcing materials, thus the composite develops improved mechanical properties. Reinforcements with enhanced thermal stability and electrical conductivity (e.g. CNT, graphene, biochar, etc.) have the potentiality to improve the thermal and electrical properties of a polymeric composite [1,2,81].

2.6 Reinforcing Theories

To fabricate a new polymer composite understanding the reinforcing mechanisms is very important. There are several theories regarding reinforcing mechanisms of the particle reinforced polymer composites such as interfacial adhesion reinforcing theory, filler inducing crystallization reinforcing theory, filler frame reinforcing theory, and synergistic reinforcing effect theory [117]. Theories behind reinforcing thermoplastic polymer composites with particles have been described in the next section.

2.6.1 Interfacial Adhesion Reinforcing Theory

When polymeric composites are bearing load, the stresses taken by the matrix and reinforcement materials are transferred through the interface between them, especially for the particulate reinforced polymer composites. Thus, interfacial adhesion reinforcing theory believes that the reinforcement of the particulates to the polymer composites depend upon the increase of the interfacial adhesion strength. In other words, the higher the interfacial adhesion strength, the better is the reinforcing effect of the polymer composites. Under the same interfacial adhesion strength, the larger the interfacial area of the particles, the better is the reinforcing effect of the polymer composites [118].

2.6.2 Filler Inducing Crystallization Reinforcing Theory

Researchers found that particulate reinforcements added to the polymer will play heterogeneous nucleation [119,120]. Therefore, the crystallization properties of the crystalline polymer will be changed after it is reinforced with particles. For example, the super-cooled degree of particle reinforced polymer composites will increase with an increase of particles, but it is lower than that of unfilled resin, this indicates that the addition of particles will make the crystallization of filled polymer easy. When the polymer is filled with a low amount of particles, the super-cooled degree is low. This illustrates that as the polymer is reinforced with small quantity particles, the melt is easy to form crystal nucleus during cooling, the crystallization accelerating effect of the polymer is maximum in this case, and the crystallization speed is the fastest. The crystallization speed of the composite decreases correspondingly with raising the filler content gradually, but the crystallization speed is faster than the unfilled polymer [120].

Generally, it is believed that the increase of crystallinity is beneficial to enhance the rigidity or to improve the strength of polymeric materials. As a result, the filler inducing crystallization reinforcing theory of particulate-reinforced polymer composites may be described as follows: when crystal polymer is reinforced with particles, the filler particles take the effect of heterogeneous nucleation in the matrix; the crystallinity is increased correspondingly, resulting in the increase of the rigidity and strength of the composite systems. On the other hand, even though particles, as nucleating agent may improve crystal structure and may enhance crystallization degree, at the same time, due to the interaction between particles and polymer molecular chains, restricts the macromolecules movement, the molecular chains participated in the crystallization decrease relevantly, leading to reduction of the crystallinity of the composites. Hence, this kind of the effects of reinforcement and increasing rigidity takes place usually in the case of the polymer composites filled with a low concentration of particles.

The above discussion indicates that the reinforcement of polymer composites is closely related to the crystallinity of the polymer matrix, while the crystallization degree of the matrix resin depends upon the competition between the reinforcement particles taking the effect of

heterogeneous nucleation in the matrix and the interaction between the matrix and particles such as polymer molecular chains restricting the macromolecules movement.

2.6.3 Filler Frame Reinforcing Theory

The theory of filler frame reinforcing and increasing rigidity in particle reinforced polymer composites is similar to the theory of filler frame reinforcing and enhancing the rigidity of the sandstone in concrete. Usually, the modulus of particulates is higher or much higher than that of resins [121]. When the polymer is reinforced with particles, the fillers will limit the movement of macromolecular chains to a certain extent, leading to a rise of the deformation difficulty of the composite material. When the composite is under loading, the stresses are shared and transferred by the matrix and filler, enhancing the rigidity and strength of the polymer composite. In other words, particles in the matrix play the role of cytoskeleton.

Liang and Wu [122] studied the influence of the surface treatment of glass beads (GB) on the tensile elastic modulus of the reinforced PP composites and observed that the relative Young's modulus of the PP-GB composites increased but not linearly with the GB volume fraction, even though for the GB with untreated surface filled PP composite system.

2.6.4 Synergistic Reinforcing Effect Theory

The studies on the reinforcing theories are relatively weaker than the toughening theories of the particle reinforced polymer composites. Hence, there have been fewer comprehensive descriptions of reinforcing mechanisms so far, even though various explanations for reinforcing mechanisms of the particulate reinforced polymer composites have been proposed. On the basis of the previous studies, the above three reinforcing theories are induced. That is, interfacial adhesion reinforcing theory, filler inducing crystallization reinforcing theory and filler frame reinforcing theory. These reinforcing theories may explain better the reinforcing mechanisms of the particulate reinforced polymer composites under given conditions.

However, the factors affecting the reinforcing mechanisms of the particle reinforced polymer composites are complex. In fact, the reinforcing mechanisms of the particle reinforced polymer composites are usually not singular, while the reinforcing mechanisms are possibly twice even triple. That means, the reinforcing effects may be provided by multiple factors, this is the synergistic reinforcing effect theory [117]. For example, in spherical particle-filled polymer composites, the interfacial adhesion between the filler and matrix is relatively weak, and the major reinforcing mechanisms should be the results of joint actions by the filler inducing crystallization reinforcing effect and the filler frame reinforcing effect. Thus, the interfacial adhesion reinforcing mechanism might be less important in this case. For polymer composites filled with block (sheet) particles or column (needle) particles, the interfacial adhesion between the particles and resin matrix is relatively strong. The major reinforcing mechanisms, in this case, should be the results of joint actions by the filler inducing crystallization reinforcing effect

and interfacial adhesion reinforcing effect, while the filler frame reinforcing mechanism might be of subordinate importance. It is, therefore, usually difficult to explain perfectly the reinforcing effect of particles to polymer materials only using singular reinforcing theory in fact. In other words, the above reinforcing theories can be combined according to the specific situation including composite type, so as to interpret more accurately the reinforcing mechanisms of the composite system.

2.7 Particle Reinforced Polymeric Composites

Polymeric composites are prepared by reinforcing the polymer matrix with suitable reinforcements (particles or fibers). The nature of the matrix varies from a synthetic to a natural polymer depending on the application requirements. On the other hand, the reinforcing materials are either particles or fibers from synthetic or natural sources. Generally, mechanical strength is a prime index of the performance of the material and it is very important for the materials used in structural applications such as machine frames and automobile bumpers. Mechanical properties mainly include tensile strength, compression strength, flexural strength, tear strength, etc. Preferable mechanical strength of a polymeric composite is usually as high as possible under the premise of meeting the use function. Polymers reinforced with particulates including rigid organic and inorganic particles, which is an important modification method of polymeric composites [123]. Factors that affect the mechanical properties of particle reinforced polymer composites are quite complicated [124]. The reinforcement of polymer composites is, therefore, one of the vital objectives of polymer modification.

There are several factors that affect the properties of particle reinforced polymer composites, such as the properties of the reinforcement and the polymer resin and the compatibility between them, the dispersion and distribution of the particles in the matrix, the reinforcing particles shape, size, surface morphology, and concentration, as well as the interfacial status [125]. Researchers found that the rigid reinforcing particles have the potentiality to increase not only the rigidity but also the strength of the composite. They also found that the reinforcing effect of particle reinforced polymer composites depends, to a great extent, on the ability to reinforce particles to modify the polymer matrix to form the appropriate aggregation structure, such as the crystallization degree and the grain size. Moreover, the crystallization degree of the composites increases with increasing the reinforcing particle content, especially for crystalline polymers, and the mechanical properties such as Young's modulus increase correspondingly in this case [124]. Thus it is believed that the reinforcing particles enhance the heterogeneous nucleation in the matrix resin, promoting the crystallization capability of the particle reinforced systems. This indicates that the addition of particle reinforcements into the polymer could change the structure of the polymeric composites. Besides, the reinforcing particles will impede the movement of the macromolecular chains of the matrix to a certain extent. Such restriction to chain movement is beneficial to increase the mechanical strength and rigidity of the reinforced composite system. Furthermore, the reinforcing particles may also develop a framework in the matrix, which has the

potentiality to improve not only the mechanical properties but also the thermal stability and the electrical conductivity of the particle reinforced composite [117].

2.7.1 Biochar Reinforced Thermoplastic Polymer Composites

Due to environmental safety and future scarcity, increasing demand for new eco-friendly products has stimulated the interest of both academic and industrial research to investigate renewable and bio-based materials, with the aim to develop a more sustainable manufacturing approach [126]. Correspondingly, the use of organic natural fibers and particles for the production of polymer-based composites has received great attention [11,14]; particularly, bio-derived materials have been utilized in several polymeric composites, showing the potential to substitute the traditionally used fillers in polymer composite systems, also because of their advantageous price–volume–performance relationships [126]. However, due to the low thermal stability of natural fibers, their use in polymer-based composites has been often problematic. Moreover, the degradation of bio-derived fibers occurs in the temperature range typical to that of polymer processing, and this feature limits the choice of the polymer matrix and significantly limits the successful fabrication of the composites [127]. In addition, natural fibers show poor compatibility with most polymers, therefore chemical and/or physical treatments of their surface are often mandatory to enhance the polymer/reinforcement interfacial interaction [17,127]. A further drawback of bio-derived fibers is the high hydrophobicity which restricts their incorporation in moisture sensitive polymeric matrices [127]. A promising alternative to the traditional natural fibers is biochar.

Biochar (BC) is a carbon-rich inexpensive material derived from the thermochemical decomposition of lignocellulosic biomass in the absence or limited supply of oxygen. In comparison with other types of carbonaceous materials, BC emerges as a new cost-effective and environmentally friendly carbon material with great potential of application in various fields. In recent years, there has been a considerable shift in research interest toward the utilization of BC in applications, such as carbon fuel cells, energy storage, and catalysis, along with its traditional uses as an adsorbent and soil amendment agent to promote carbon sequestration [133]. The use of biochar has found plenty of applications due to its interesting mechanical and temperature-related properties. Usually, costly carbon and glass fillers (e.g., carbon fiber, carbon nanotube, graphene, glass fiber) are used to increase mechanical properties of reinforced plastics [130] but are experiencing decrease popularity for real scale production. This is because of the high cost and problems correlated to low yields of productive processes [126]. Thus, low-cost waste and bio-derived carbon fillers like biochar have become very attractive. Tuneability of the BC properties represents an interesting route to improve the mechanical exploitation of thermoplastic composites [130, 131]. Arrigo et al. [127] demonstrated the beneficial effect of spent coffee biochar on the thermal and mechanical properties of polyethylene composites. Furthermore, the enhanced electrical conductivity of polymeric composites by biochar addition was reported [18]. On the other hand, rice husk derived biochar was found to improve the thermal stability of

polyolefin composites [128]. Rice husk is abundant and cheap. Application of rice husk biochar as a reinforcing agent in the polymer matrix is a smart choice due to its high surface area, porosity, and renewability [128].

The consumption of reinforced plastic composites has been growing rapidly and accordingly the carbon-based filler composites as well. Production of petro-based carbon materials needs a tedious synthetic process and is not environmentally or economically viable. Efforts have been made to explore various renewable carbon resources as the feedstock that is cost-effective, environment-friendly, and are abundant in nature. According to recent researches, there is a scope for the successful application of biochar in thermoplastic composites due to its high carbon content, porous structure, large surface area, which could facilitate the physical bonding with the polymer matrix. Biochar has been successfully incorporated with different types of polymer matrices for improving their mechanical, electrical and thermal properties [14].

2.8 Review of Related Research Works

Application of biochar as reinforcement to produce bio-based composites is currently getting much attention due to its low cost and favorable properties such as high thermal stability, excellent electric conductivity, and large surface area compared to natural fibers [127]. Biochar is being incorporated in different polymers to develop composites with improved mechanical, electrical and thermal properties. Significant research works in the field of biochar reinforced thermoplastic composite is presented below in Table 2.5.

Table 2.5: Remarkable studies on biochar reinforced polymeric composites

Polymer Matrix	Reinforcement	Observations	Reference
High-density polyethylene (HDPE)	Poplar biochar	Poplar biochar addition increased flexural strength, reduced impact toughness, and promoted early crystallization of the composite	[126]
High-density polyethylene (HDPE)	Spent coffee ground biochar	Biochar improved the thermo-oxidative stability and modified the melting enthalpy of the composite	[127]
High-density polyethylene (HDPE)	Rice husk biochar	The developed composite exhibited improved bending and tensile strength than wood-plastic composites	[17]
Starch	Rice husk biochar	Rice husk biochar addition improved the mechanical and thermal properties of the composite	[128]
Polyester resin	Rice husk biochar	Impact strength and dielectric constant of the composite increased but tensile strength reduced	[11]
epoxy resin	Coffee waste biochar	Developed composite exhibited better electric conductivity and improved	[129]

		mechanical performances	
epoxy resin	Olive pruning biochar	Tuneability of the mechanical properties of composites according to the thermal history of the biochar	[130]
Styrene-butadiene rubber (SBR)	Waste lignin biochar	Composite exhibited improved tensile strength and elongation at break	[131]
Poly (trimethylene terephthalate) (PTT)	Lignin residue biochar	weight reduction coupled with increased heat deflection temperature and flexural strength of the composite was reported	[132]
Polypropylene (PP)	Date palm biochar	PP biochar composite exhibited improved thermal stability and stiffness	[133]
Polypropylene (PP)	Date palm biochar	Biochar incorporation in PP enhanced tensile strength and electrical conductivity but reduced the crystallinity of the composite	[14]
Polypropylene (PP)	Waste pinewood biochar	Biochar in PP composites was found to improve mechanical strength and thermal stability	[2]
Polypropylene (PP)	Landfill pinewood biochar	Developed composite showed improved tensile and flexural properties with a relatively low peak heat release rate	[134]
Polypropylene (PP)	Pinewood biochar	Biochar addition increased presence of free radicals, thermal conductivity and crystallization temperature of the composite but did not disrupt the crystal structure	[135]
Polyvinylidene fluoride (PVdF)	Wood biochar	Prepared biochar composite membranes have high mechanical strength and a porous structure with promising adsorption capacities	[136]
Polyvinyl alcohol (PVA)	Mixed hardwood biochar	Addition of biochar promoted electrical conductivity, thermal decomposition temperature and tensile modulus of the PVA composites	[18]

Accordingly, Zhang et al. [126] prepared poplar biochar by pyrolyzing poplar wood in a muffle furnace at different temperatures and heating rate of 15⁰C/min. Poplar biochar was mixed with high-density polyethylene via blending and extruding to form a poplar biochar-HDPE composite. The developed composite exhibited enhanced flexural strength due to the interlocking structure between poplar biochar and HDPE. Poplar biochar addition found to decrease the impact strength of the composite but did not affect the microcrystalline structure of HDPE. HDPE composite was also developed by Arrigo et al. [127] by incorporating spent coffee ground biochar in HDPE by melt compounding method. Biochar was prepared from waste coffee powder via pyrolysis in a tubular furnace at a heating rate of 5⁰C/min and heating up to 700⁰C. The thermo-oxidative stability of the composite was improved and polymer crystallinity was

decreased by the biochar addition. Zhang et al. [17] in another study reinforced HDPE with rice husk biochar (RHB). Biochar was prepared by fast pyrolysis of rice husk in a fluidized bed reactor at 700°C and was mixed with HDPE via the extrusion method. HB reinforced HDPE composites showed higher bending, tensile, and impact strength than that of wood-plastic composites and rice husk biochar reduced the crystallization rate of HDPE. The researchers concluded that the RHB is feasible to reinforce thermoplastic polymers such as HDPE. RHB was investigated by other researchers also as reinforcement in different polymers. Correspondingly, Amin et al. [128] reinforced *Tacca leontopetaloides* starch with RHB and reported significant improvement in mechanical and thermal properties. Especially, tensile strength and thermal degradation temperature were improved. On the other hand, Richard et al. [11] reinforced polyester resin with RHB. Biochar was prepared by pyrolyzing rice husk in an electric muffle furnace at 450°C and the obtained rice husk derived biochar was mixed with polyester resin by resin transfer molding method. It was reported that the impact strength and dielectric constant of the RHB –polyester composite increased by 77.5% and 7% respectively due to RHB addition compared to pure resin. However, a decrease in tensile strength was also reported by the researchers.

Coffee waste biochar was again utilized by Giorcelli et al. [129] to reinforce epoxy resin polymer. The researchers reported that, even though coffee biochar had less conductivity compared with carbon black in powder form, but it created composites with better conductivity in comparison with carbon black composites. The mechanical properties of the composite were also improved with respect to neat epoxy resin. Thus the researchers concluded that considering the sustainability of biochar production, biochar-derived carbon could be a sound replacement for oil-derived carbon fillers. Bartoli et al. [130] also reinforced epoxy resin but with different biochar. They prepared biochar from olive pruning by pyrolysis in a tubular furnace in N₂ atmosphere. It was found that the mechanical properties of the olive pruning biochar-epoxy resin composites could be tuned according to the thermal history of the biochar applied. Jiang et al. [131] investigated a rather different composite, where they reinforced styrene-butadiene rubber (SBR) with waste lignin biochar and reported increased tensile strength and elongation at break of the rubber composite. Lignin biochar was also utilized by Myllytie et al. [132] to reinforce poly-trimethylene terephthalate (PTT) and their study revealed that weight reduction coupled with increased heat deflection temperature and flexural strength of the composite was achieved by biochar incorporation.

Polypropylene (PP) reinforced with date palm biochar composite was developed by Elnour et al. [133] to study the effect of pyrolysis conditions on both the biochar and composite. They obtained biochar from lignocellulosic biomass of date palms via slow pyrolysis carried out at different temperatures with a heating rate of 10⁰C/min for 2 h and the biochar was mixed with PP by melt mixing process followed by injection molding. The developed date palm biochar reinforced PP composites showed improved thermal stability and the stiffness was also increased. However tensile strength and ductility of the composite remained unaffected and

biochar acting as a nucleating agent enhanced the overall crystallization process. Thus, the researchers concluded that biochar can be used as a potential reinforcing material in PP and other polymeric composite systems. Date palm biochar reinforced PP composite was also studied by Poulose et al. [14] to investigate the electrical, mechanical, thermal and rheological properties of the composite. The electrical conductivity of date palm biochar PP composite was increased by four orders of magnitudes on increasing the biochar content from 0 to 15% w/w. The tensile modulus of the composites was also improved when compared with neat PP. On the other hand, Das et al. [2,134,135] in a series of study investigated different aspects of biochar/PP composites. Das et al. [2] in one study developed waste pinewood biochar reinforced PP composite and investigated the mechanical and flammability characteristics of the bio-composite. The fabricated biochar/PP bio-composites showed improved flexural strength and thermal stability when compared with neat PP. Das et al. [134] in a second study, added four types of waste biomass (rice husk, coffee husk, coarse wool fiber, and landfill pine wood) with biochar and polypropylene (PP) to manufacture bio-composites. It was found that wood base biomass incorporated biochar/PP bio-composites offer good mechanical and thermal properties. In another study, Das et al. [135] characterized the chemical and thermal properties of biochar incorporated wood/PP composites. The study revealed that, biochar addition reduced surface roughness of the composite but did not affect the crystal structure of PP and higher amounts of biochar incorporation promoted the thermal conductivity of the composites. A. Ghaffar et al. [136] also used wood biochar to fabricate biochar/polymer composite but with a different polymer, which is polyvinylidene fluoride (PVdF). Composite membrane fabricated by the researchers exhibited high mechanical strength and a porous structure with promising adsorption capacities. Finally, Nan et al. [18] investigated the composites prepared from polyvinyl alcohol (PVA) and mixed hardwood biochar and reported that the addition of biochar enhanced thermal decomposition temperature, electrical conductivity, and tensile modulus of the PVA composites.

2.9 Viability of Rice Husk Pyrolyzed Biochar Reinforced PP Composite Fabrication

In order to reduce the dependence on fossil resources, two countermeasures are commonly adopted by the researchers. The first one is to explore new renewable materials that have the potentiality to replace petroleum-based products, and the second is to develop a viable pathway of recycling and reusing industrial, agricultural, and domestic wastes [131]. Especially, the disposal of solid wastes from different sources is a challenging issue for many nations because of the lack of high-tech treatment infrastructure to transform waste into high-value products. The landfill and incineration of solid wastes are mainly adopted worldwide. However, soil and air contaminations are generated from the degradation and burning of these solid wastes. Therefore, converting those wastes into usable and renewable products to replace current petroleum-based products is a win-win strategy.

Waste biomass sources can be processed via the pyrolysis technique for biochar and other value-added production. Paddy rice is among the highest cultivated agricultural crop around the world and paddy rice cultivation is increasing almost every year [25] and Bangladesh is the fourth largest milled rice-producing country [26]. The paddy rice cultivation produces a significant amount of byproducts such as rice bran, straw, and rice husk. Usually, straw and rice bran are used for animal feeding. On the other hand, rice husk (RH) is a waste product that has limited uses. An average of 20 kg husk is produced during 100 kg milled rice is processed [28]. The huge amount of rice husk produced during paddy rice processing is poorly utilized, especially in developing countries, causing environmental and health threats [29]. High-quality biochar can be produced from rice husk via the pyrolysis process and it can be utilized as fillers/reinforcements in polymeric composites [17,128]. Biochar has additional advantages than natural fiber as reinforcement in polymer composites since the properties of biochar can be altered by modifying the pyrolysis conditions to obtain biochar with desired properties and to obtain greater compatibility with the polymer matrix than the hydrophilic natural fibers [14]. The thermal stability of the resulting biochar composites has been reported to be higher than the composites with natural fibers such as jute, sisal, flax, hemp, coir, and cotton. Rice husk biochar (RHB) was found to be advantageous for biochar polymer composite synthesis. RHB reinforced polymer composites exhibited improved mechanical, thermal and electrical properties [11,128]. Thus, researchers concluded that the RHB is a potential reinforcing material for thermoplastic polymers [17].

Polypropylene (PP) is a versatile commodity polymer and has excellent processing characteristics. PP has been extensively replacing engineering plastics due to its economic viability, reduced weight, excellent mechanical properties, and ease of processing. Researchers were able to fabricate composites with superior properties by reinforcing PP with biochar prepared from various biomasses [2,14,133] and they concluded that biochar has the potentiality to be a potential reinforcing material for PP systems [133].

As RHB is a potential reinforcement for polymeric composites and PP has excellent interaction with biochar fillers, so RHB reinforced PP composites are expected to possess superior mechanical, thermal and electrical properties. However, to date, there are no vital studies exploring the fabrication and properties of RHB reinforced PP composites. As a consequence, in this report, a comprehensive study on RHB reinforced PP composites fabrication and characterization of their mechanical, thermal and electrical properties have been performed. Successful fabrication of RHB reinforced PP composite will not only develop high-quality material but also ensure the conversion of agricultural waste into value-added products and save the environment.

2.10 Likely Applications of Rice Husk Pyrolyzed Biochar Reinforced PP Composites

Polymers have become the backbone in the day-to-day applications such as food packaging, medical products, household goods, and automobile parts, due to its alluring and long life properties [95]. Especially, in automotive industries, the application of polymers and composites is increasing very rapidly. Tailoring new efficient products to maintaining a sustainable environment is a major challenge to the researchers of this era.

PP is an excellent engineering plastic, with favorable mechanical properties, lightweight due to its low density, and impressive chemical resistance. Particulate reinforced PP composites offer superior qualities and deliver improved chemical, mechanical, environmental, and electrical properties [137]. Reinforcement of RHB in PP is expected to improve the mechanical properties such as impact strength (toughness), flexural strength, and dimensional stability, reduce cost and increase the thermal stability of the composite. The composite with such improved properties is suitable for various engineering applications, especially in automotive industries. The potential applications of the new composite may include vehicle interior component (armrests, pillars, consoles, etc.), air cleaner bodies, heater housings, heater baffles, and other interior component with improved aesthetics, car dashboards, dashboard components, side protective strips, high flexible bumper with high impact, high stiffness, self-supporting bumpers, underbody aerodynamic covers, cowl linkage covers, spoilers, plugs, engine fans, wheelhouse trims, steering wheel coverings, trim panels, radiator headers, air cleaner bodies, etc.

The composite is expected to reduce the application of metal, wood, ceramic, and glass in the automotive industries. Moreover, improved properties of the developed composite might prove to be a better choice for applications in other sectors such as home appliances, and industrial components.

CHAPTER 3
EXPERIMENTAL PROCEDURE

3.1 Materials

3.1.1 Rice Husk (Precursor of Biochar)

Rice husk (RH) used in this research was collected from a local rice mill situated in Dohar near Dhaka of Bangladesh. The husk was of freshly milled BRRI-28 paddy as mentioned by the mill manager. Firstly, the obtained RH was inspected properly for dirt and other unwanted substance removals. Then, it was washed with deionized water three times and dried properly in sunlight. Finally, the dry RH was kept inside an airtight container for future use. The image of the RH used in this work is presented in Figure 3.1

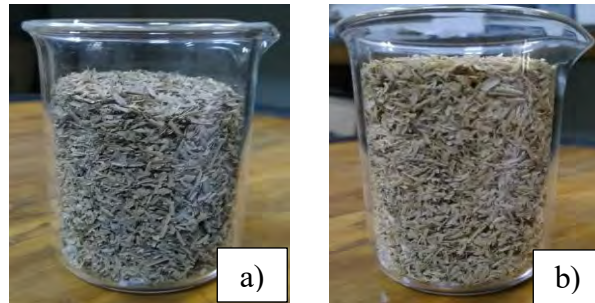


Figure 3.1: Picture of rice husk a) as obtained from the mill, b) washed and dried.

3.1.2 Virgin PP Resin

Polypropylene (PP) as a polymer matrix used in this study was SABIC PP 575P from Saudi Arabia and it was specially developed for producing rigid injection molding articles for general purpose applications. The PP resin was collected locally from Rahim Plastic Center, Dhaka-1211. Typical properties of the PP resin (as provided by Sabic) used in this study are given below in Table 3.1

Table 3.1: Properties of the PP resin used in this study (from Sabic website for SABIC PP 575P).

Properties of PP	Typical Value	Unit	Test Method
Density at 23°C	905	kg/m ³	ASTM D1505
Melt Flow Rate, at 230°C & 2.16kg load	11	g/10 min	ASTM D 1238
Vicat Softening Point	153	°C	ASTM D1525
Heat Deflection Temperature, at 455kPa	98	°C	ASTM D648
Rockwell Hardness	104	HRR	ASTM D785
Notched Izod Impact Strength, at 23°C	22	J/m	ASTM D256
Strength @ Yield	35	MPa	ASTM D 638
Elongation @ Yield	11	%	ISO 527-2 1A

Image of PP sack from which PP resin was collected and granulates of PP is shown below in Figure 3.2

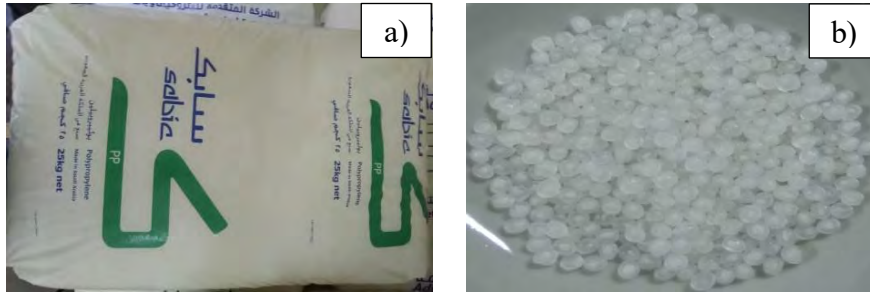


Figure 3.2: Polypropylene (PP) - a) A sack of PP, b) Virgin PP granulates.

3.1.3 Other Accessories

Rice husk derived biochar and polypropylene are the two components used for composite fabrication. However, some other supporting materials were also needed to aid the total process. Silicone mould release spray from Bosny, Thailand was applied for better release of the composite from the mould, acetone from Merck, India was used for mould cleaning, a stainless steel cylindrical pot with perforated lid was used for rice husk pyrolysis, and airtight plastic containers were used for biochar and other materials storage. All these accessories were collected from local market.

3.2 Biochar Preparation

Biochar was prepared from cleaned RH via the slow pyrolysis method. Firstly, the clean RH was dried for 2 hours at 110°C in an oven (Figure 3.3 a). Then, 200 g of dry RH was weighted and kept inside a stainless steel cylindrical pot (Figure 3.3 b) to perform pyrolysis. The pot has a lid with a 1mm hole in the middle to allow gaseous volatile removal during pyrolysis. The slow pyrolysis was performed in an electrical muffle furnace (Figure 3.3 c) supplied by Nabertherm GmbH, Bremen, Germany.

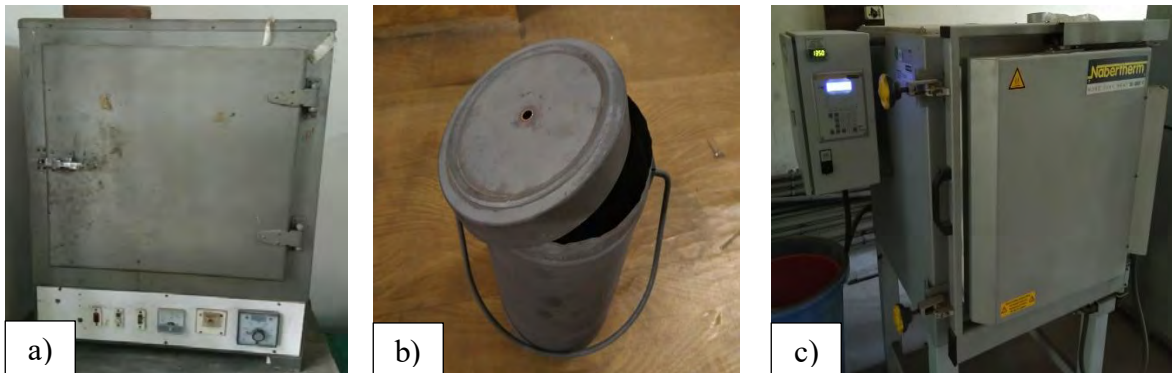


Figure 3.3: a) Oven, b) the pot inside which pyrolysis was performed, c) Muffle Furnace.

RH was pyrolyzed under slow pyrolysis conditions [30]. Accordingly, 200 g RH in the pot covered with lid was slow pyrolyzed in the muffle furnace. Pyrolysis was performed at four different temperatures 400, 550, 700, and 850°C, while the heating rate was 10°C per minute. The temperature of the furnace was kept stable for 1 hour after reaching the target temperature to ensure the completion of the slow pyrolysis process. After pyrolysis for an hour, the biochar was allowed to cool down inside the furnace overnight. Figure 3.4 is the schematic representation of the slow pyrolysis process performed to produce RHB.

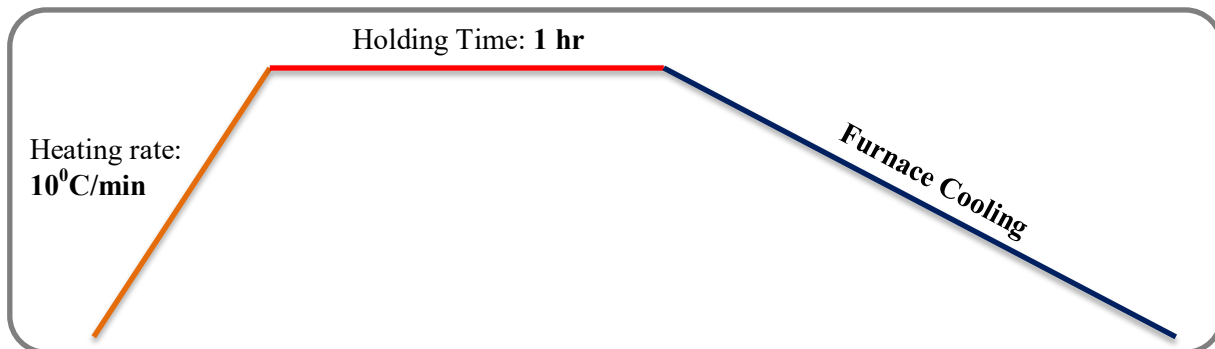


Figure 3.4: Slow pyrolysis of rice husk.

The produced RHB was taken out next day and subjected to grinding by a porcelain mortar and pestle to obtain fine powder of RHB. The grinding was done by hand for 2 hours with 10 minutes interval after every 30 minutes. Figure 3.5 presents RH before and after slow pyrolysis and the hand grinding RHB by a porcelain mortar and pestle.



Figure 3.5: a) Dry RH before pyrolysis, b) rice husk biochar (RHB)
c) Grinding of RHB

After completion of the grinding process, the RHB fine powder was stored inside an airtight plastic jar. Following the process mentioned above, biochar prepared at four different temperatures were ground and stored in four different jars for characterization and application in the composites. The jars were labeled as RHB400, RHB550, RHB700, and RHB850, where

RHB stands for rice husk biochar and the digits reveal the pyrolysis temperature of the RH. RHB stored in labeled plastic jars is shown below in Figure 3.6.



Figure 3.6: RHB fine powder stored in labeled jars.

The schematic presentation of the entire rice husk derived biochar powder production process is given in Figure 3.7 below.

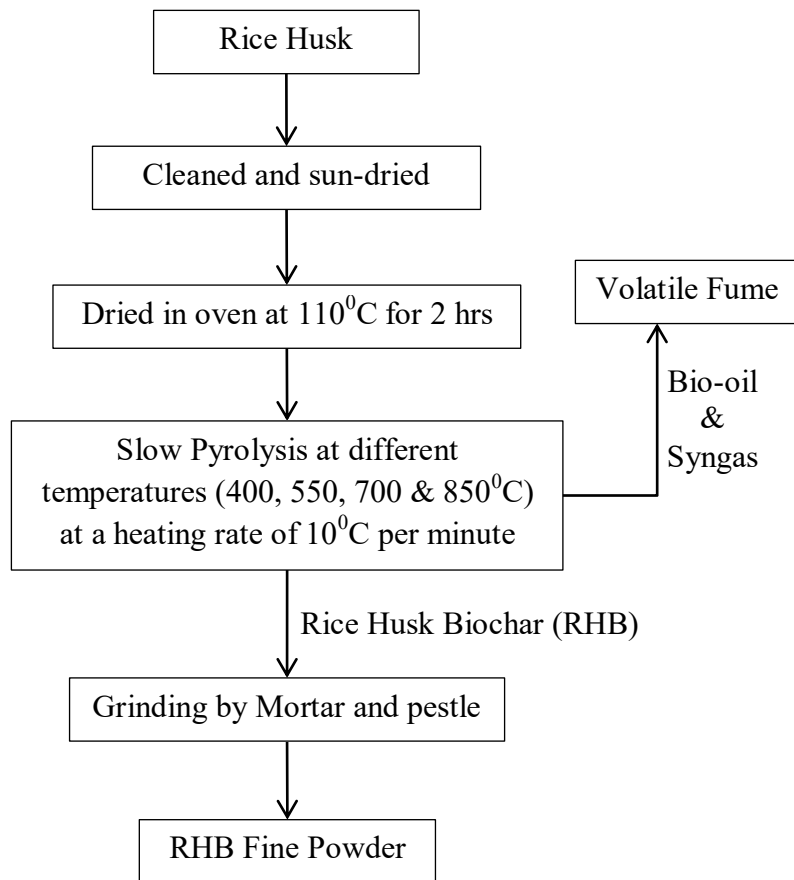


Figure 3.7: Flowchart of RHB powder preparation.

3.3 Composite Fabrication

The components of the composites were mixed together by melt blending machine and then formed into composite sheets using a hot press. A total of eight composites were developed in this study. 10 wt% and 15 wt% of each four biochar were mixed with PP individually and thus, eight different composite samples were fabricated. Table 3.2 demonstrates the name of the composites and the wt% of constituents present in the composites.

Table 3.2: Name and constituents of the developed composites

Biochar Used	RHB Content (wt%)	PP resin Content (wt%)	Composite sample Name
RHB400	10	90	PP-10RHB-400
	15	85	PP-15RHB-400
RHB550	10	90	PP-10RHB-550
	15	85	PP-15RHB-550
RHB700	10	90	PP-10RHB-700
	15	85	PP-15RHB-700
RHB850	10	90	PP-10RHB-850
	15	85	PP-15RHB-850

Details of the melt blending and hot pressing during the composites fabrication process are being described below in section 3.3.1 and 3.3.2.

3.3.1 Melt Blending

For melt blending of RHB powder with PP, an internal mixer (Figure 3.8) was used, which is a small polymer melting and mixing unit designed to meet the purpose of scientific research works. The advantage of this internal mixer unit is that it can mix the polymeric materials uniformly within a controlled temperature environment. The controllable temperature range of this unit is between 0 and 450°C, while the rotational speed reaches up to 60 rpm.



Figure 3.8: Internal mixer unit.

Prior melt blending, required amounts of PP resin and RHB powder were weighted by a precision balance and dried in an oven for 2 hrs at 110°C. Then the dried RHB and PP were

transferred inside the preheated internal mixer chamber at 170⁰C and the mixing was started at 35 rpm for 10 minutes. After 10 minutes the temperature of the internal mixer was raised to 190⁰C and the second mixing session of another 10 minutes at 35 rpm was done. Mixing the composite in two seasons was found to improve the dispersion of RHB particles into the PP matrix. Finally, the mixed composite was brought out from the mixing chamber and subjected to the next processing step. Figure 3.9 shows a composite sample after mixing when it was not hot-pressed yet.



Figure 3.9: Composite sample after melt blending.

3.3.2 Hot Press Molding

The identical shape is important to compare the properties of the developed composites. To mould the composites into identical sheet form (150 mm × 150 mm × 2 mm), hot molten composite as obtained from the internal mixer was transferred into an aluminium mold (Figure 3.10 a) and hot pressed in Fontijne hydraulic compression hot press machine (Figure 3.10 b). The Fontijne hydraulic hot press has a fixed upper platen and movable lower platen with induction coil type heating system and water supply system for cooling. The mold was placed between the platens and a pressure of 30 kN was applied. Initially, the temperature was raised to 170⁰C and kept there for 5 minutes. Then the temperature was increased to 190⁰C and kept steady for another 5 minutes. Then the composite sample was allowed to solidify by turning the water supply system at the same pressure. After cooling pressure was released, the composite sheet was taken out and stored in a sealed plastic bag for characterization.

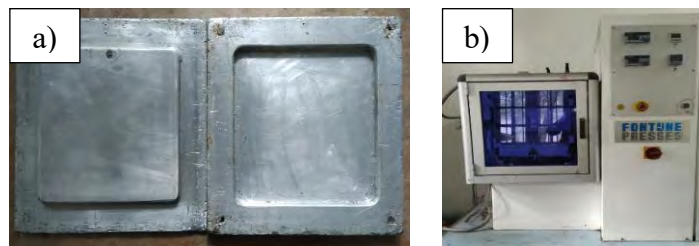


Figure 3.10: Hot press molding a) aluminium mold, b) Fontijne hydraulic hot press machine.

It is important to mention that the aluminium mold was cleaned properly and silicon spray was applied to ensure the easy release of composite from the mold. The above mentioned process was applied to fabricate composite sheets of all eight samples. Finally, a 100% PP polymer sheet was

also prepared by the same procedure and named 100PP to compare the properties of developed composites with PP sheet. Figure 3.11 presents the image of the developed PP and composite sheet.

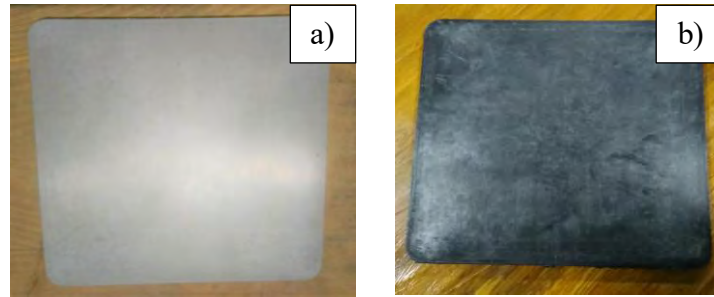


Figure 3.11: Hot pressed sheet of a) PP, b) RHB reinforced PP composite.

The schematic illustration of the composite fabrication process is presented below in Figure 3.12.

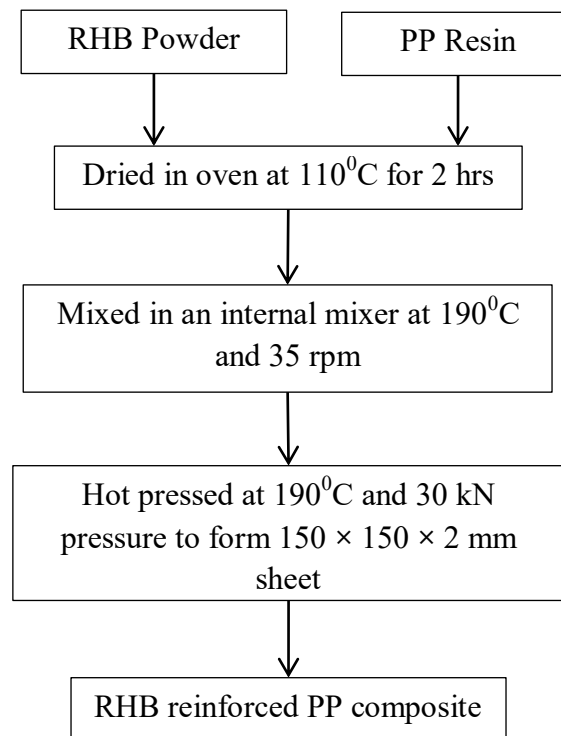


Figure 3.12: Flowchart of RHB reinforced PP composite preparation.

3.4 Characterization of RHB

Properties of the RHB were characterized to better understand the effect of pyrolysis temperature on the char quality and its effect on composites.

3.4.1 Biochar Yield

The yield of rice husk derived biochar was determined from the initial weight of the dry feedstock and the final weight of the biochar sample [138]. The calculation is as follows:

$$Yield(\%) = \frac{\text{Mass of RHB (g)}}{\text{Oven dry mass of feedstock (g)}} \times 100\%$$

3.4.2 Proximate Analysis and pH

The proximate analysis was performed to measure volatile matter (VM) and ash content. The contents of VM and ash were determined using the ASTM D3172 – 13 method [139]. VM content was determined as weight loss after heating a certain amount of moisture-free RHB in a covered crucible to 950⁰C and holding for 7 min. The calculation is as follows:

$$\% VM = \frac{\text{Loss of weight}}{\text{Weight of RHB}} \times 100\%$$

Ash content was determined as weight loss after combustion at 750⁰C for 6 hr with no ceramic cap. The calculation is as follows:

$$\% Ash = \frac{\text{Weight of residue}}{\text{Weight of RHB}} \times 100\%$$

Fixed C content was calculated by the following equation:

$$\text{Fixed Carbon \%} = 100\% - (\% Ash + \% VM)$$

The RHB sample was soaked in distilled water at a 1:5 biochar/water ratio and stirred for 30 minutes at room temperature [138]. The pH was observed using a digital pH meter (HANNA Microprocessor pH meter, model: pH 211). The pH measurement process of RHB is presented below in figure 3.13.

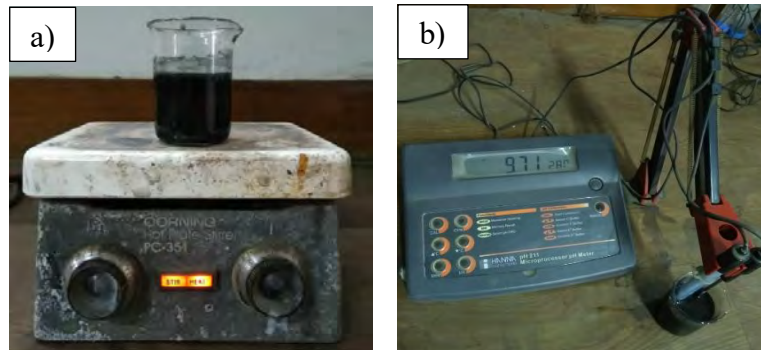


Figure 3.13: pH test- a) Solution preparation, b) pH measurement of RHB.

3.4.3 Morphological Characterization

3.4.3.1 Optical Microscopy

Optical microscopy is a very useful tool to examine the morphology and surface structure of materials. The technique basically developed in metallography was found to be useful for examining metals, ceramics, polymers, and other organic/inorganic solid materials. Clean RH, pyrolyzed RHB and RHB powder was firstly examined by the means of an optical microscope (OPTIKA microscopes, Italy) as presented in Figure 3.14. The micrographs are discussed in the Results and Discussion section.



Figure 3.14: Optical microscope

3.4.3.2 Scanning Electron Microscopy (SEM)

The morphology and microstructure of RHB were also characterized by using Scanning Electron Microscope (ZEISS, Germany) at the acceleration voltage of 5.00 kV. Prior to scanning, RHB was placed on a disc and held in place using a double-sided carbon tape, then coated with gold particles via sputtering technique. Since RHB is not highly conductive, the thin gold coating helps to avoid sample charging. The model of the microscope was EVO 18 Research.

3.4.4 Energy Dispersive X-Ray (EDX) Analysis

Surface element analysis of RHB was conducted simultaneously with the SEM at the same surface locations using energy dispersive X-ray (EDX) analysis. The Zeiss, EVO 18 Research scanning electron microscope was coupled with an EDX system (ZEISS Smart EDX). The EDX can provide rapid qualitative, or with adequate standards, semi-quantitative analysis of elemental composition with a sampling depth of 1-2 microns [44].

3.4.5 Fourier Transform Infrared Spectroscopy (FTIR)

Fourier transform infrared (FTIR) analysis of the RHB samples was carried out to characterize the surface organic functional groups. To obtain the observable FTIR spectra, RHB was ground and mixed with KBr to 0.1 wt.% and then pressed into pellets. The spectra of the samples were measured using a Cary 630 FTIR spectrometer from Agilent Technologies (Figure 3.15). The FT-IR spectra of the samples were recorded between 650 and 4000 cm^{-1} , using 32 scans at a resolution of 8 cm^{-1} .



Figure 3.15: Cary 630 FTIR spectrometer.

3.4.6 Thermogravimetric Analysis (TGA)

The thermal stability evaluation of the RHB samples was performed by a thermogravimetric analyzer (TA instrument TGA Q50, model: V6.4 Build 193). Approximately 20 mg of biochar was weighed into an alumina crucible and was subjected to a thermogravimetric analysis from room temperature to 800 $^{\circ}\text{C}$ at the heating rate of 10 $^{\circ}\text{C min}^{-1}$ and in a nitrogen flow rate of 50 $\text{mL}\cdot\text{min}^{-1}$. TGA with DTG (Derivative thermogravimetry) curves of RHB samples were obtained to better understand the thermal degradation and number of degradation steps.

3.4.7 Differential Scanning Calorimetry (DSC)

Further thermal analysis of RHB was done by differential scanning calorimetry (DSC). DSC analysis of RHB was performed with a DSC131 EVO analyzer (SETARAM Instrumentation). About 20 mg of the ground and dried RHB sample in an aluminum pan was heated from room temperature to 600 $^{\circ}\text{C}$ and at the heating rate of 10 $^{\circ}\text{C min}^{-1}$. The heat flow to or from the sample was monitored as a function of temperature during the heating. N_2 with a flow rate of 50 mL min^{-1} was used as flushing gas.

3.5 Characterization and Testing of RHB Reinforced PP Composite

The fabricated RHB reinforced PP composite sheets were tested and characterized according to test methods defined by the world's reputed standards developing organizations, such as the American Society for Testing and Materials (ASTM), The International Organization for Standardization (ISO), etc. A standard testing method makes comparing a certain property present in different materials more meaningful and the use of similar language to communicate possible.

3.5.1 Mechanical Properties Test

When a new material is developed, usually mechanical properties are evaluated first to analyze the material's specifications. Mechanical properties such as tensile strength, flexural strength, and hardness of the developed composites were tested according to standard test methods as they were described below in consecutive sections and evaluation of properties by comparing with PP sheet was also performed.

3.5.1.1 Tensile Test

Tensile properties (i.e. strength, modulus, and elongation) data are very useful to compare different types of plastic materials. Tensile tests were carried out according to ASTM D 638-03 [140] using a universal testing machine (Instron UTM machine, USA, max. capacity 50 kN). The crosshead speed of the machine was 5 mm/min and tests were continued until tensile failure. Tensile test specimens were cut from the fabricated composite sheets according to ASTM D 638-03 instructions (Figure 3.16).

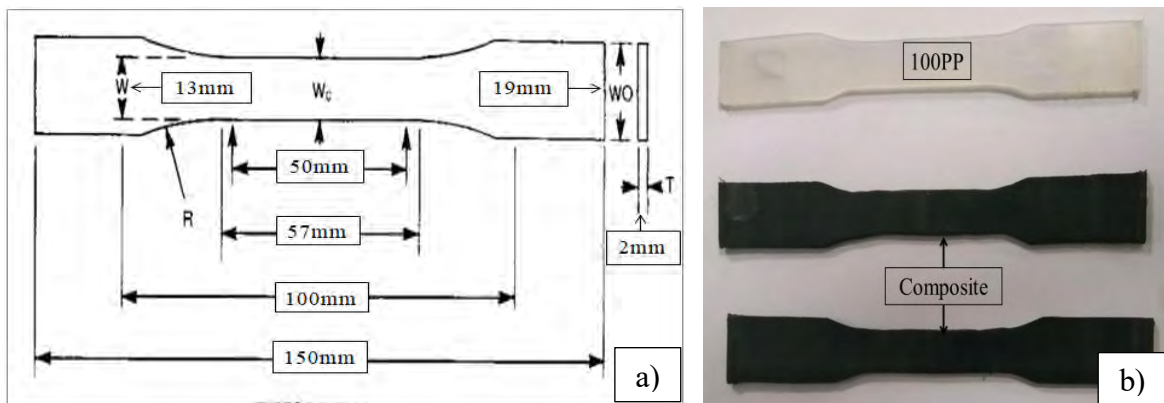


Figure 3.16: Tensile test specimens a) specimen measurements, b) prepared specimens

The prepared specimens were subjected to the tensile test according to followed steps:

- I. The thickness and width of the gauge length of the specimen were measured.
- II. The specimen was placed in the grips of the UTM machine.

- III. The crosshead speed was set to 5 mm/min and continued until the specimen failed under tension.
- IV. Obtained data was recorded and the ultimate tensile strength (σ) was calculated using the following formula:

$$\text{Ultimate Tensile Strength}(\sigma) = \frac{\text{Maximum Load (F in Newton)}}{\text{Cross Section Area (A in mm}^2\text{)}} \text{ MPa}$$

The tensile strength of the developed PP sheet was also measured by the same technique.

3.5.1.2 Flexural Test

The flexural test is a measurement of the materials stiffness or resistance to bending when a force is applied perpendicular to the long edge of a sample. The three-point method and the four-point method are the two basic test methods. The three-point flexural test was performed on the composite samples following the ASTM D 790 – 03 standard test method [141]. Accordingly, the support span shall be 16 times the thickness of the beam. Specimens that have 3.2 mm or less thickness shall be 12.7 mm in width. As the thickness of the composite sheets was 2 mm, so the support span distance was 32 mm and the specimen width was 12.7 mm as shown in Figure 3.17.

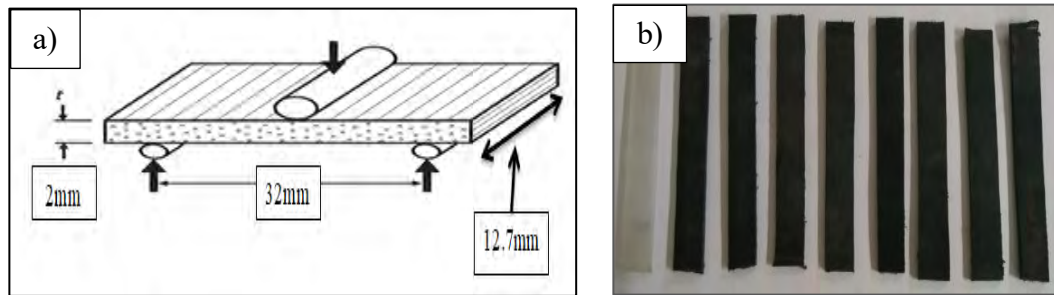


Figure 3.17: Flexural test specimens a) specimen measurements, b) prepared specimens.

- I. The thickness and width of the specimen were measured.
- II. The UTM machine was calibrated and the specimen was set in such way so that the axis of the cylindrical surfaces was parallel and the loading nose was midway between the supports.
- III. The load was applied to the specimen at the specified crosshead motion and simultaneously load-deflection data was taken till rupture occurred at the outer surface of the test specimen.
- IV. The flexural strength was calculated by the following equation:

$$\text{Flexural Strength}(\sigma_f) = \frac{3FL}{2bd^2} \text{ MPa}$$

Where, F= load (N)

L = support span distance (mm)

b = width of beam (mm)

d = depth of beam (mm)

Flexural strength test of the developed PP sheet was also carried out by the same technique.

3.5.1.3 Hardness Test

The hardness of the developed composites and 100PP sheets were measured by a Shore Durometer hardness testing machine (Figure 3.18). The Shore Durometer hardness test method is based on the penetration of a specific type of indenter when forced into the material under specified conditions. The indentation hardness is dependent on the viscoelastic behavior and elastic modulus of the material and is inversely related to the penetration. This test provides an empirical test value that doesn't necessarily correlate well to other properties or fundamental characteristics. Thus, no simple relationship exists between indentation hardness determined by this test method and any fundamental property of the material tested. Among the existing Shore hardness scales, Shore A and D scales are the most commonly used. The Shore A scale is preferred for softer plastic materials, while the D scale is usually for harder ones. Shore D hardness of the composites was measured according to ASTM D2240 – 15 protocols [142].

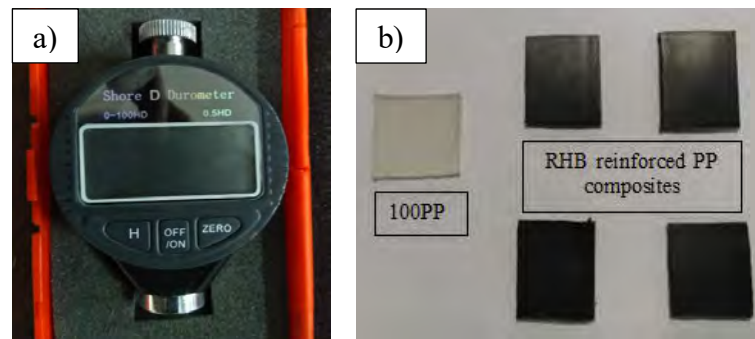


Figure 3.18: Hardness test a) Shore D Durometer, b) test specimens.

3.5.2 Morphology and Structure

Morphological analysis of the fabricated composites was done by a field emission scanning electron microscopy (FESEM) and the effect of RHB particles on the crystal structure of PP resin was studied by an X-ray diffraction (XRD) analyzer as described below.

3.5.2.1 Scanning Electron Microscopy (SEM)

The SEM image of the tensile fracture surface of the composites was carried out to understand the surface morphology of the composites and investigate the tensile fracture patterns. The scanning electron microscope used was ZEISS EVO 18 Research (Figure 3.19) and the tests were carried out at 5.00 kV acceleration. Prior to scanning, the composite specimen was placed on a disc and held in place using a double-sided carbon tape then coated with gold particles via sputtering technique to avoid sample charging.



Figure 3.19: ZEISS EVO 18 Research Scanning Electron Microscope.

3.5.2.2 Energy Dispersive X-Ray (EDX) Analysis

To investigate the existence of RHB particles in the PP matrix, EDX analysis simultaneously with the SEM was conducted at the same surface locations. The Zeiss, EVO 18 Research scanning electron microscope was coupled with an EDX system (ZEISS Smart EDX). The EDX can provide rapid qualitative, or with adequate standards, semi-quantitative analysis of elemental composition components present in the composite's surface [44].

3.5.2.3 X-Ray Diffraction (XRD)

X-Ray Diffraction (XRD) is a non-destructive analytical method used to investigate the structure of crystalline materials. XRD analysis is performed to identify the crystalline phases present in a material and thereby reveal chemical composition information. Moreover, XRD is a prime technique to determine the degree of crystallinity in polymers and polymeric composites. X-ray diffraction (XRD) analysis was done by the Emma (enhanced mini-materials analyser) X-Ray Diffractometer (Figure 3.20) from GBC Scientific Equipment, with scattering angle 2θ scanned from 10° to 80° at 30 kV using Cu $K\alpha$ radiation.



Figure 3.20: The Emma (enhanced mini-materials analyser) X-Ray Diffractometer.

3.5.3 Thermal Properties Test

Thermal properties of the developed composite sheets were measured by the means of thermogravimetric analysis (TGA) and differential scanning calorimetry (DSC) tests as described in section 3.5.3.1 and 3.5.3.2 below.

3.5.3.1 Thermogravimetric Analysis (TGA)

Thermogravimetric analysis (TGA) is a useful technique to determine a material's thermal stability and the fraction of volatile components present in a material by monitoring the weight change that occurs as a sample is heated at a constant rate. The TGA analysis of the composite sheets was performed to study the effect of RHB particle's presence on the thermal stability of PP matrix and thermal degradation rate of the composite at different temperatures. TGA test was carried out on about 20 mg RHB reinforced PP composite at a heating rate of 10°C/min in a nitrogen atmosphere using a Thermo-gravimetric Analyzer (TA instrument TGA Q50, model: V6.4 Build 193) (Figure 3.21). TGA test started at room temperature and the end temperature was 550°C.



Figure 3.21: TGA Q50 Thermo-gravimetric Analyzer.

3.5.3.2 Differential Scanning Calorimetry (DSC)

Differential scanning calorimetry (DSC) is a thermo-analytical technique in which the variation of heat requirements to raise the temperature of a sample compared to a reference is measured as a function of temperature. It is an effective technique to investigate the response of polymeric composites to heating. DSC can be used to study the melting temperature (T_m) and the glass transition temperature (T_g) of polymers and polymeric composites. DSC analysis of fabricated composites was performed with the DSC131 EVO analyzer from SETARAM Instrumentation (Figure 3.22). About 20 mg of composite sample in an aluminum pan was heated from room temperature to 300°C and at the heating rate of 10°C min⁻¹. The heat flow to or from the sample

was monitored as a function of temperature during the heating. N_2 with a flow rate of 50 mL min^{-1} was used as flushing gas.



Figure 3.22: Differential scanning calorimeter (DSC131 EVO).

3.5.4 Impedance Analysis (IA)

The impedance analysis (IA) was performed using a Precision Impedance Analyzer, 6500B series from Wayne Kerr Electronics, UK (Figure 3.23 a). The impedance analysis was conducted to measure the impedance (Z) and resistance (R) of the fabricated composites and compare them with the impedance (Z) and resistance (R) of the 100PP sheet. The tests were carried out at 18°C and the applied frequency was 100 Hz. The dimensions of the test specimens were $20 \text{ mm} \times 20 \text{ mm} \times 2 \text{ mm}$ (Figure 3.23 b).

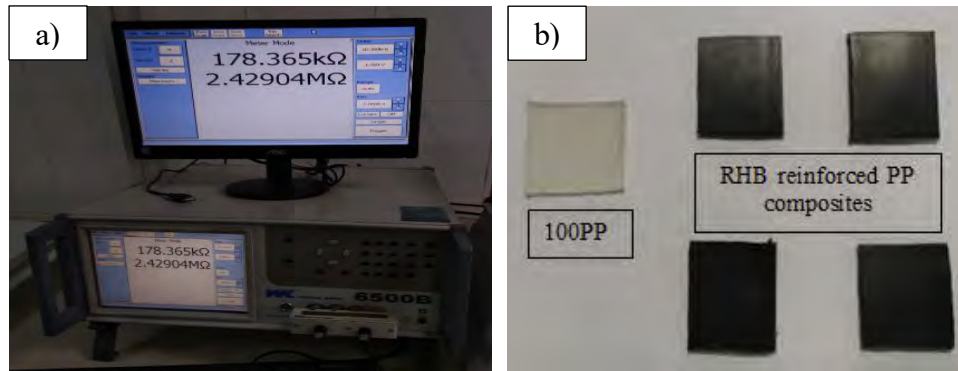


Figure 3.23: Impedance analysis- a) Precision Impedance Analyzer, 6500B series, b) Test specimens.

CHAPTER 4
RESULTS AND DISCUSSION

4.1 Evaluation of RHB Characteristics

4.1.1 Biochar Yields and pH

The yield of RHB decreased as the pyrolysis temperature increased from 400-850°C. The highest biochar yield of 47.07% was obtained from the slow pyrolysis of rice husk at 400°C (RHB400) and the lowest yield was 34.54% at 850°C (RHB850). Figure 4.1 shows the yield of rice husk derived biochar (RHB) at different pyrolysis temperatures.

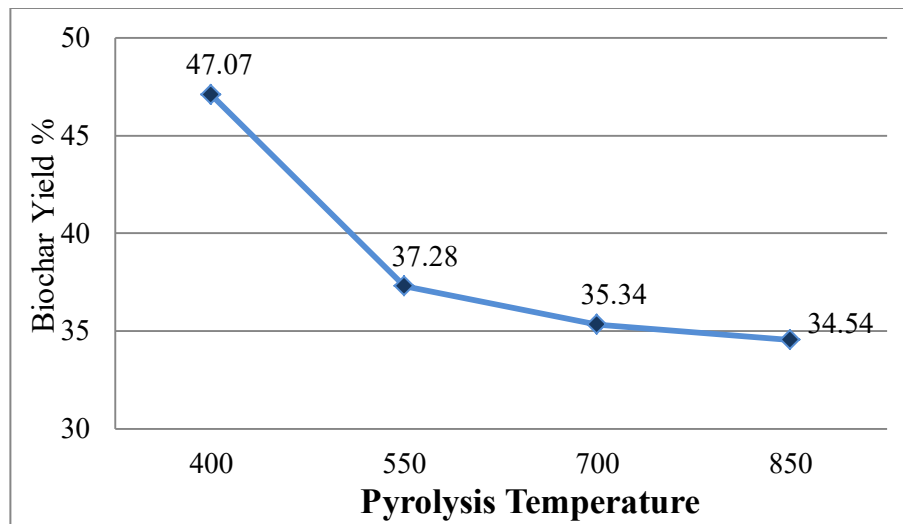


Figure 4.1: Biochar yield at different pyrolysis temperatures.

A large decline of biochar yield was observed between 400 and 550°C but the reduction in yield between 550 and 850°C was little. The pyrolysis temperature range of 400 to 850°C was chosen, because the related previous study investigation had shown that at around 300°C conversion of the feedstock to biochar was poor and at above 850°C the biochar yield was decreased dramatically due to high decomposition of volatile materials and intermediate melt in the biochar structure [143]. Demirbas, in a study, found that the biochar yield depends on the destructive reaction of the cellulose and polymerization process of biochar [144]. Moreover, the reduction of biochar yield with increasing pyrolysis temperature can be due to either greater primary decomposition of feedstock (rice husk) or secondary decomposition of the biochar (lignocellulosic residue) at higher temperatures [145]. As the pyrolysis temperature increases, the final solid residue decreases, as a result of the competition between charring and de-volatilization reactions, of which the latter is more favored [143].

The synthesized biochar samples were alkaline ($\text{pH} > 7$) in nature and the pH of RHB increased from 7.17 to 9.71 when the pyrolysis temperature escalated from 400 to 850°C (Figure 4.2).

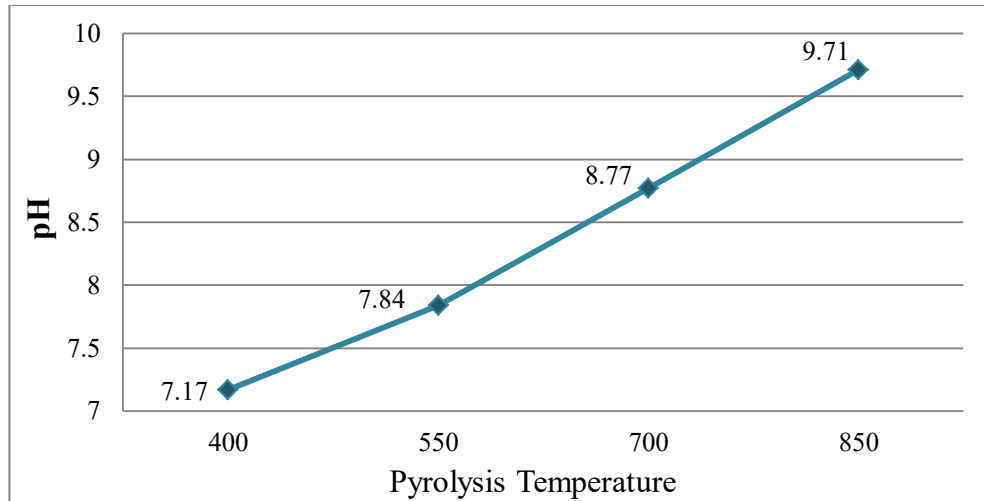


Figure 4.2: pH of 1:5 wt% of RHB/water solution containing RHB pyrolyzed at four different temperatures.

Minerals that are contained in the rice husk separates from the organic matrix during pyrolysis. The separation of the organic compound (carbon) and inorganic compounds (alkali elements) in the biochar increases with increasing pyrolysis temperature, which can significantly increase the pH value of RHB [143]. On the other hand, minerals begin to separate from the organic matrix when ashes are formed at pyrolysis temperatures above 350°C [146] causing an increase in pH values of RHB.

4.1.2 Micrographs of RHB

4.1.2.1 Optical Micrograph

To get a better view of rice husk and RHB optical micrograph at 40 times magnification was obtained. Figure 4.3 shows the optical image of rice husk and its biochar.

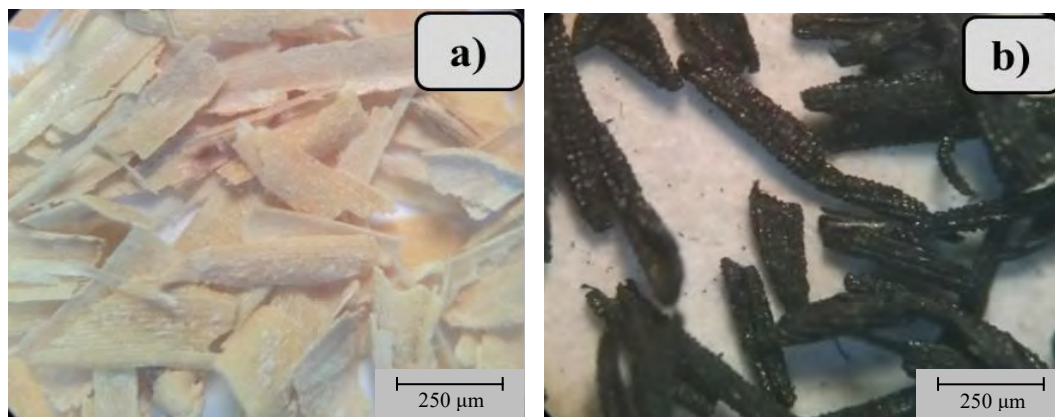


Figure 4.3: Rice husk a) before pyrolysis, b) after pyrolysis (RHB).

Rice husk has a rough surface with small spikes [147]. Pyrolysis of rice husk produced good quality biochar as there is no sign of rice husk portions that were not pyrolyzed. Moreover, significant ash formation is not observed.

Micrograph of ground RHB was also obtained at 40 and 1000 times magnification as presented in Figure 4.4.

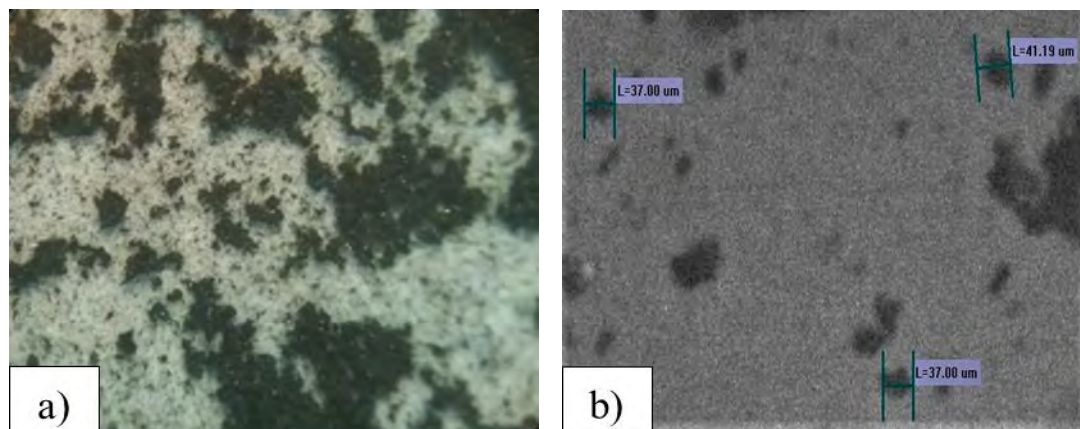


Figure 4.4: RHB after grinding a) $\times 40$, b) $\times 1000$.

RHB powder with fine particle size is obtained after grinding as observed from the figure (figure 4.4 a). The optical micrograph at 1000 times magnification is not very clear but a better understanding of particle size can be obtained (figure 4.4 b). RHB particles having a diameter less than $50 \mu\text{m}$ were observed.

4.1.2.2 SEM Analysis

Surface morphology of RHB samples (RHB400, RHB550, RHB700, and RHB850) were further investigated by obtaining SEM micrographs at different magnifications. The rice husk biochar shows an obviously porous structure, with varied pore size and shape. Figure 4.5 presents the typical morphology of RHB400 at 1000 times magnification. The lignocellulosic residue, pore structure and spike in the surface can be observed in the RHB400 sample, which are some common features of rice husk derived biochar [147]. The porous structure of RHB400 is clearly seen in the SEM micrograph, exposing a variety of shapes in the macro-pores, and micro-pores. The biochars contain tissue that was not fully decomposed; hence the pores were not fully developed [143]. The outer surface of RHB400 is compact and has a corrugated structure. On the other hand, the inner part has a porous structure. Thus, the morphology is different for the outer and inner surfaces of rice husk derived biochar. According to the study done by Deshmukh et al. [138], most of the silica was present in the outer epidermal cells of rice husk and after pyrolysis, the silica obtains a highly porous structure with large internal surface area.

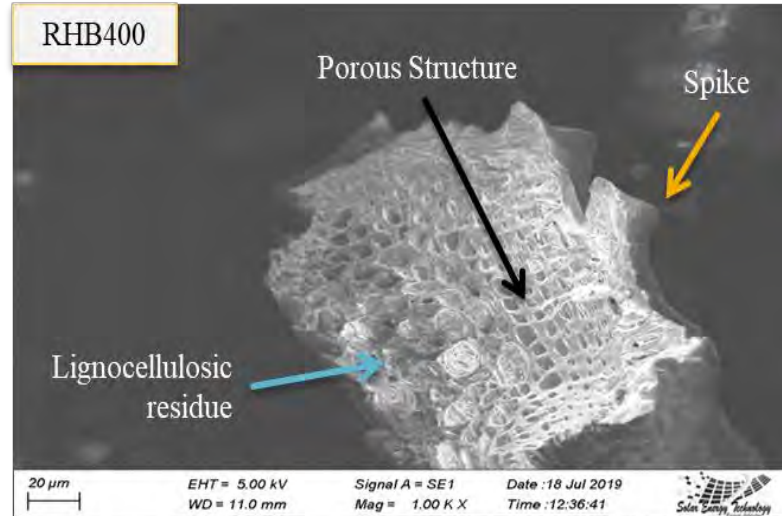


Figure 4.5: SEM micrograph of RHB400.

Figure 4.6 presents the SEM image of RHB550 at 1000 times magnification. The rice husk has broken up during the thermal decomposition of organic lignocellulosic materials, thus leaving a highly porous structure [143]. The structure of RHB550 has a higher degree of porosity than that of RHB400. The generation of pores with varying size and structure indicates that a large amount of organic compounds might be driven off during pyrolysis. Moreover, the presence of lignocellulosic residue is less evident in the micrograph.

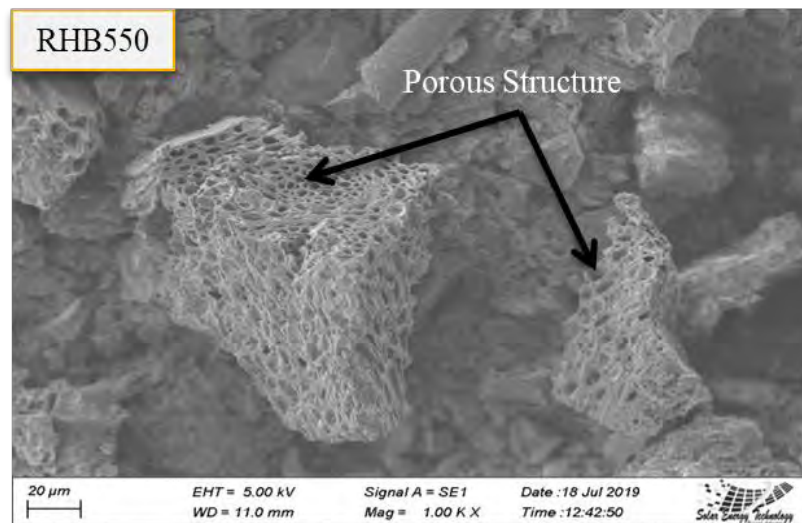


Figure 4.6: SEM micrograph of RHB550.

SEM image presented in Figure 4.7 illustrates the morphology of RHB700 is at 1000 times magnification. At 700°C, the morphology of the biochar became a honeycomb-like structure with cylindrical holes. The micrographs of the biochar show many pores formed over the surface

and they are arranged in an orderly fashion. According to Guo et al. [149] properly arranged pore structures of biochars possess high surface area and adsorptive capacity.

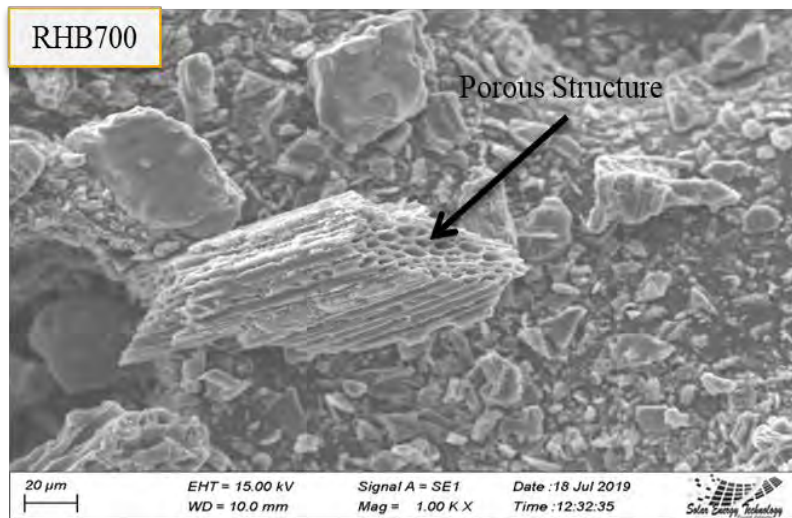


Figure 4.7: SEM micrograph of RHB700.

Finally, Figure 4.8 presents the SEM micrograph of RHB850 at 10000 times magnification for better understanding of the structure. The RHB850 had a loose and porous shape. Fine materials around the outer surface of the pores could be observed falling down and closing the pores. These materials were mainly silicon and calcium minerals as evident by the EDX spectrum [143]. Cracks and shrinkages could be observed on the surface of the biochar due to high temperature. RHB pyrolyzed at 850°C has highly porous, hollow, and well-arranged structures (Figure 4.8). The macro-pores of the char are interconnected by micro-pores. The structures seemed to be fragile because of their thin walls.

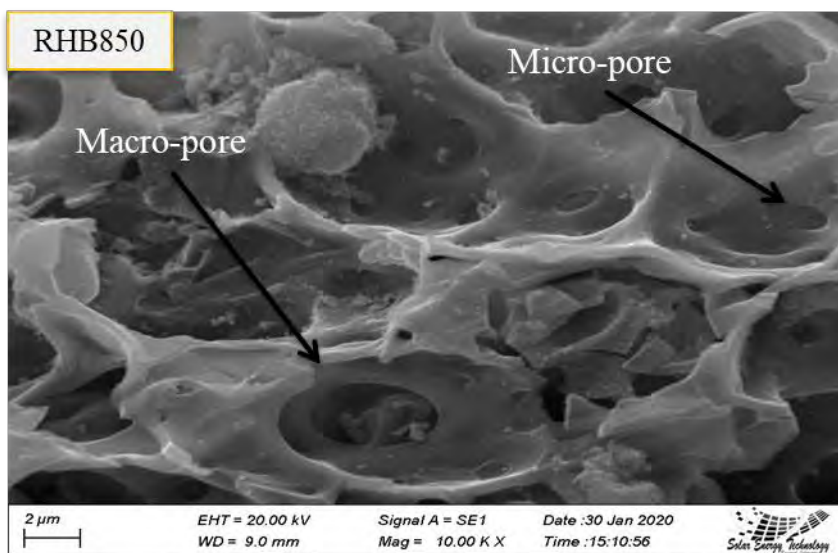


Figure 4.8: SEM micrograph of RHB850.

All the biochar samples exhibited clear porous characteristics and the voids development. At higher pyrolysis temperatures, the structure of RHB became more ordered because the number of micro-pores decreased while the number of macro-pores increased. A large number of pores lengthwise and crosswise in the rice husk biochar might be able to strengthen the interface with the polymer matrix, due to the ultrahigh surface area, providing the possibility of the preparation of biochar-based polymeric composites. Highly porous rice husk biochar has the potentiality to strengthen the interface with the polymer matrix [150].

4.1.3 Proximate Analysis

Proximate analysis of the biochar samples was performed according to ASTM D3172 – 13 test method. Table 4.1 presents the proximate analysis results of RHB samples as a function of pyrolysis temperature. The results showed that the ash content of RHB increased with increasing pyrolysis temperature. This was because increased devolatilization during pyrolysis at higher temperatures resulted in biochar with an increased amount of non-volatile matter. The percentage of ash content was 35.06, 39.19, 43.79, and 45.60% for RHB400, RHB550, RHB700, and RHB850, respectively. In general, the increased ash content is due to the reduction in the content of other elements during pyrolysis. Elements such as C, H, N, O, and S are volatilized during heating while the inorganic salts such as quartz and calcite are not fully volatilized. According to Tsai et al. [146], the increase in ash content in the biochar with an increase in pyrolysis temperature is because of the progressive concentration of minerals and destructive volatilization of lignocellulosic matters.

Table 4.1: Proximate analysis data for RHB samples produced at four different temperatures

Sample	Ash Content (%)	Volatile Matter (%)	Fixed Carbon (%)
RHB400	35.06	22.97	36.66
RHB550	39.19	17.33	38.16
RHB700	43.79	11.24	37.14
RHB850	45.60	9.91	36.62

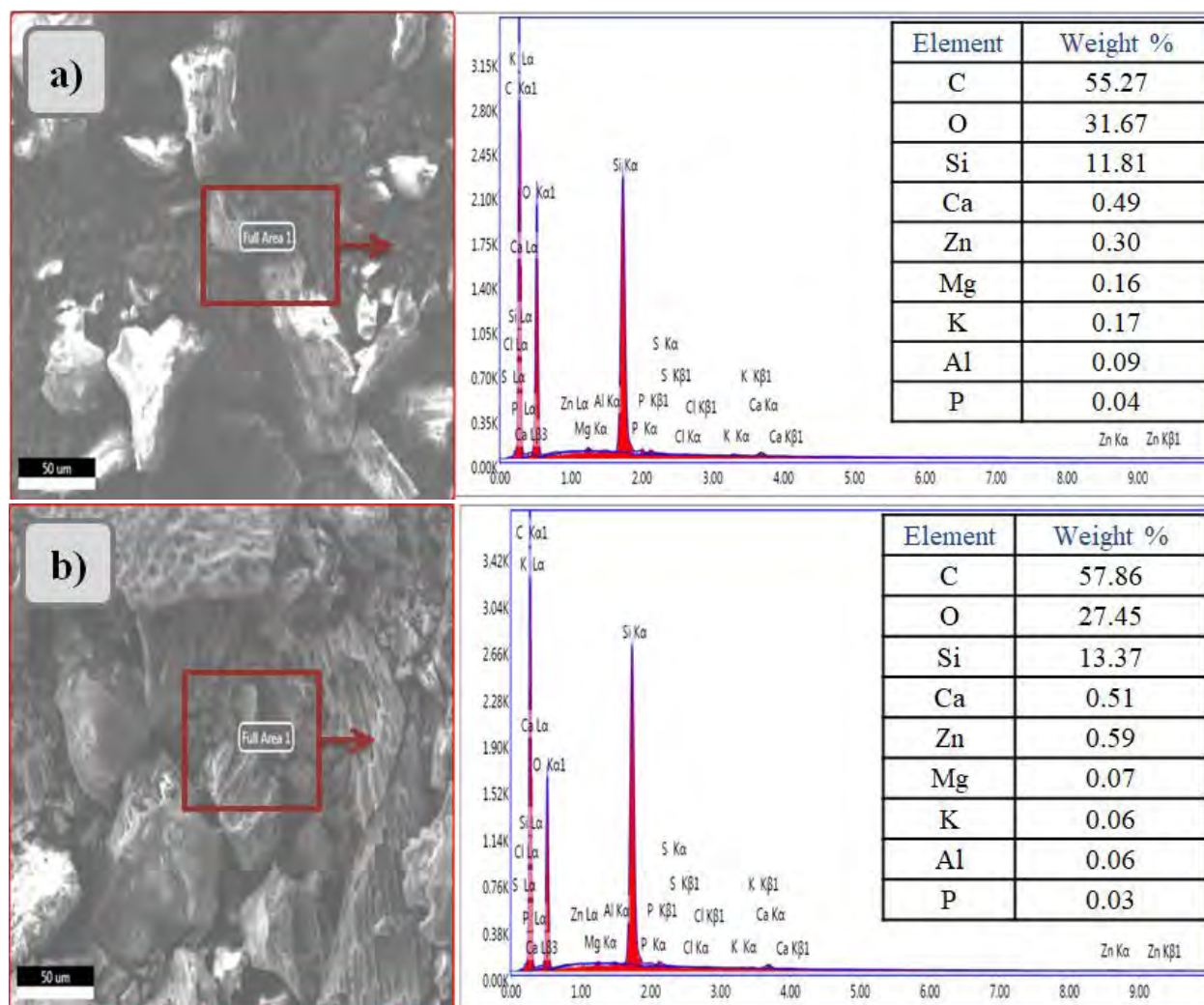
The content of volatile matter (VM) for the prepared biochar samples ranged from 9.91% to 22.97%. An increase in the pyrolysis temperature decreased the content of VM, exhibiting a similar trend with the biochar yield. This might due to the fact that the increasing temperature resulted in the further crack of the volatile fractions into low molecular weight gases and liquids instead of biochar [138]. Meanwhile, the dehydration of hydroxyl groups and thermal degradation of cellulose and lignin might also occur with the increasing pyrolysis temperature

[143]. These results confirmed that the increase in temperature enhanced the stability of biochar for the loss of volatile fractions [138].

The fixed C content of RHB increased with pyrolysis temperature due to increasing concentrations of the volatile matter being released. However, the amount of fixed C increased up to 550°C but not at higher temperatures (table 4.1). This confirmed the observations of Jindo et al. [151]. The slight reduction of fixed C in the RHB700 and RHB850 might be due to the dehydration of hydroxyl groups and the thermal degradation of carbonaceous materials at higher pyrolysis temperatures [143].

4.1.4 SEM-EDX Analysis

EDX images of RHB samples at their marked specific area surface constituents are shown in Figure 4.9.



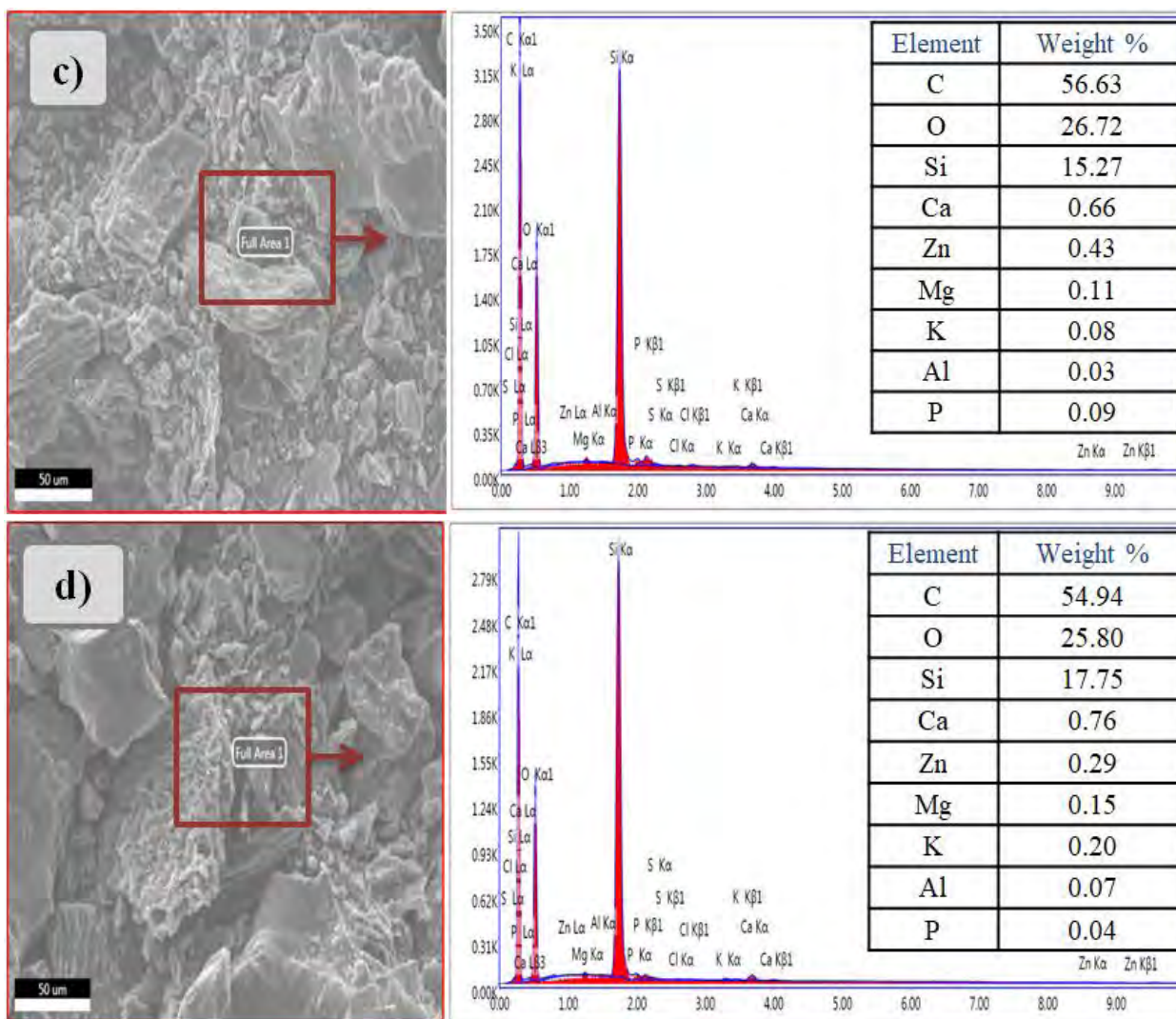


Figure 4.9: EDX spectra of rice husk biochar samples a) RHB400, b) RHB550, c) RHB700, and d) RHB850.

According to the EDX data, carbon (C) was the major element (>50 wt%) in all RHB samples. Next to C, oxygen (O) and silicon (Si) were the prominent elements in all the RHB samples with small amounts of calcium (Ca), zinc (Zn), and magnesium (Mg). In addition, K, Al, and P were present, though in a very small quantity. The highest Si presence of 17.75 wt% was obtained in the RHB850, and with increasing pyrolysis temperature the spectra of metals (Ca, Zn, and Mg, etc.) were observed to emerge revealing enrichment of inorganic constituents in the biochar at higher temperatures. Maximum Ca concentration of 0.76 wt% was recorded in RHB850, while the highest Zn concentration (0.59 wt%) was found in RHB550. Table 4.2 illustrates the major elements of RHB samples and the change of elemental concentration in RHB as a function of pyrolysis temperature.

Table 4.2: Major elements of RHB prepared at different temperatures

Sample	C (wt %)	O (wt %)	Si (wt %)
RHB400	55.27	31.67	11.81
RHB550	57.86	27.45	13.37
RHB700	56.63	26.72	15.27
RHB850	54.94	25.80	17.75

The C concentration in the RHB samples initially increased with pyrolysis temperature due to the increasing valorization of volatile matter. But, the amount C exhibited a decreasing trend after 550°C because of the thermal decomposition of carbonaceous materials at higher pyrolysis temperatures [143]. Fixed C content results in the proximate analysis also followed the same trend (Table 4.1). The O concentration was found to decrease with increasing pyrolysis temperatures. This might be due to the dehydration of various groups present in the lignocellulosic residue of the biochar [138]. In contrast, the concentration of Si in the RHB increased with rising pyrolysis temperatures. According to proximate analysis results, ash content increases with increasing pyrolysis temperature (Table 4.1) and Si in the form of silica remains in the residue when rice husk is thermally decomposed [147,152]. This could be the prime reason behind increasing Si concentration at higher pyrolysis temperatures.

4.1.5 FTIR Analysis

FTIR (Fourier Transform Infrared) spectroscopy was performed to determine the functional groups of the developed RHB, while simultaneously gaining an insight into the changes in chemical reactions due to various pyrolysis temperatures. The FTIR spectra of rice husk biochars produced at four pyrolysis temperatures are presented in Figure 4.10.

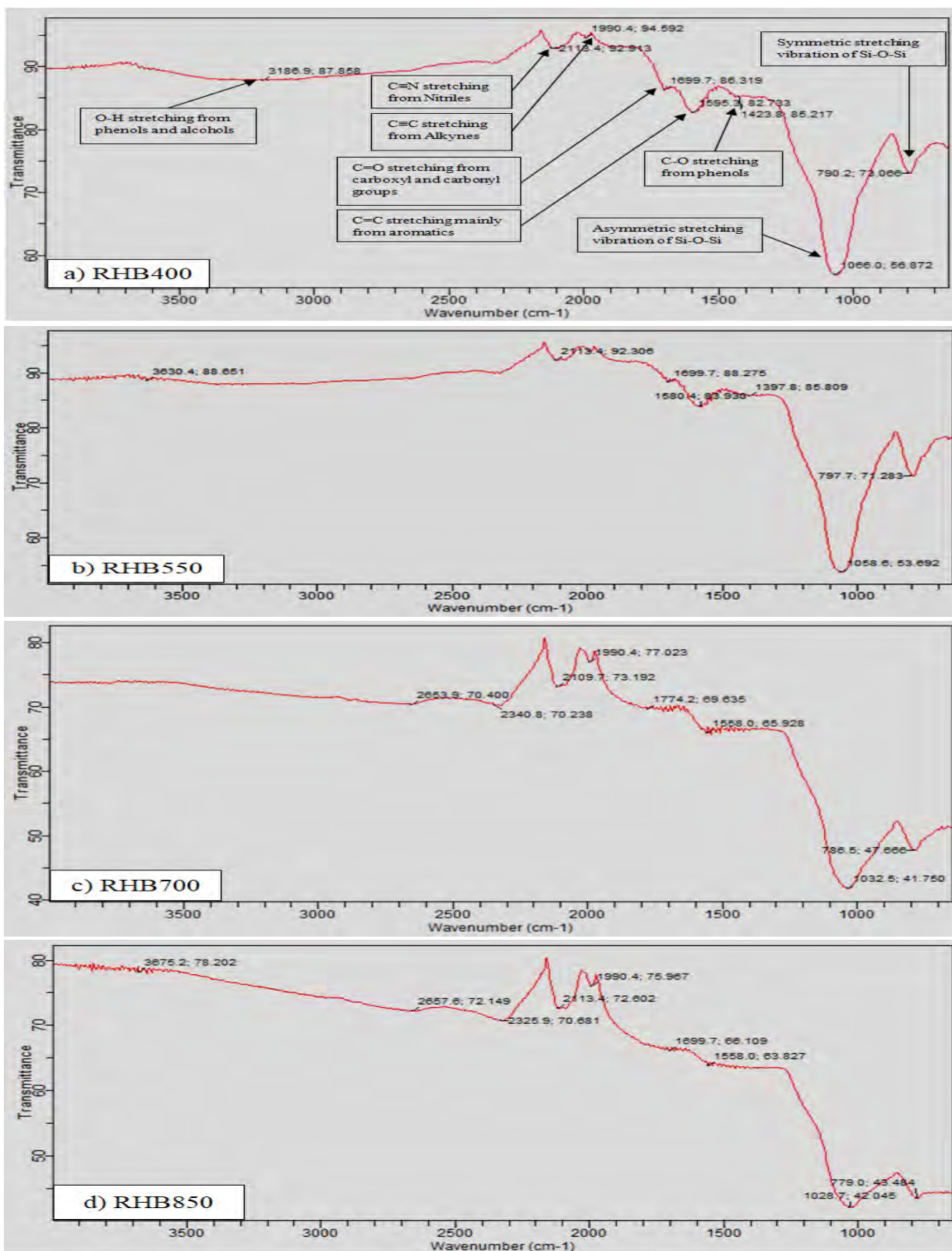


Figure 4.10: FTIR spectra of biochar samples- a) RHB400, b) RHB550, c) RHB700, and d) RHB850.

The FTIR spectra showed various remarkable bands. The band at between 3750 cm^{-1} and 3200 cm^{-1} correspond to -OH stretching from phenols and alcohols, which indicates dehydration of cellulose and lignin [153]. The broad band at around 2113 cm^{-1} was assigned to the stretching vibration of $\text{C}\equiv\text{N}$ from nitrile [155]. The peaks at 1990.4 cm^{-1} were assigned to stretching vibration of $\text{C}\equiv\text{C}$ from alkyne [155]. The band at 1780 cm^{-1} to 1680 cm^{-1} was presented as the stretching vibration of $\text{C}=\text{O}$ from the carboxyl and carbonyl groups [153]. The transmittance peak at the wavenumbers of 1650 cm^{-1} to 1450 cm^{-1} was the stretching vibration of the $\text{C}=\text{C}$ benzene ring skeleton mainly from aromatics [156]. The peak at 1420 cm^{-1} to 1380 cm^{-1} can be assigned to C-O stretching vibration from phenols [154]. A sharp peak at 1088 cm^{-1} to 1028 cm^{-1} was observed in all samples. This corresponds to the asymmetric stretching vibration of Si-O-Si bridges in SiO_x and the relatively weak band at 798 cm^{-1} to 778 cm^{-1} observed in all samples was related to the symmetric stretching vibration of Si-O-Si present in silica [156,157]. The band assignments for all RHB samples are summarized in Table 4.3.

Table 4.3: Peak position of functional groups observed in the FTIR spectra of RHB samples

Wave Number (cm^{-1})	Characteristic Vibrations	Reference
3675.2 - 3186.9	Stretching vibration of O-H from phenols and alcohols	[153]
2657.6 - 2623.9	Stretching vibration of O-H from carboxylic acid	[154]
2340.8 - 2325.9	Stretching vibration of $\text{C}=\text{O}$ from ketene	[154]
2113.4 - 2109.7	Stretching vibration of $\text{C}\equiv\text{N}$ from Nitrile	[155]
~ 1990.4	Stretching vibration of $\text{C}\equiv\text{C}$ from alkyne	[155]
1774.2 - 1699.7	Stretching vibration of $\text{C}=\text{O}$ from carboxyl and carbonyl groups	[153]
1595.3 - 1558.0	Stretching vibration of $\text{C}=\text{C}$ benzene skeleton mainly from aromatics	[156]
1423.8 - 1397.8	Stretching vibration of C-O from phenols	[154]
1088.0 - 1028.7	Asymmetric stretching vibration of Si-O-Si	[156,157]
797.7 - 779.0	Symmetric stretching vibration of Si-O-Si	[156,157]

Different spectra reflected changes in the surface functional groups of RHB produced at different temperatures. This result is likely due to the degradation and depolymerization of cellulose, and lignin [143]. For example, intensities of $\text{C}=\text{C}$ and $\text{C}=\text{O}$ stretching vibration changed with temperature and peaks of C-O stretching vibration from phenols disappeared which may suggest that phenolic and carboxylic compounds in lignin had been degraded [138]. On the other hand, intensities of peaks from symmetric and asymmetric stretching vibration of Si-O increased with increasing pyrolysis temperature which indicates that Si compounds (mainly silica) in RHB have increased [157] and it is well agreed with the EDX results presented in Table 4.2.

4.1.6 Analysis of Thermal Properties

4.1.6.1 Thermogravimetric Analysis

Thermogravimetric analysis (TGA) and derivative thermogravimetry (DTG) curves for all four biochars are presented in Figure 4.11.

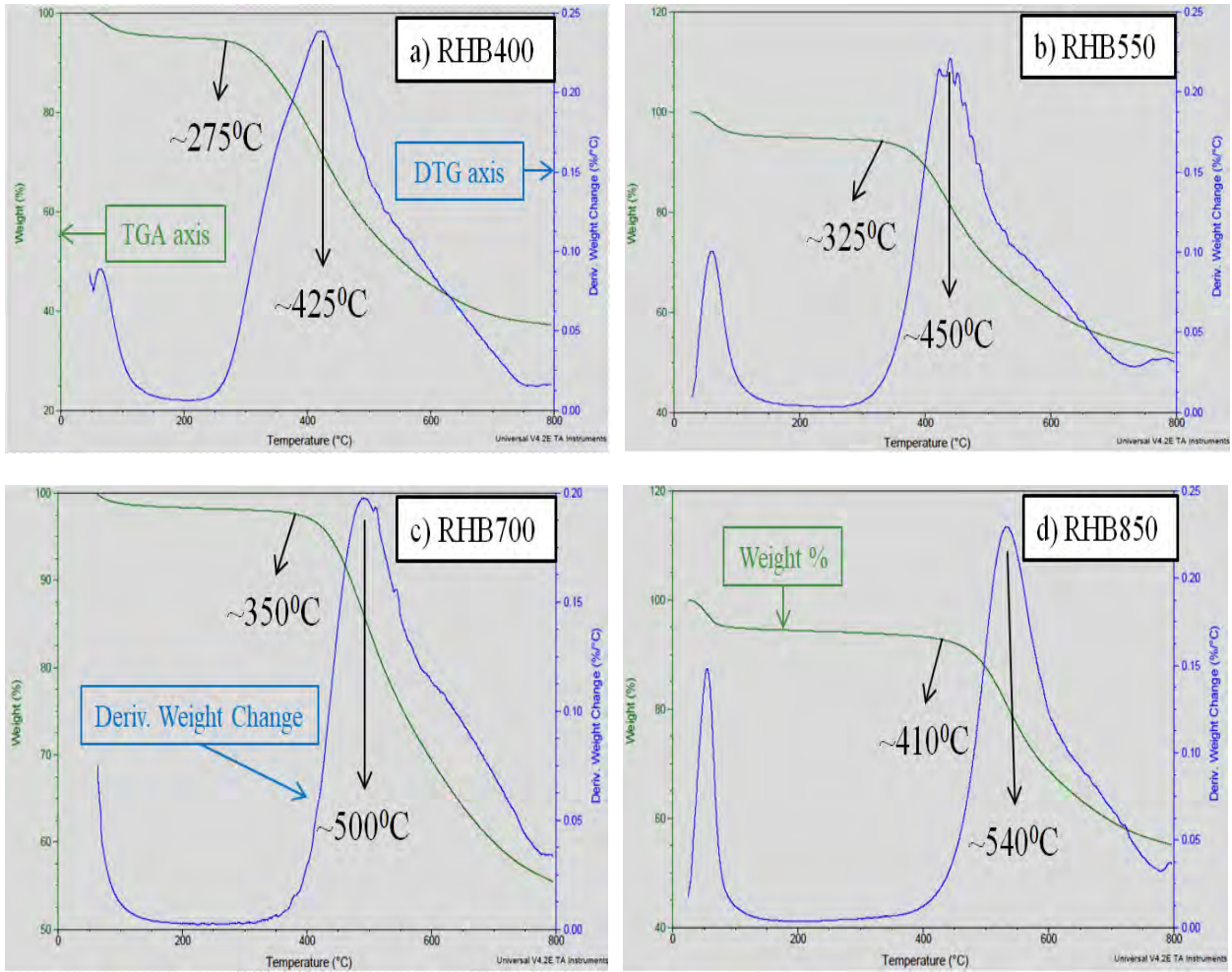


Figure 4.11: TGA with DTG curves of biochar samples- a) RHB400, b) RHB550, c) RHB700, and d) RHB850.

During thermal degradation in the TGA process, two-stage weight losses were observed (green lines), which was also implied by the DTG curves (blue lines). The mass loss occurred close to 100°C , suggesting that this reduction in weight commonly associated with the removal of the initial moisture and volatiles of the samples [158]. After the initial mass loss, the main weight loss started at around 275°C , 325°C , 350°C , and 410°C for RHB400, RHB550, RHB700, and RHB850 respectively, and the weight loss occurred over a wide temperature range. This was likely due to the fact that the prepared biochars had undergone a previous heat treatment process before the thermal analysis, thus, the tested biochar samples exhibited higher thermal stabilities

with increasing pyrolysis temperatures [138]. For each of the tested RHB samples, only one peak was found during the main weight losses on the DTG curves (blue lines). In general, if the testing temperature exceeds the biochar preparation temperature, then a secondary pyrolysis reaction could be observed and easily detected [158]. Thus, the weight loss over a wider temperature range might be attributed to the decomposition and degradation of organic materials [159]. The maximum weight loss occurred at around 425^oC, 450^oC, 500^oC, and 540^oC for RHB400, RHB550, RHB700, and RHB850 respectively, suggesting that the higher the pyrolysis temperature was, the better thermal stability the biochar showed, which is consistent with the literature [138]. The biochars pyrolyzed at lower temperatures were less thermally stable than the higher temperature derived biochars, probably because they were not fully carbonized [159]. At around, 750-800^oC the decomposition for all the RHB samples finished, and the curves became stable.

4.1.6.2 DSC Analysis

To further investigate the thermal properties of RHB, DSC tests were carried out. Figure 4.12 shows the DSC curves for all biochar samples.

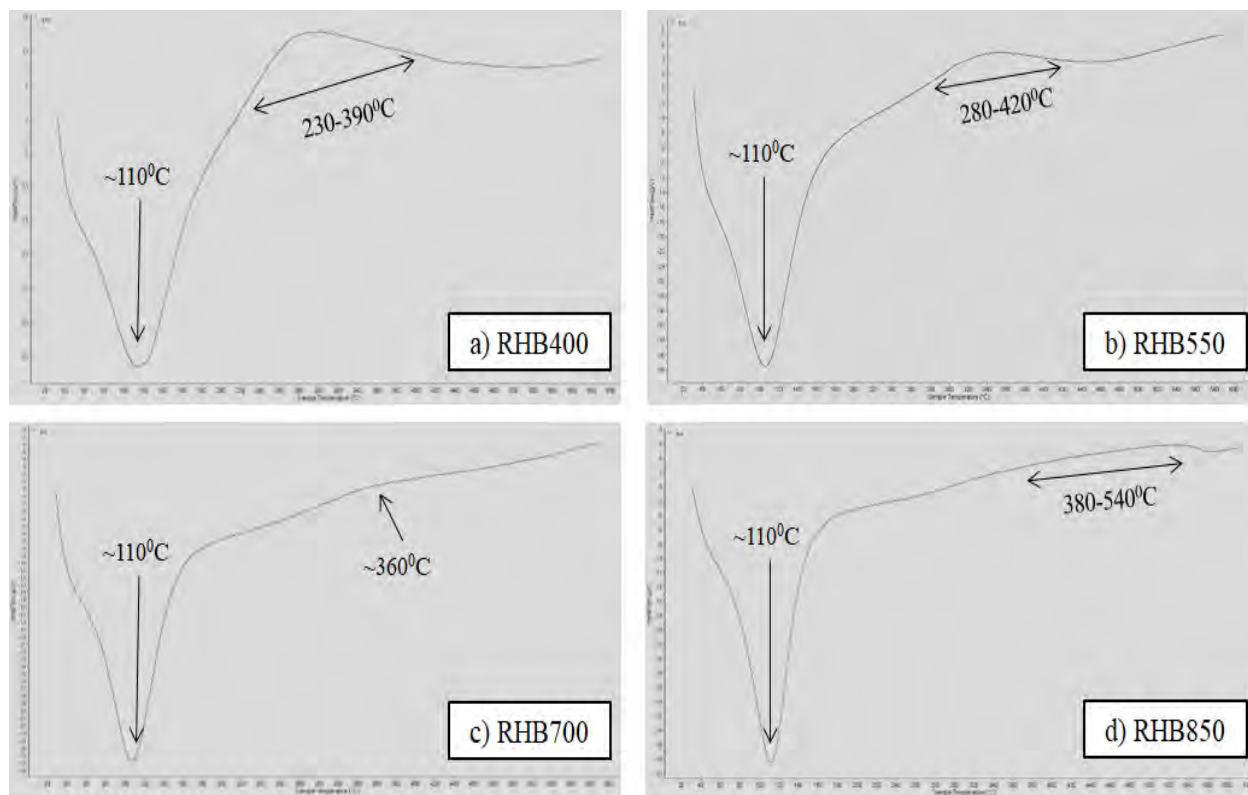


Figure 4.12: DSC curves of a) RHB400, b) RHB550, c) RHB700, and d) RHB850.

The first peak present in the DSC curves of all RHB samples appeared around 110^oC as an endothermic peak was due to the evaporation of moisture [160]. After the initial endothermic

peak, the DSC curves exhibited an exothermic peak in the temperature range of 230-540⁰C, which was due to the decomposition and combustion of organic materials [161]. According to Brebu et al. lignin decomposes slowly over a wide temperature range (200-500⁰C) than cellulose and the hemicellulose components of biomass [162]. Thus the unpyrolyzed lignocellulosic residues in the biochar showed an exothermic peak during DSC heating and this peak considerably decreased in the RHB pyrolyzed at higher temperatures, indicating that organic residues had degraded due to pyrolysis [163]. The DSC curve of RHB400 exhibited a broad exothermic peak at the temperature range of 230-390⁰C, indicating the higher presence of lignocellulosic residue in the biochar. In the DSC curves of RHB550, RHB700, and RHB850 the intensity of the exothermic peak gradually decreased, indicating that the amount of lignocellulosic residue in biochar decreased with increasing pyrolysis temperatures. Moreover, the exothermic peak consistently moved towards higher temperatures with increasing pyrolysis temperatures. This demonstrates that RHB pyrolyzed at higher temperatures undergo thermal decomposition at higher temperatures. As a consequence, biochars produced at high temperatures could be more stable and resistant to thermal degradation [161,163]. This observation is well agreed with the TGA results discussed in the previous section.

4.2 Characteristics and Properties of RHB Reinforced PP Composite

A large number of factors influence the properties of a biochar reinforced polymer composite. The composite properties are usually dependent on matrix properties, reinforcing agent and to a certain extent, upon the interfacial adhesion strength [117]. The mechanical, thermal, and electrical properties of the fabricated RHB reinforced PP composites were characterized thoroughly and compared with the properties of PP for better assessment.

4.2.1 Mechanical Properties Analysis

4.2.1.1 Tensile Test

The tensile strength or ultimate tensile strength refers to the maximum stress that a composite can withstand before failure occurs when an external force is exerted to pull the composite. The incorporation of particle reinforcements can modify the mechanical properties of polymeric composites in many ways depending on the particulate size, loading, composites microstructure, and the particle-matrix interfacial adhesion [133]. Similarly, the maximum strength sustained by composites under uniaxial tensile loading depends on the effective stress transfer between the matrix and reinforcements [11]. Determination of tensile strength is important for the evaluation of different polymers, especially for designing of plastic components for load-bearing applications, and for predicting the in-service performance of plastics. In that perspective, tensile tests of fabricated composites and PP were performed according to the ASTM D638 standard and the test results are shown in Table 4.4. From the tensile test results, it can be observed that the addition of RHB has considerably affected the tensile strength of the composites compared to the neat PP.

Table 4.4: Tensile test results of RHB reinforced PP composites

Sample Name	Sample No	Tensile Strength (MPa)	Average Tensile Strength (MPa)
100PP	1	33.93	34.57
	2	34.94	
	3	34.85	
PP-10RHB-400	1	24.19	27.94
	2	30.14	
	3	29.48	
PP-15RHB-400	1	29.53	30.25
	2	30.99	
	3	30.22	
PP-10RHB-550	1	25.10	27.01
	2	27.90	
	3	28.03	
PP-15RHB-550	1	30.61	31.41
	2	32.21	
	3	31.41	
PP-10RHB-700	1	24.01	26.74
	2	28.51	
	3	27.69	
PP-15RHB-700	1	25.42	27.17
	2	29.33	
	3	26.75	
PP-10RHB-850	1	24.73	27.22
	2	27.87	
	3	29.05	
PP-15RHB-850	1	27.53	29.03
	2	30.16	
	3	29.41	

The tensile strength of the RHB reinforced composites reduces upon the introduction of biochar particles. This may be due to the reduction in the extensibility by rigid particles and the formation of clusters of the PP matrix, which resulted in the increase of stress concentration zones and weakened the interfacial bonding strength of the sample [164]. However, for all biochar samples, tensile strength increased with increasing biochar content. Sound interfacial

bonding between the polymer matrix and the additive is crucial for the enhancement of the tensile strength of a composite. More RHB addition in the PP system indicates that more carbon content in the RHB reinforced PP composite. The porous structure of RHB (Figure 4.5–4.8) allowed more penetration of PP and provided more reinforcement as interlocking between RHB and PP increased. Hence, the tensile strength of the composites increased with increasing RHB content. Figure 4.13 presents the effect of RHB addition in the tensile strength of PP.

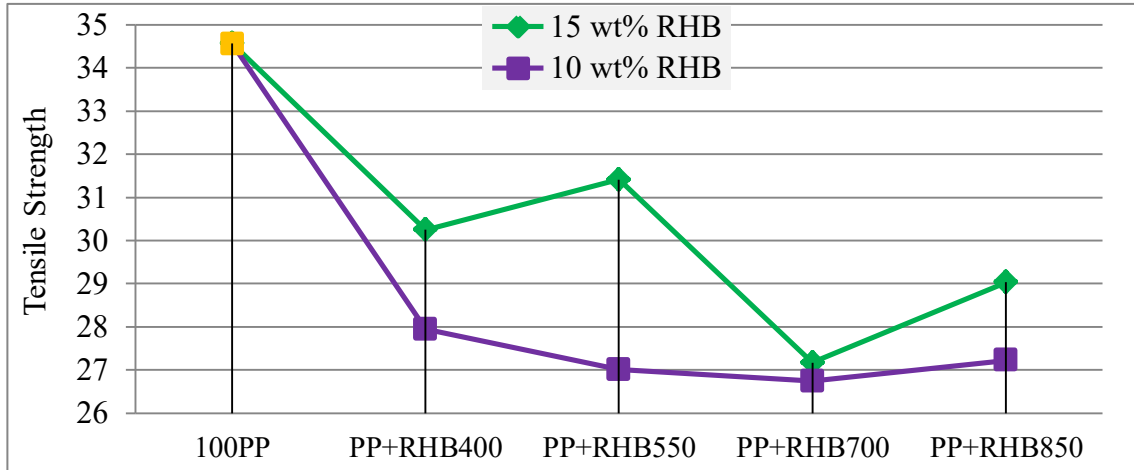


Figure 4.13: Variation of tensile strength due to RHB addition.

From the figure, the best tensile strength of 31.41 MPa was shown by PP-15RHB-550 composite, though the value is less than that of PP. The tensile strength of biochar reinforced polymer composites depends mainly on the interfacial adhesion and compatibility between the matrix and the reinforcement which enables the transfer of a portion of stress to the reinforcing particles at the time of deformation [11]. RHB pyrolyzed at 550⁰C has the highest C content among the developed RHB samples (Table 4.1) and the biochar has a large amount of surface functional groups (FTIR results, Figure 4.10), which is necessary for the interfacial bonding between biochar and PP. Moreover, the porous structure of RHB550 (Figure 4.6) allowed the PP to infiltrate in its pores, resulting in an interlocked system between RHB550 and PP. These could be the reasons behind the highest tensile strength of PP-15RHB-550 composite among the fabricated composites. On the other hand, the varying trend of tensile strength change in the developed composites might be due to the difference in mixing uniformity in the fabricated composites [134].

4.2.1.2 Flexural Test

In the flexural test, the upper half of the specimen is in compression while the lower half is in tension. The compressive stresses tend to close the cracks rather than opening them. Thus, cracks cannot easily propagate towards the compression side [2]. The flexural test results obtained for PP and the RHB reinforced PP composites are shown in Table 4.5.

Table 4.5: Flexural test results of RHB reinforced PP composites

Sample Name	Sample No	Flexural Strength (MPa)	Average Flexural Strength (MPa)
100PP	1	63.45	64.06
	2	66.19	
	3	62.54	
PP-10RHB-400	1	54.95	61.26
	2	69.62	
	3	59.20	
PP-15RHB-400	1	61.08	65.90
	2	68.43	
	3	68.18	
PP-10RHB-550	1	57.72	59.07
	2	61.26	
	3	58.24	
PP-15RHB-550	1	67.55	65.02
	2	60.43	
	3	67.09	
PP-10RHB-700	1	64.57	63.09
	2	67.03	
	3	57.68	
PP-15RHB-700	1	66.04	67.13
	2	67.47	
	3	67.89	
PP-10RHB-850	1	62.95	61.34
	2	63.63	
	3	57.43	
PP-15RHB-850	1	68.56	70.61
	2	69.62	
	3	73.66	

From the flexure test results, it is observed that flexural strength increased as the RHB content increased from 10 wt% to 15 wt%. Moreover, RHB prepared at higher temperatures found to further improve the flexural strength of the composites. The maximum flexural strength of 70.61 MPa was exhibited by PP-15RHB-850, which was 10.22% higher than that of PP (64.06 MPa). On the other hand, the lowest flexural strength value of 61.26 MPa was exhibited by PP-10RHB-

400 and the value is 4.73% less than that of PP (64.06 MPa). The flexural strength of a particle reinforced composite is dependent on factors such as wetting, filler content, mixing uniformity of filler and matrix and particle dispersion [126]. The porous structure of RHB could allow molten PP to flow inside the biochar, thus, a physical/mechanical interlocking might occur. Besides, biochar from rice husk has lignocellulosic residue and high silica content (Table 4.1 and 4.2.), which could facilitate an efficient stress transfer within the composite structure [2]. For all the biochar samples, the flexural strength increased with an increase in the amount of biochar in the composite. Uniform and even dispersion of RHB particles throughout the matrix and a higher percentage of particles are capable to withstand higher bending stress. Therefore, biochar particles caused a reinforcing effect in neat PP consequently improving its flexural strength. Similar results were reported by Das et al. [2], and Ho et al. [164]. RHB prepared at higher temperatures was also found to enhance the flexural strength. The effect of biochar addition on the flexural strength of the composites is presented in Figure 4.14.

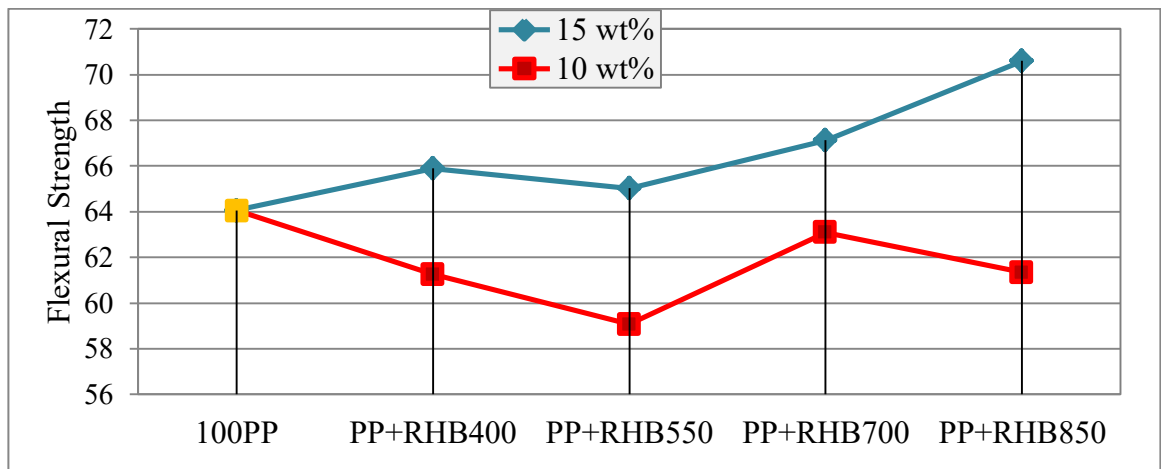


Figure 4.14: Variation of flexural strength due to RHB addition.

At lower RHB content (10 wt%), flexural strength of the fabricated composites was lower than that of PP. This was probably due to the poor load transfer between the RHB particles, as the content of RHB was low. As a result, stress gets accumulated at certain points of the composites and highly localized strains occur in the matrix, causing deterioration of flexural strength [117]. On the other hand, at higher RHB content (15 wt%), the composites showed excellent flexural strength improvements with increasing pyrolysis temperatures, where the flexural strength was higher than that of PP. Rice husk derived biochar prepared at higher temperatures has a lower amount of volatile matter and higher Si content in the silica form (Table 4.1 and Figure 4.9), which has the potentiality to increase the stiffness of the composites [117,121,122]. However, the flexural strength of the fabricated composites did not follow a common trend, which could be due to the lack of similarity of particle dispersion and mixing uniformity in the fabricated composites [164]. Biochar particles are rigid in nature with low ductility and good compressive strength [17]. As a result, the incorporation of RHB in the PP matrix increased the flexural strength but reduced the tensile strength of the fabricated composite.

4.2.1.3 Hardness Test

Hardness test (Shore hardness in D scale) of the RHB reinforced PP composites and PP sheet was carried out using a durometer device. The shore hardness D test results are presented in Table 4.6.

Table 4.6: Shore hardness (D scale) test results of RHB reinforced PP composites

Sample Name	Sample No	Shore Hardness (D Scale)	Average Shore Hardness (D Scale)
100PP	1	76.00	75.50
	2	75.00	
	3	75.50	
PP-10RHB-400	1	77.50	78.33
	2	79.50	
	3	78.00	
PP-15RHB-400	1	78.50	78.83
	2	79.50	
	3	78.50	
PP-10RHB-550	1	79.00	78.83
	2	78.50	
	3	79.00	
PP-15RHB-550	1	80.00	79.50
	2	79.00	
	3	79.50	
PP-10RHB-700	1	78.00	78.17
	2	79.00	
	3	77.50	
PP-15RHB-700	1	79.00	79.00
	2	79.50	
	3	78.50	
PP-10RHB-850	1	78.00	78.33
	2	79.00	
	3	78.00	
PP-15RHB-850	1	79.50	80.00
	2	80.00	
	3	80.50	

From the results, it was also observed that the hardness of the composites increased when biochar prepared at higher temperatures were incorporated, and the hardness (shore D) values of all the composites were higher than that of PP. Moreover, the Shore D hardness increased with increasing RHB wt% in the composites and the trend was similar for all four biochar samples. The incorporation of biochar particles in polymeric matrix increased the hardness, which was due to the stiffening behavior of particle addition [117,165]. Thus, the presence of comparatively hard RHB particles in the PP matrix resulted in more rigid composite systems, and the more the RHB content, the higher the hardness of the composite. Figure 4.15 presents the hardness of 100PP and composites containing 10 wt% and 15 wt% of biochar prepared at different pyrolysis temperatures.

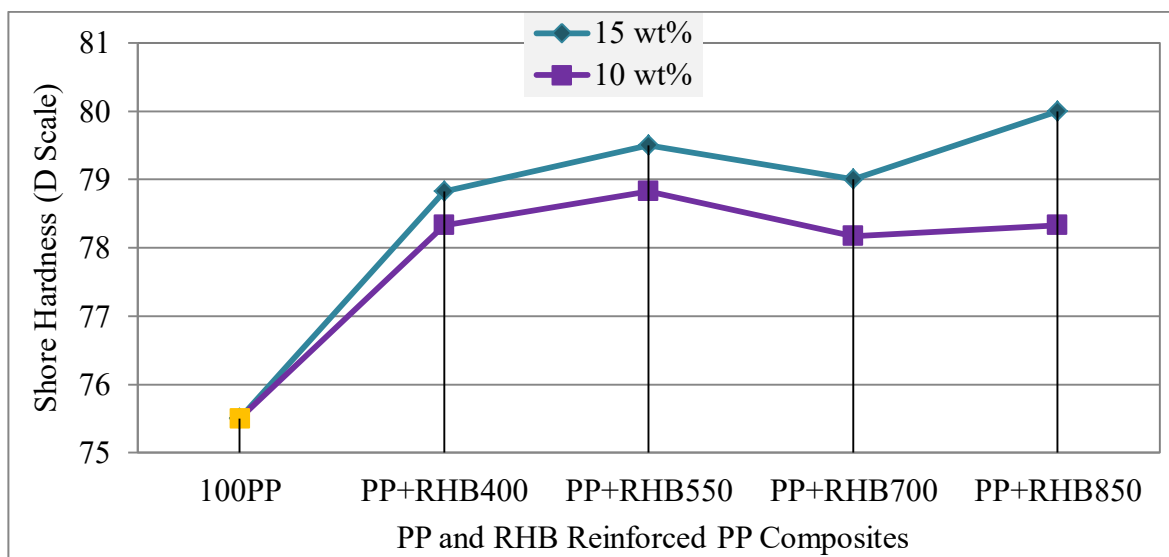


Figure 4.15: Hardness (Shore D) of composites containing 10 wt% and 15 wt% of prepared RHB reinforcements at different temperatures.

Composites with 10 wt% of RHB reinforcement exhibited better hardness than PP, maybe due to the inclusion of rigid particles as mentioned earlier. However, the results were very close and the hardness (shore D) values were between 78 and 79. The low amount of reinforcement addition (only 10 wt%) was not able to reveal the effect of biochar quality (due to temperature change) on the hardness of the composites. Incorporation of 15 wt% of RHB in composites resulted in further improvement of hardness than the 10 wt% biochar inclusion. Moreover, biochar pyrolyzed at higher temperatures found to be beneficial to improve the hardness of the composites. With increasing pyrolysis temperature ash and Si content of the RHB increases, moreover, the amount of volatile matter decreases. As a result, RHB prepared at higher temperatures could have more rigid particles [164]. The addition of hard reinforcing material in the PP matrix increased the ability to resist plastic deformation. Thus, increased rigidity of RHB particles with increasing pyrolysis temperature and a decrease in the inter-particle distance with increasing particle loading in the matrix increased the hardness of the composites. As a result,

highest hardness (shore D) was exhibited by PP-15RHB-850 composite which had higher biochar content and the biochar was prepared at the highest temperature among the RHB samples. Even though, the same technique was applied to fabricate every composite, ensuring much-defined particle dispersion pattern in every composite is very difficult. This could be the reason behind the varying trend of hardness change in the developed composites.

4.2.2 Morphological and Structural Analysis

4.2.2.1 EDX Analysis

There were RHB-like porous particles seen on the tensile fracture surface of the fabricated composites. As a result, SEM-EDX was utilized to confirm that the porous particles present on the surface were RHB. The EDX elemental analysis of a representative tensile fracture surface is shown in Figure 4.16.

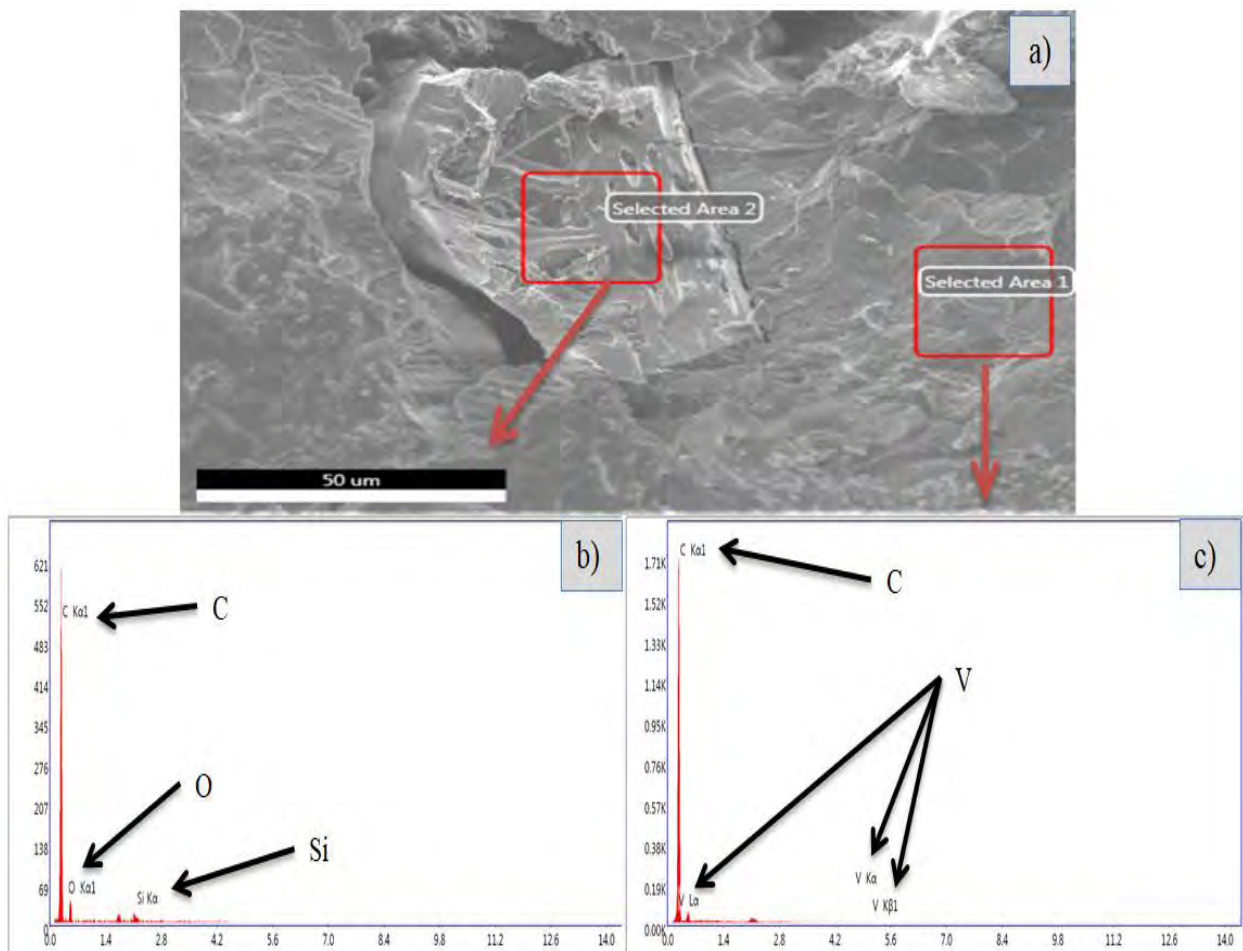


Figure 4.16: EDX analysis of the composite- a) area of analysis, b) EDX spectra of the point representing RHB particle in the composite (Area 2), c) EDX spectra of the point representing PP matrix in the composite (Area 1).

Figure 4.16 (a) presents the tensile fracture surface area of the composite where the EDX analysis was performed. A porous structure can be seen embedded in the matrix. Figure 4.17 (b) is the EDX spectra of the porous particle, where the presence of C, Si, and O can be observed. The spectra exhibited the main elements of the RHB (according to the EDX analysis of RHB, Figure 4.9), ensuring that the porous particles were RHB. However, in the spectra, the C concentration was much higher than that of RHB, maybe due to the penetration of PP in the pores of RHB. Finally, the EDX spectra presented in Figure 4.17 (c) shows a high C concentration with a trace amount of vanadium (V). This high C concentration was probable from the C skeleton of PP chains, hydrogen was not detected in the EDX spectra and the presence of V was maybe from the catalyst residue that was used for PP resin synthesis and left in the PP matrix. High C concentration and presence of transition metal (Ti, V, Pt, Ni, etc.) in the EDX spectra of PP was also reported by other researchers [166].

4.2.2.2 SEM Analysis

To study the morphology and structure of the composites, typical SEM images of the tensile fractured surface of PP and the composites were obtained. The RHB particles were homogeneously dispersed within the polymer matrix and do not tend to form agglomerates; besides, it can be observed that the particles were firmly embedded within the polymer matrix, indicating a good matrix-filler adhesion. In addition, in some composite samples, the porous structure of RHB was no longer observable, suggesting a partial filling of RHB porosity by PP. Figure 4.17 presented the SEM image of the tensile fracture surface of the PP sheet at a magnification of 1000 times.

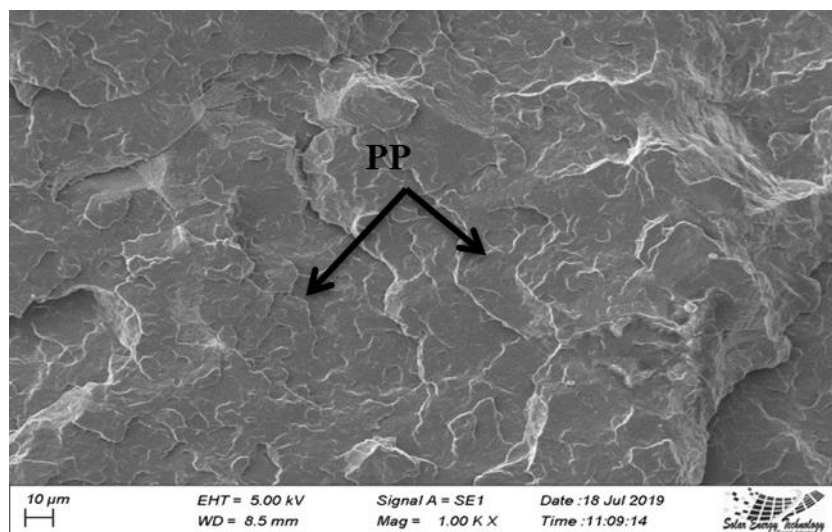


Figure 4.17: SEM micrograph of tensile fracture surface of PP.

The tensile fracture surface of PP presents a rough homogeneous surface with almost no sign of elongation. This was because the PP resin used in this study was SABIC PP575P, which is specially developed for rigid injection molding applications and the polymer exhibits very low

elongation (Table 3.1). Now, figure 4.18 shows the SEM image of tensile fracture surface of PP-10RHB-400 composite at a magnification of $\times 1000$.

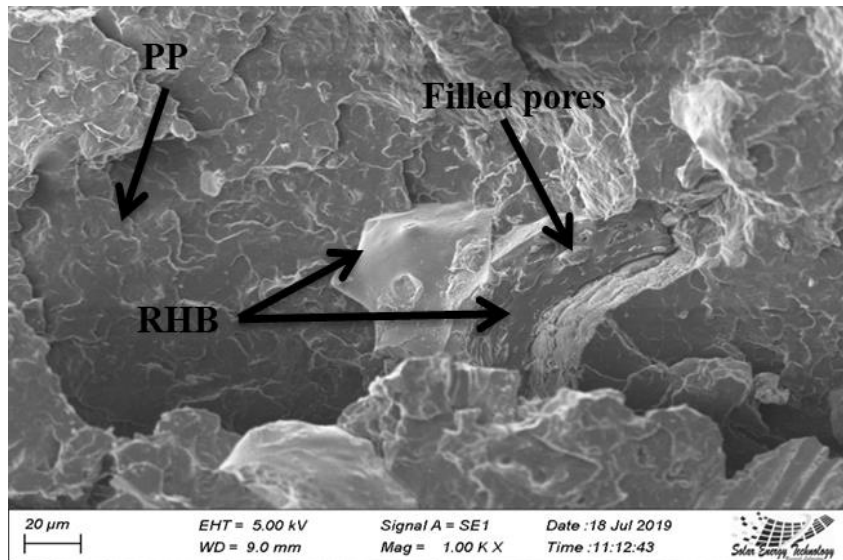


Figure 4.18: SEM micrograph of tensile fracture surface of PP-10RHB-400.

The image clearly revealed the spikey surface and internal porous of RHB (Figure 4.5) embedded in the PP matrix. The pores are filled and the filling material is most probably PP [133]. The RHB particle is well implanted in the PP matrix, indicating good surface adhesion and compatibility between RHB and PP. The SEM image of tensile fracture surface of PP-15RHB-400 at 1000 times magnification also revealed similar results (Figure 4.19). However, from the image it can be seen that the central pores of RHB particle were not filled, suggesting that PP only filled the pores located at the surface of the RHB particle.

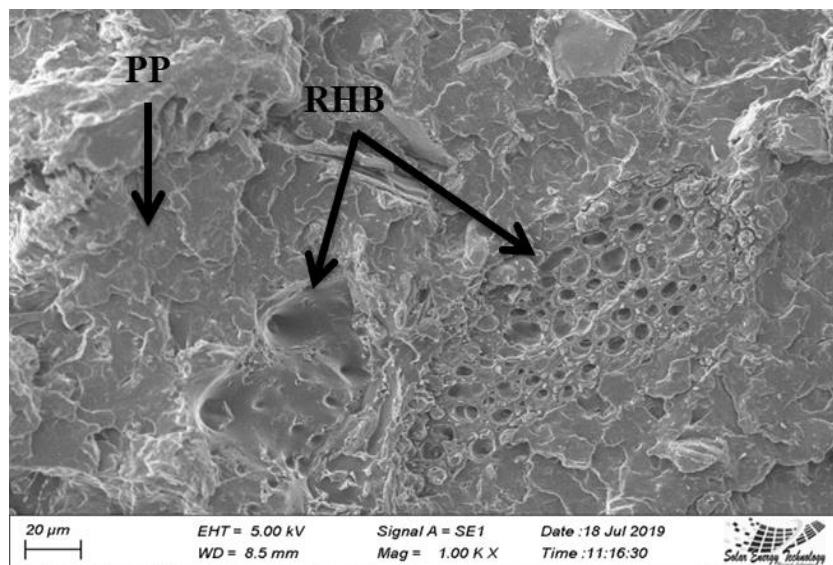


Figure 4.19: SEM micrograph of tensile fracture surface of PP-15RHB-400.

The tensile fracture surface of composites containing 10 and 15 wt% of RHB550 was investigated in Figure 4.20 and 4.21. The SEM images were captured at 1000 times magnification and according to the images RHB550 also exhibited good surface bonding and compatibility with PP. Similar to the SEM images explained above, some pores of RHB were not blocked (Figure 4.20) and some others were filled most probably by PP (Figure 4.21). Thus as expected, the molten PP had infiltrated into the surface pores of RHB particles in the composites, and a physical/mechanical interlocking was formed, which is so different from fiber-polymer composites [126] and this is the cause for enhanced mechanical strength in the composites.

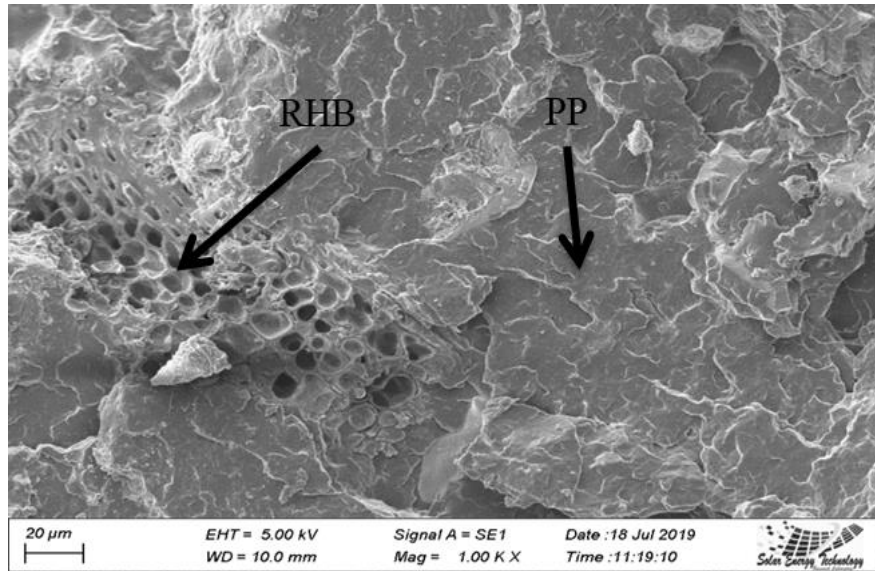


Figure 4.20: SEM micrograph of tensile fracture surface of PP-10RHB-550.

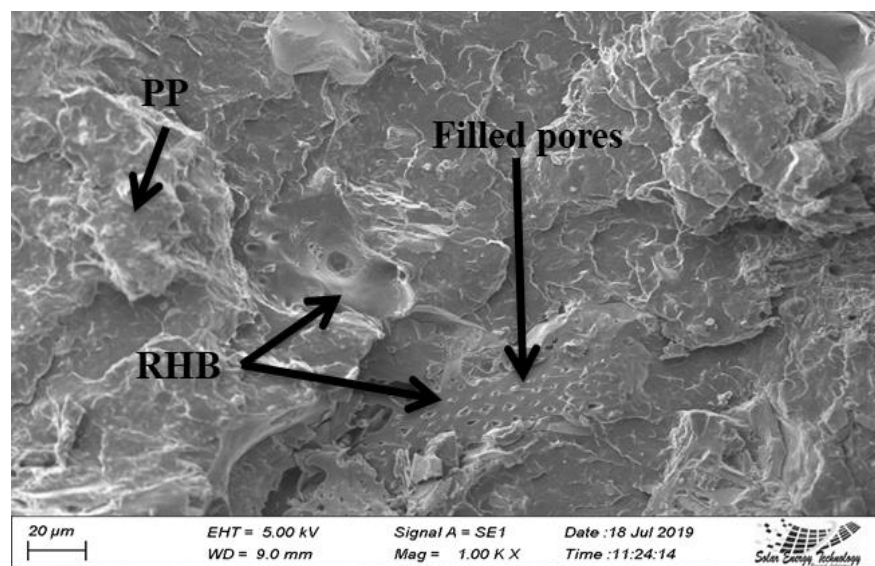


Figure 4.21: SEM micrograph of tensile fracture surface of PP-15RHB-550.

The SEM micrograph of the tensile fracture surface of the composite containing RHB700 (PP-10RHB-700) at 1000 times magnification was presented in Figure 4.22.

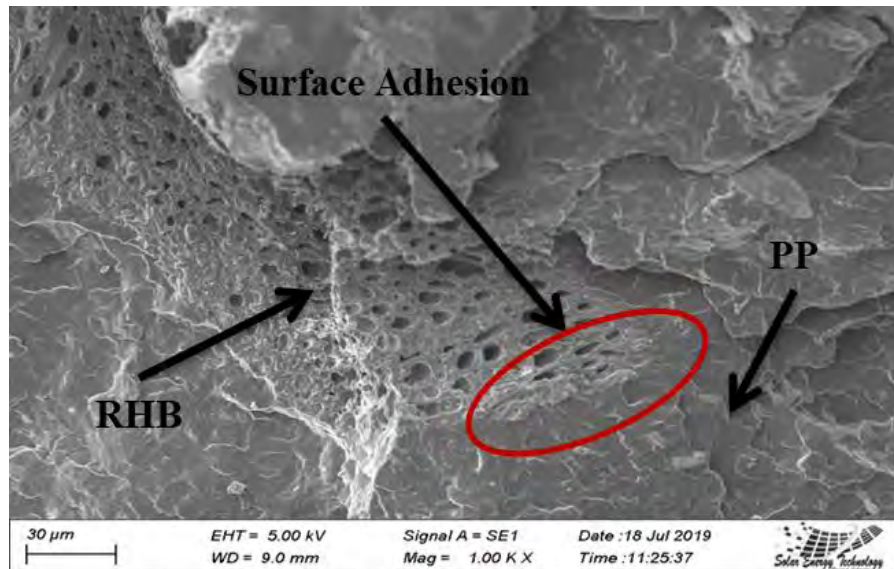


Figure 4.22: SEM image of tensile fracture surface of composite containing RHB700.

The SEM image showed a porous structure of the RHB700 particle embedded in the PP matrix similar to the pictures presented above. The image also presented a smooth and uniform interface (red circle), which revealed a good surface adhesion and compatibility between RHB and PP. RHB particles were embedded in the PP matrix and the matrix held the RHB particle very tightly. Figure 4.23 showed the red circled area in Figure 4.23 with a higher magnification of $\times 5000$.

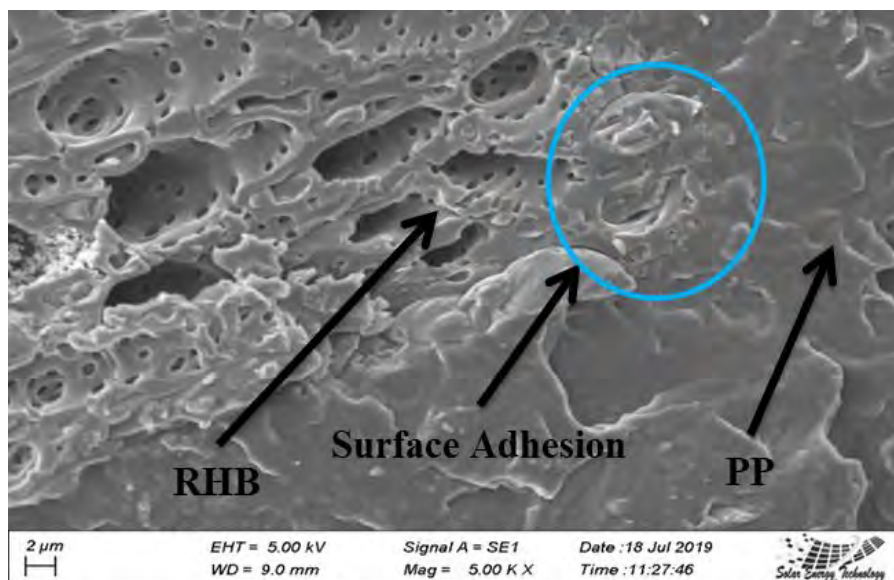


Figure 4.23: Image of circled area in figure 4.24 with $\times 5000$ magnification.

The SEM image in Figure 4.23 clearly showed the micro-pores and macro-pores present in the honeycomb structure of RHB700 (upper left side), the PP matrix (right side), and the excellent interfacial bonding between RHB700 and PP (blue circle). It should also be noted from the SEM image (Figure 4.23) that although surface bonding and compatibility can be observed, the amount of PP penetrated the pores of biochar was minimal, which meant that not only the interlocking between RHB and PP in the composite but also the bonding effect of PP were greatly weakened. This could be the reason behind the comparatively low tensile strength of composites containing RHB700 (Table 4.4). The morphology of the tensile fracture surfaces after the uniaxial tensile test of the composite containing RHB850 (PP-10RHB-850) is shown in Figure 4.24.

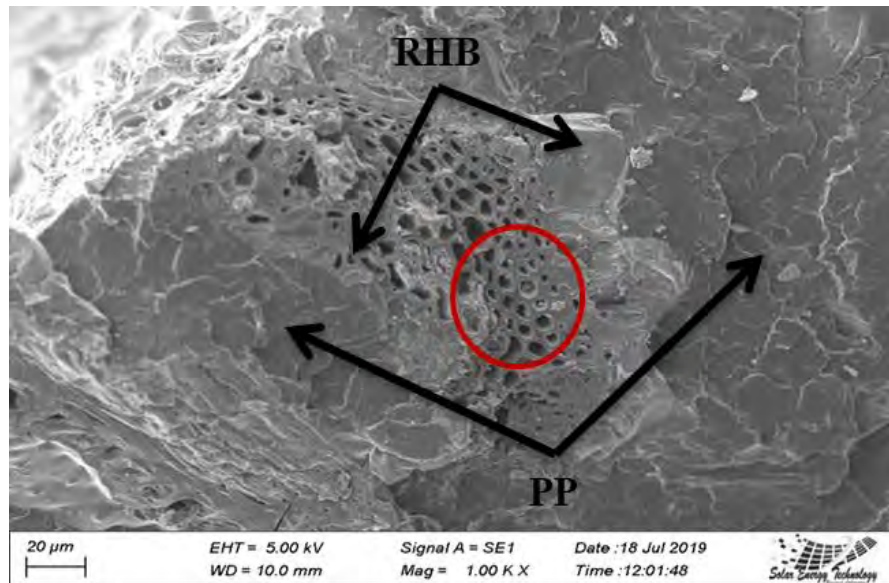


Figure 4.24: SEM image of tensile fracture surface of composite containing RHB850 at $\times 1000$ magnification.

It can be seen from Figure 4.25 that an RHB850 particle is embedded uniformly in the PP matrix and both the spikey outer surface and the honeycomb internal structure of the biochar were properly bonded with the PP matrix. This revealed the excellent compatibility between RHB850 and PP in the composite. Moreover, the penetration of PP in the honeycomb structure of RHB was also observed. The RHB850 showed comparatively better interfacial interaction between the matrix and the reinforcement, as compared to other composites prepared with RHB obtained at lower pyrolysis temperatures. This improved interfacial bonding can be attributed to the large surface area and porous structure of RHB synthesized at higher temperatures [133]. For better observation of the PP filled RHB pores, the circled area in Figure 4.24 was shown in Figure 4.25 below with higher ($\times 5000$) magnification, which revealed that a large number of pores were filled with PP. However, PP was not able to penetrate all the pores, especially the central pores following the complex pore channels in the honeycomb structure of RHB.

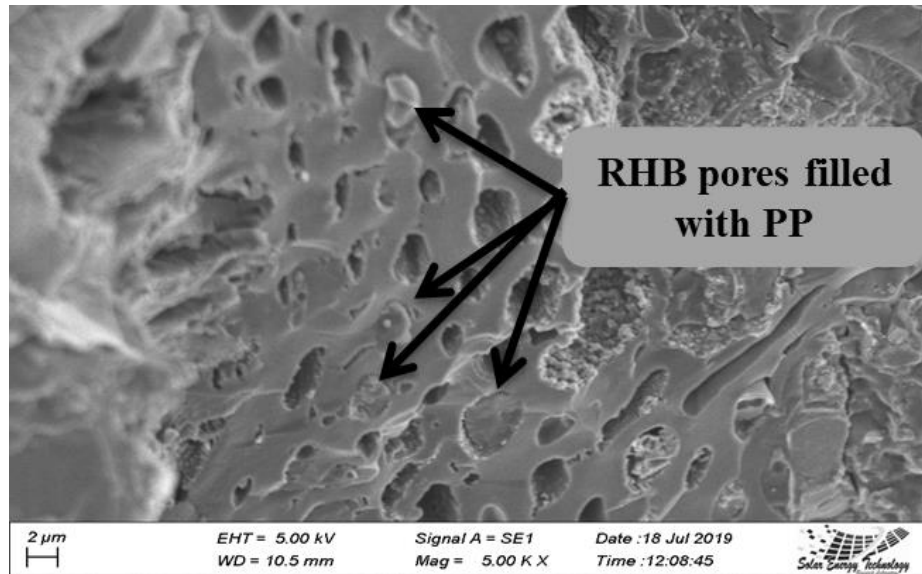


Figure 4.25: SEM micrograph of tensile fracture surface of PP-10RHB-850 composite at $\times 5000$ magnification.

The tensile fracture surface of PP-15RHB-850 composite also exhibited an RHB particle, in which pores were filled with PP (Figure 4.26).

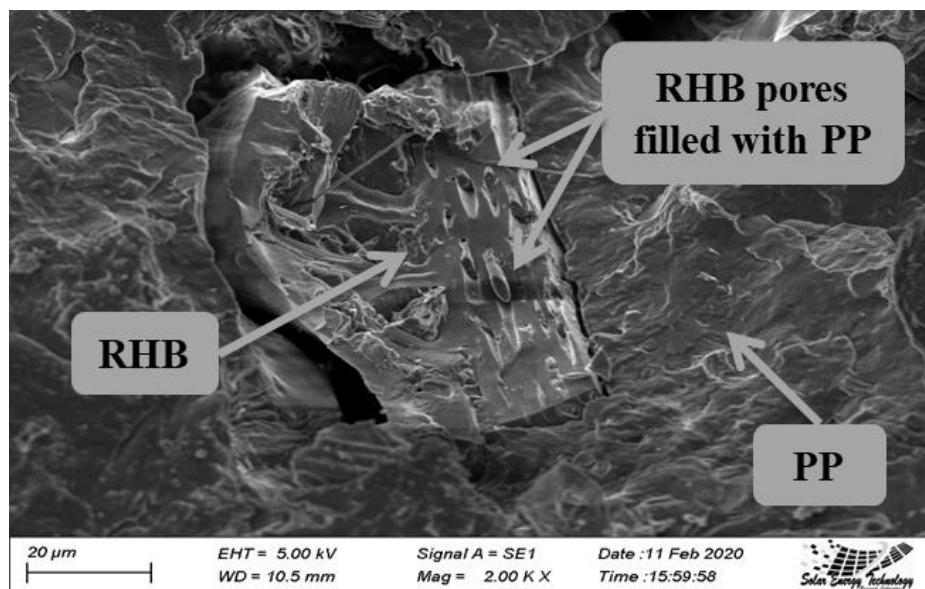


Figure 4.26: SEM micrograph of tensile fracture surface of PP-10RHB-850 composite at $\times 5000$ magnification.

As presented in Figure 4.26, the RHB850 embedded in PP has its pores filled with PP. The molten PP resin, during composite processing, penetrates into RHB pores, which results in better interlocking between reinforcement particle and matrix [127]. The RHB particle shown in Figure 4.26 was smaller and more filled with PP than the RHB particle in Figure 4.25, suggesting that

smaller particles allow better PP penetrations. This could be due to the fact that smaller RHB particles contain less complex pore channels in the honeycomb structure, allowing better infiltration of PP resin.

For good mechanical strength, proper interfacial bonding between the reinforcing particles and the matrix is very crucial, and ultimately it must lead to an efficient and uniform transfer of applied stress. The reinforcing particles might pull out from the matrix due to the lack of interfacial adhesion and cause degradation of the reinforcing effect [133]. In all the RHB reinforced PP samples, it was observed that the biochar particles were firmly embedded in the PP matrix due to their porous structure and potential compatibility with PP resin. Moreover, the molten PP has penetrated a large number of pores of the biochar particles in almost all the composite samples. This resulted in large networks of mechanical interlocking between the RHB particles and the matrix, which consequently enhanced the flexural strength and the hardness (shore D) of the composites. It is apparent, that, with the increase in the wt% of RHB, the pore infiltration in particles would be more extensive. Thus, the mechanical properties might improve with increasing wt% of RHB in the composites [2]. This statement is in agreement with the mechanical properties test results found in this study.

4.2.2.3 XRD Analysis

Figure 4.27 presents the XRD spectra of the PP used in this study. It can be clearly observed that the semi-crystalline nature of PP had contributed for the peaks at around 14°, 16°, 18°, 21°, 22°, 25°, 29°, and 43°.

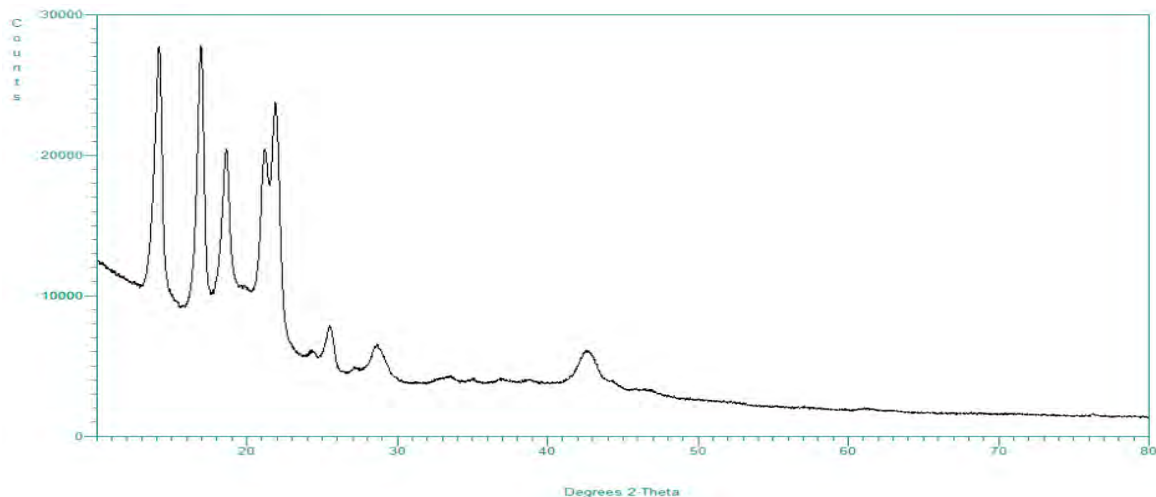


Figure 4.27: XRD spectra of PP.

The PP exhibited sharp spectra, suggesting that peak shape is not only affected by the degree of crystallinity but also by crystal size [135]. Consequently, the percentage of crystallinity in PP was high. The XRD spectra of the RHB reinforced PP composites are shown in Figure 4.28 and compared with neat PP.

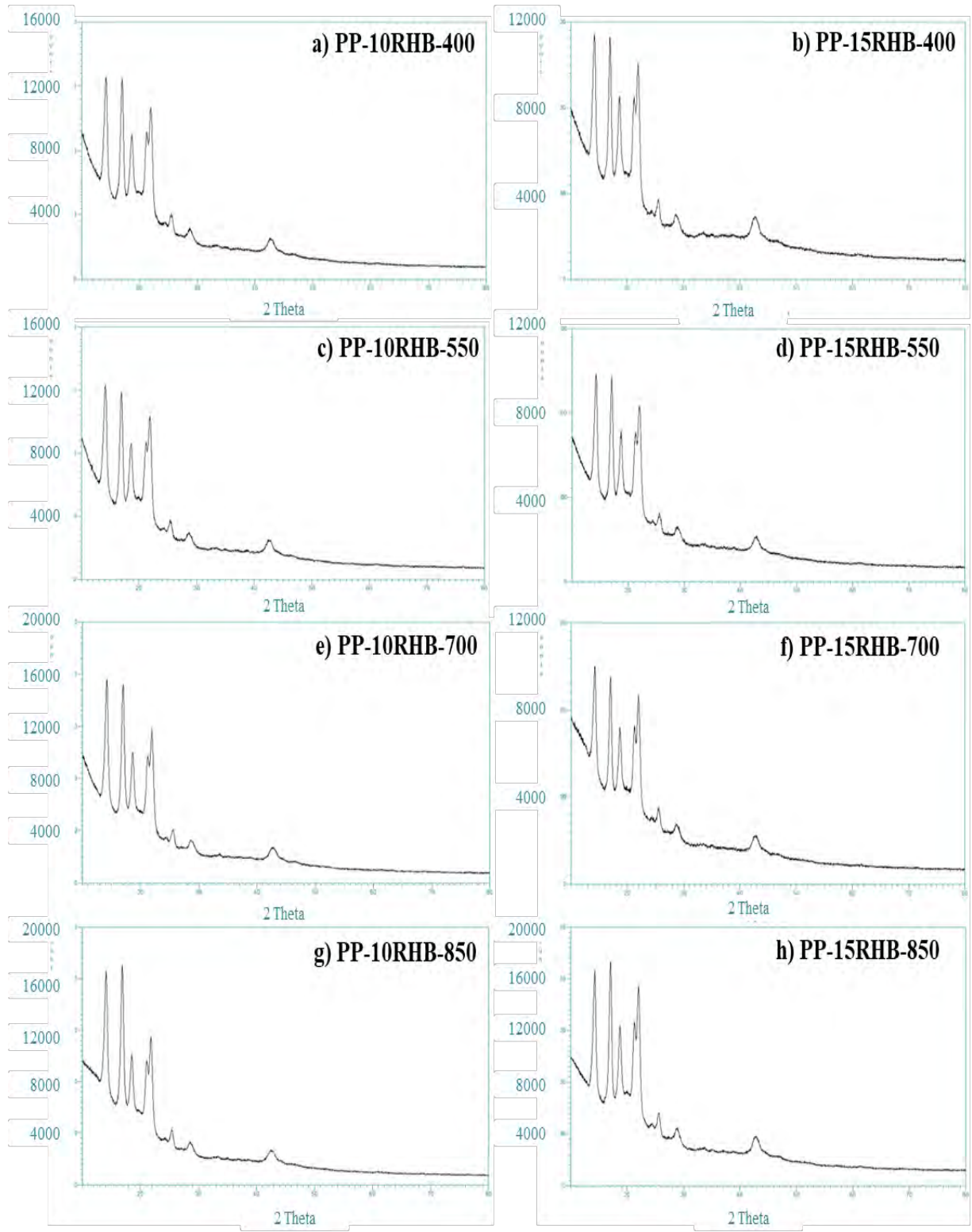


Figure 4.28: XRD spectra of RHB reinforced PP composite- a) PP-10RHB-400, b) PP-15RHB-400, c) PP-10RHB-550, d) PP-15RHB-550, e) PP-10RHB-700, f) PP-15RHB-700, g) PP-10RHB-850, and f) PP-15RHB-850.

From Figure 4.28 it can be observed that the crystallinity of the RHB reinforced PP composites was contributed mostly by the PP, as the shape and position of different peaks were similar to the spectra of PP. Thus, all the main diffraction peaks appearing in the spectra of the composites were contributed by PP rather than RHB, which revealed that RHB was amorphous in nature. It is important to mention that, as RHB samples were prepared at temperatures below 1000⁰C, the silica present in the biochar was mostly amorphous in nature [152]. Besides, it should be noted that with increasing RHB content, the intensity of the peaks decreased for all four biochar samples, which indicated that the increase of RHB content may have a negative effect on the crystallinity of PP. The reason was that the lack of crystalline PP in the composites with a high loading of RHB caused the reduction of XRD peak intensities. A similar reduction of peak intensity in the biochar reinforced polymer composites was observed by other researchers also [2,126,135,164].

On the other hand, by comparing spectra (a) with (g) and/or (b) with (h) in figure 4.29, it is clear that a general reduction in peak intensity was observed when biochar pyrolyzed at lower temperatures were added in the composites. RHB has a high presence of silica and the amount of silica increased with increasing pyrolysis temperatures [11]. Moreover, the crystallinity of the RHB derived silica increases with increasing process temperature [152]. Thus, RHB850 has the best crystallinity among the developed RHB samples. As a result, composites containing RHB850 exhibited a higher degree of crystallinity among the fabricated composites.

To observe the effect of RHB incorporation on the crystal structure of PP in the composites, Figure 4.29 illustrates the XRD spectra of 100PP and the fabricated composite PP-15RHB-400 in one image.

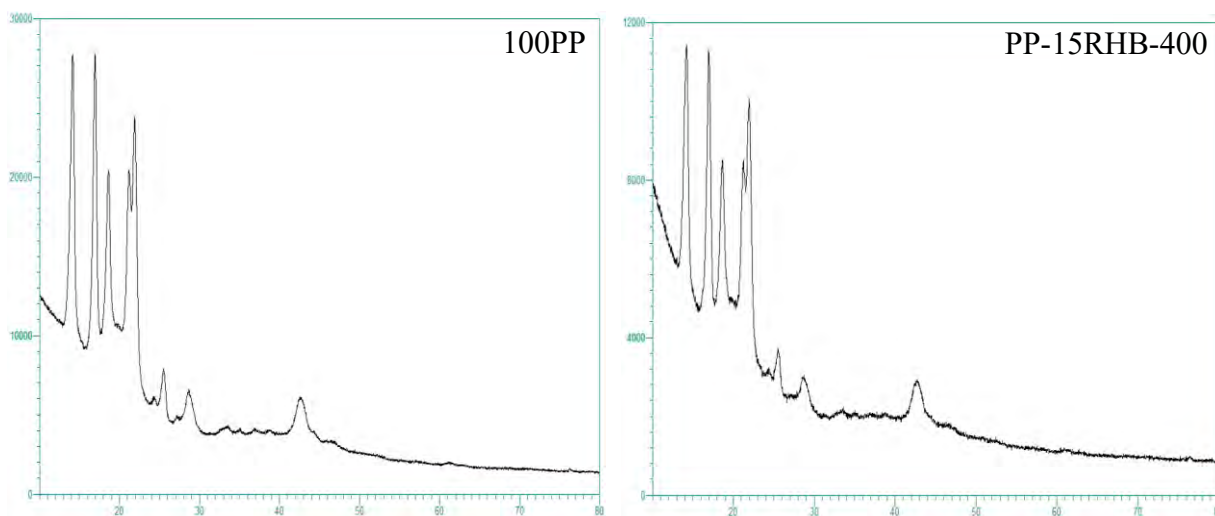


Figure 4.29: Comparison of the XRD spectra of 100PP and PP-15RHB-400

Figure 4.29 indicates that the addition of RHB samples showed almost no effect on the crystal structure of the PP. This could be due to the lower content of RHB in the composites and the

absence of major reactions between RHB and PP, except surface adsorption. Similar results were also reported by Zhang et al. and Das et al. [126,167]. As a result, the addition of RHB had very little effect on the crystalline structure of PP though RHB incorporation could change the crystallinity of the RHB reinforced PP composites.

4.2.3 Analysis of Thermal Properties

4.2.3.1 Thermogravimetric Analysis

The thermal stability of polymeric composites is a crucial parameter since the thermal stability of the thermoplastic polymer matrix can be a limiting factor in both processing and end-use applications of the developed composite [6]. Thermal degradation of the PP and RHB reinforced PP composites was determined from the weight loss during heating. The weight loss % (TGA) and the derivative weight change (DTG) curves are discussed in this section. The thermogravimetric curves (TGA and DTG) of PP are illustrated in Figure 4.30 below.

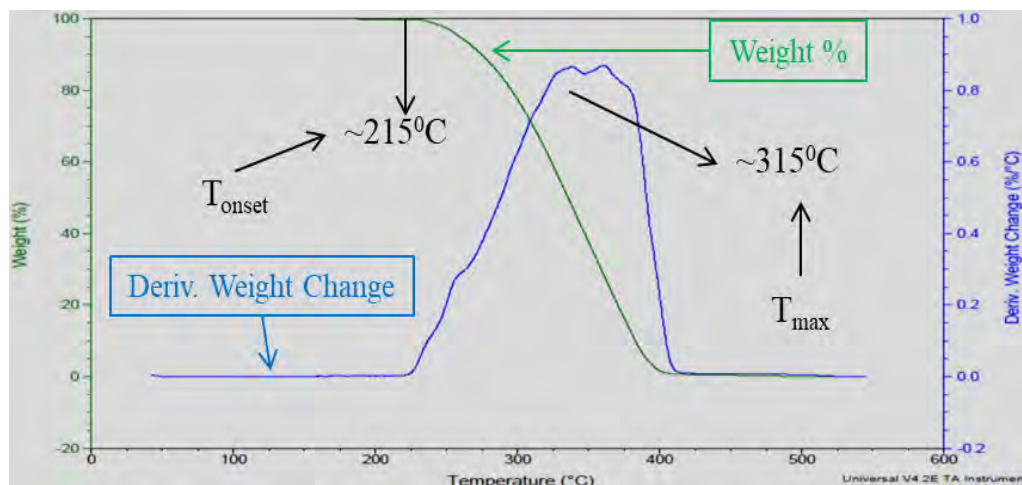


Figure 4.30: TGA and DTG curves of PP.

In Figure 4.31 the green line is the weight loss (TGA) curve and the blue line is the derivative weight loss (DTG) curve. The thermal decomposition of PP was marked by two distinct points, one was at around 215^oC (onset degradation temperature, T_{onset}) and another one was at around 315^oC (the temperatures at the maximum mass loss rates, T_{max}). The thermal decomposition of PP occurred mainly by chain transfer and random chain scission reactions and released decomposed products such as pentane and heptane [167]. From Figure 4.30 it is also observed that the degradation of PP occurred in one step leaving almost no residue [134].

Now the thermal degradation behavior (TGA and DTG curves) of the RHB reinforced PP composites are presented in Figure 4.31 for better understanding the effect of RHB on the thermal stability of the composites.

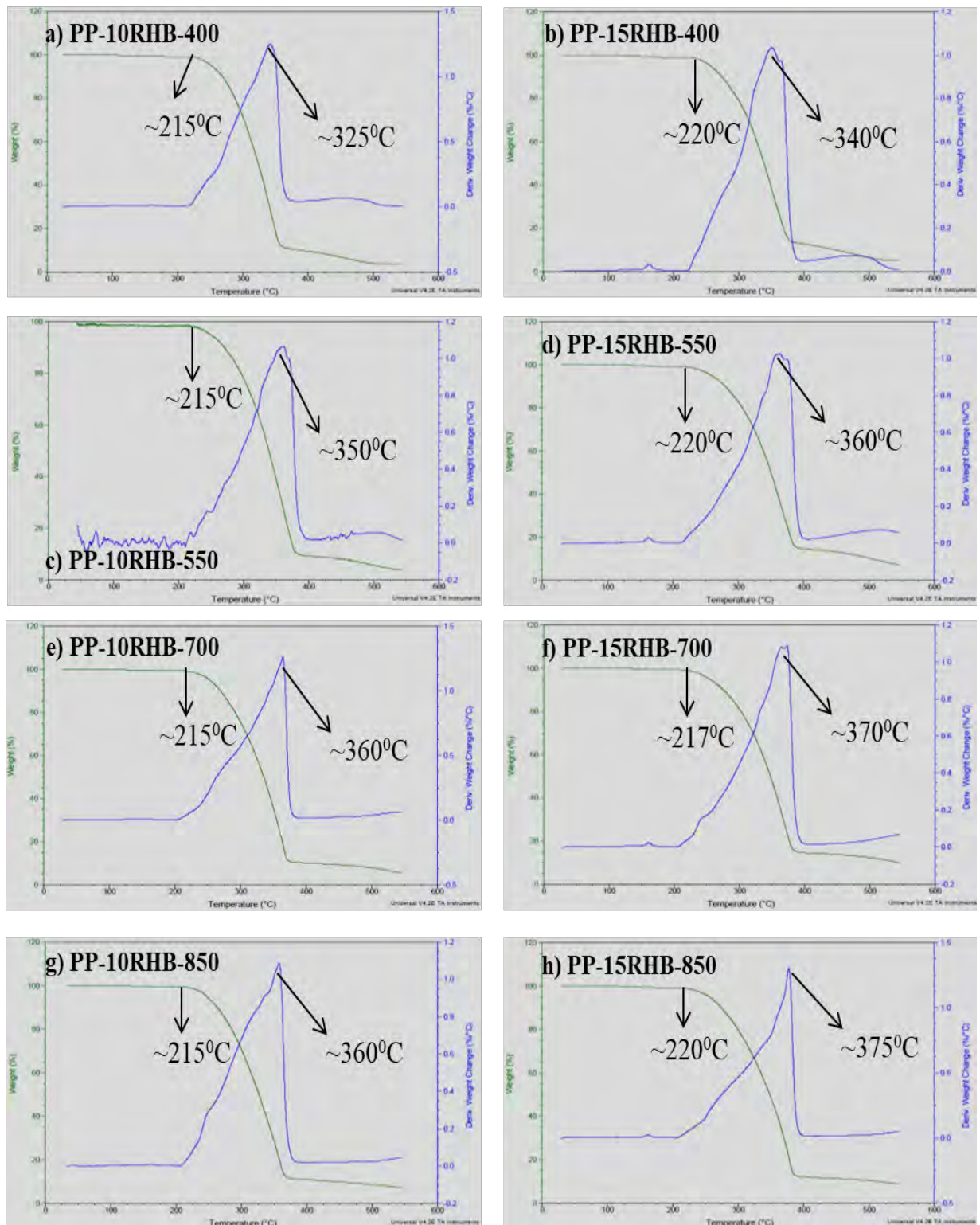


Figure 4.31: TGA and DTG curves of RHB reinforced PP composite- a) PP-10RHB-400, b) PP-15RHB-400, c) PP-10RHB-550, d) PP-15RHB-550, e) PP-10RHB-700, f) PP-15RHB-700, g) PP-10RHB-850, and f) PP-15RHB-850.

The values of the degradation initiation temperature/ onset degradation temperature, T_{onset} (left) and the temperatures at the maximum mass loss rates, T_{max} (right) were marked on every thermogravimetric curve as shown in Figure 4.31. It can be observed from the figure that the thermal degradation of the composites occurred in a single step which was similar to the degradation curve of PP. Figure 4.32 also indicated that RHB reinforced PP composite with 10 wt% of the developed RHB samples showed onset degradation temperatures similar to that of PP. However, a composite containing 15 wt% of the developed RHB samples exhibited a delayed onset degradation temperature compared to the neat PP. On the other hand, the temperature at maximum mass loss rates, T_{max} of the composites was also delayed by not only the higher RHB content but also by increasing the pyrolysis temperature of the RHB. This delay in thermal decomposition is an indication of improved thermal stability of the composites, which was due to the incorporation of the thermally stable biochar [2,18,133,134,167]. Amongst the fabricated composite samples, it can be observed that the PP-15RHB-850 showed higher thermal stability than the other composites.

This improved resistance toward thermal degradation can be attributed to the barrier effect of the added RHB to the PP matrix, causing mass transfer limitations of volatile gases produced during thermal transformation [133]. The biochar is considered to be an amorphous material that is structurally disordered in nature [2]. Some rearrangement of molecular layers in the biochar takes place between the carbon chains and/or carbon molecules depending on the temperature of pyrolysis and residence time [133]. Such type of carbon network transformation into the turbostratic stack-like structure of the biochar has already been reported [18,133]. This thermally stable turbostratic stack-like structure of the biochar helps to delay the thermal degradation of the polymeric matrix. From the above discussion, it becomes clear that the addition of RHB in the PP based composites has a positive response when thermal stability is concerned. Moreover, the inherent thermal stability increment of RHB with increasing pyrolysis temperature helps the fabricated composites to sustain higher thermal decomposition temperatures.

4.2.3.2 DSC Analysis

Figure 4.32 illustrates the heating thermogram of PP.

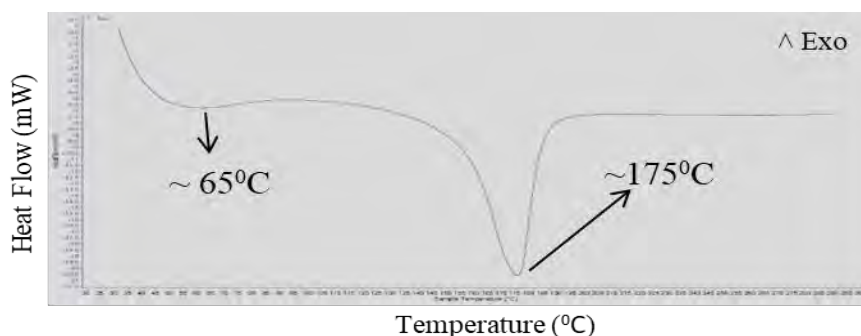


Figure 4.32: DSC curve of PP.

The DSC thermogram of neat PP showed two endothermic peaks. The first endothermic wide peak around 65°C was due to the moisture and volatile removal [168] and the second sharp peak was due to the endothermic melting of PP at around 175°C . Now the DSC curves of all the RHB reinforced PP composites are presented in Figure 4.33 below.

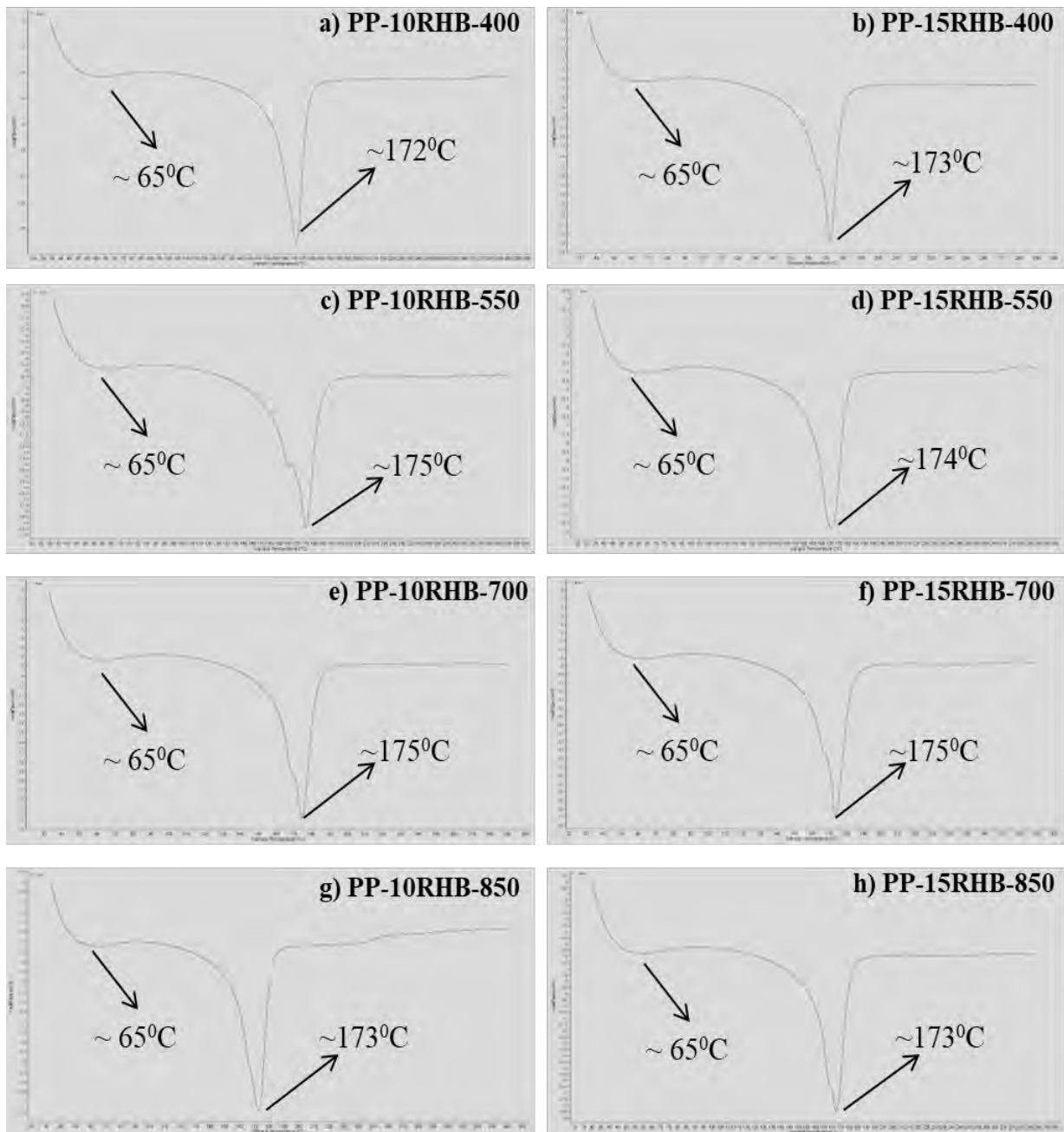


Figure 4.33: DSC curves of RHB reinforced PP composite- a) PP-10RHB-400, b) PP-15RHB-400, c) PP-10RHB-550, d) PP-15RHB-550, e) PP-10RHB-700, f) PP-15RHB-700, g) PP-10RHB-850, and f) PP-15RHB-850.

As presented in Figure 4.33, the composites exhibited DSC curves similar to that of PP. Accordingly, the first endothermic curve was due to the moisture and volatile removal [168] and the second endothermic peak was caused by the melting of the composites. The melting temperature of RHB reinforced PP composites had almost no shift compared to neat PP, which means that the endothermic melting in between 172⁰C and 175⁰C was caused by a typical melting behavior of PP, and the addition of RHB had a negligible effect on the melting temperature of the composites [14]. The PP resin used in this study had an isotactic structure. The isotactic PP has the highest melting temperature among the three types of PP and the melting temperature might be reduced if the tacticity of PP is altered [169,170]. During composite fabrication, the melt-blending of PP resin and addition of RHB particles has the potentiality to disrupt the tacticity of PP causing a slight decrease in the melting temperature [171]. Thus, the little reduction of melting temperature observed in some composites was probably due to the change of tacticity, rather than RHB addition. Moreover, the type of RHB was also found to have almost no impact on the melting temperature of the fabricated composites. A similar result was also found by several researchers while studying different biochar reinforced polymer composites [18,126,133]. Thus, the RHB incorporation into the PP matrix had a negligible effect on the melting temperature (T_m) of the developed composites.

4.2.4 Analysis of Electrical Properties

4.2.4.1 Resistance Measurement

Generally, biochar contains a notable amount of amorphous carbon structures and turbostratically stacked graphene sheets, especially when the biochar is prepared at higher temperatures [18,129]. Moreover, rice husk derived biochar has a significant amount of silica (Table 4.2) that is semiconducting material. Thus, the incorporation of RHB has the potentiality to improve the electrical properties of the resulting composites. Table 4.7 presents the resistance (R) of PP and the developed composites at 100 Hz and 18⁰C.

Table 4.7: Resistance of PP and the developed RHB reinforced PP composites

Test Sample	Resistance, R ($\times 10^{07} \Omega$)
100PP	4.30
PP-10RHB-400	6.09
PP-15RHB-400	6.24
PP-10RHB-550	4.50
PP-15RHB-550	5.81
PP-10RHB-700	3.84
PP-15RHB-700	3.71
PP-10RHB-850	4.22
PP-15RHB-850	3.53

As presented in Table 4.7, the resistance of PP at 100 Hz was $4.30 \times 10^7 \Omega$. On the other hand, the resistance of the composites followed two different trends. Composites containing RHB pyrolyzed at lower temperatures (400 and 550°C) exhibited much higher resistance than PP and the resistance of the composites increased with increasing biochar content. This could be due to the higher presence of lignocellulosic residue in the RHB prepared at lower temperatures (section 4.1.6.2). The lignocellulosic residue is nonconductive and thus increases the resistance of the composite. Figure 4.34 shows the resistance of composites containing 10 wt% of RHB prepared at different temperatures and presents the change of resistance with changing pyrolysis temperatures.

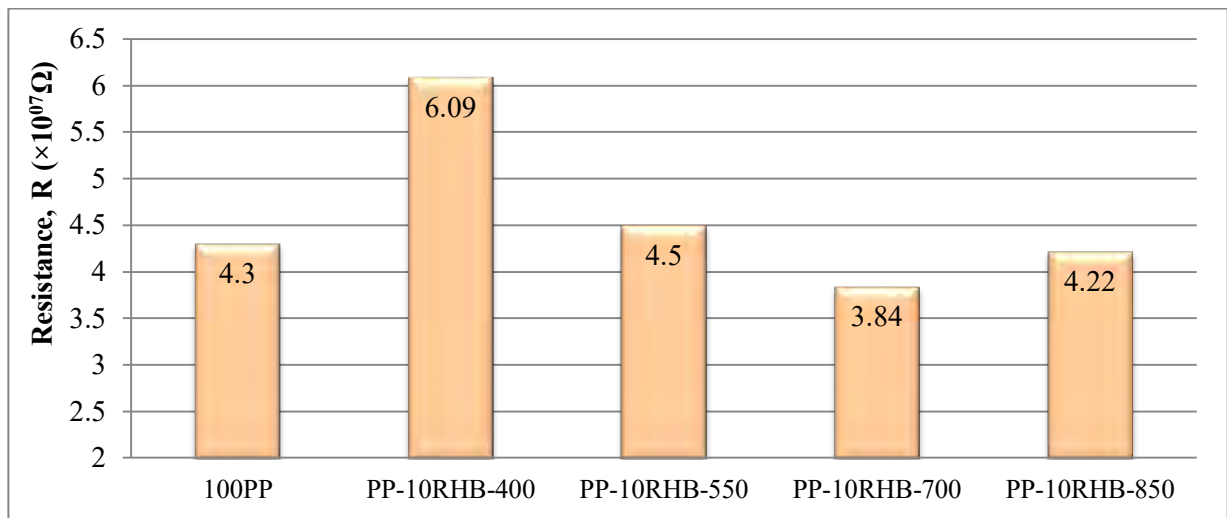


Figure 4.34: Resistance of PP and composites containing 10 wt% of four different RHB samples.

Composites containing 15 wt% of prepared RHB samples also exhibited a similar trend and the resistance of the composites decreased with increasing pyrolysis temperatures (Figure 4.35).

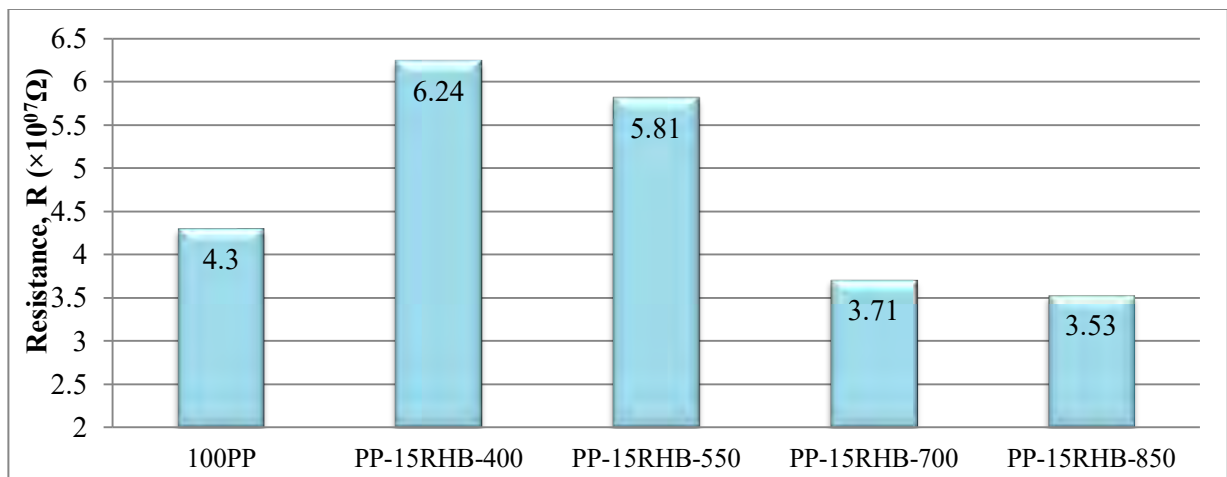


Figure 4.35: Resistance of PP and composites containing 15 wt% of prepared RHB samples.

Biochar prepared at higher temperatures exhibit better conductivity due to the formation of graphitic structures [129]. However, enough conductive particles are needed to create a proper conductive network in the polymer matrix, which can significantly reduce the resistance of the composite [18]. So, the low carbon content of RHB850 could be the reason behind higher resistance of PP-10RHB-850 composite, and with increasing biochar loading there were enough particles present in the PP matrix, which reduced the resistance of PP-15RHB-850. Moreover, the silica content of the RHB increased with increasing pyrolysis temperature. Thus, the presence of graphite and high silica content (Figure 4.10) could be the reason behind reduced resistance of the composites containing RHB700 and RHB850, where increasing RHB loading further decreased the resistance of the composites.

RHB prepared above 700⁰C has the potentiality to decrease the resistance of PP matrix and increasing RHB content (prepared at higher temperatures) was found to have a positive impact when the reduction of resistance is concerned.

5.1.4.2 Impedance Measurement

Impedance, denoted Z, is the total effective resistance of a material when subjected to alternating current, and arising from the combined effects of resistance and reactance [172]. Table 4.8 presents the impedance (Z) of PP and the fabricated composites at 100 Hz and 18⁰C.

Table 4.8: Impedance of PP and the fabricated RHB reinforced PP composites

Test Samples	Impedance, Z ($\times 10^{08} \Omega$)
100PP	1.66
PP-10RHB-400	1.53
PP-15RHB-400	1.56
PP-10RHB-550	1.57
PP-15RHB-550	1.61
PP-10RHB-700	1.60
PP-15RHB-700	1.40
PP-10RHB-850	1.54
PP-15RHB-850	1.46

The impedance of all the composites was found to be less than that of PP. Similar to resistance measurement results, composites containing low-temperature biochar (400 and 550⁰C) exhibited increased impedance with increased RHB content, but composites containing biochar prepared at higher temperatures (700 and 850⁰C) exhibited decreased impedance with increased RHB content. On the other hand, among the fabricated composites lowest impedance was exhibited by

PP-15RHB-700, rather than PP-15RHB-850. Impedance is a complex measure, where overall effective resistance due to alternating current is taken into account. The electrical conductivity of biochar is highly dependent on its carbon content [173]. RHB700 was found to have higher C content than RHB850, which could be the reason behind the lower impedance of PP-15RHB-700. Thus, RHB prepared at higher temperatures has the potentiality to decrease the impedance of the RHB reinforced PP composites if the C content of the biochar is high. A schematic illustration of the change of impedance due to RHB type and loading is presented in Figure 4.36.

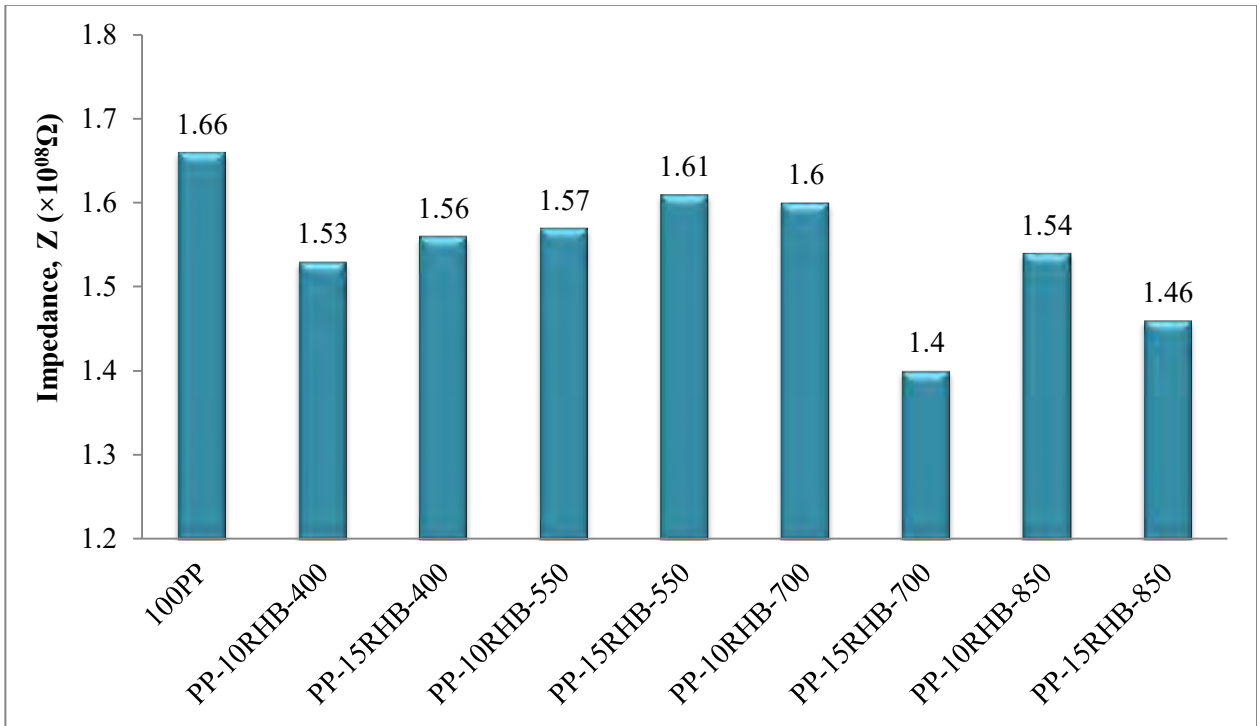


Figure 4.36: Impedance of PP and fabricated composites.

Therefore, the fabricated RHB reinforced PP composites exhibited noteworthy improvements in several mechanical, thermal and electrical properties when compared with PP and other comparable composites. A general comparison of the properties of RHB reinforced PP composites fabricated in this study with PP and other related composites so far developed is attached in Appendix A.

Chapter 5

Conclusion and Recommendations for Future Work

5.1 Conclusion

Biochar with high carbon and silica content was obtained by slow pyrolysis of rice husk and it was used to fabricate RHB reinforced PP composite. After investigating the properties of biochar and the developed composites the results can be interpreted as follows:

- Biochar derived from rice husk via slow pyrolysis exhibited high yield and the char was basic ($\text{pH} > 7$) in nature. With increasing pyrolysis temperature, the ash and silica content of the biochar increased, while the C content slightly decreased after 550°C . The biochar samples had a porous structure and the thermal stability of the samples increased with increasing pyrolysis temperature.
- The tensile strength of all composites decreased when compared with neat PP. However, a slight increase of tensile strength was observed with increasing RHB content and the best tensile strength was exhibited by PP-15RHB-550. On the other hand, flexural strength and hardness of the composites increased. Accordingly, PP-15RHB-850 composite exhibited the maximum flexural strength of 70.61 MPa (10.22% higher than that of PP) and hardness of 80 in the Shore D scale (5.96% higher than that of PP). However, the flexural strength of composites containing 10 wt% of all biochar samples was lower than that of PP, but it increased with increasing biochar content and became higher than the flexural strength of PP. On the other hand, all composites exhibited higher hardness than PP.
- SEM images and EDX analysis revealed good interfacial adhesion and compatibility in the composite between RHB and PP.
- The addition of RHB did not affect the crystal structure of PP in the developed composites but reduced the intensity of the crystalline peaks of the composites.
- RHB prepared at higher temperatures (700 & 850°C) has the potentiality to increase the thermal stability of the composites, but RHB incorporation has a negligible effect on the melting temperature of the PP matrix.
- Composites containing RHB prepared at higher temperatures (700 & 850°C) and have higher RHB content showed lower resistance and impedance.

Evaluating the characteristics of the developed biochar and composite, it can be concluded that rice husk derived biochar is a potential reinforcing material for composite fabrication. RHB reinforced PP composites exhibited improvements in mechanical, thermal, and electrical properties, when compared with neat PP. Except for a little deviation, the improvements of the composite properties were found to be better when the RHB content in the composites was increased (15 wt%) and the incorporated RHB was pyrolyzed at higher temperatures (700 and 850°C). The minor deviation might be due to the lack of homogeneous mixture formation of light RHB powder into the PP matrix during composite fabrication.

5.2 Recommendations for Future Work

Based on the findings of the present research work the recommendations for future work in this field of research involve the following:

- Composites with RHB contents higher than 15 wt% can be studied to determine the trend of different properties changes.
- The effect of the RHB particle size on the properties of the composite can be investigated.
- The extent of uniform mixing of RHB particles in the PP matrix can be examined to determine the effect of particle dispersion on the properties of the composite.
- In this study, RHB prepared at higher temperatures exhibited better performances. So, composites containing RHB pyrolyzed at higher temperatures (higher than 850⁰C) can be studied.
- RHB is organic reinforcement, so biodegradability of the composite can be studied in further research.
- The water absorption test can be carried out in order to determine the effect of RHB addition on the water absorption ability of the composite.

References

- [1] W. Yao, S. Qian, K. Sheng, and H. Zhang, (2016) "Composites of Polypropylene Reinforced with Ultrafine Bamboo-char: Morphology, Mechanical and Thermal Properties," in *2016 ASABE Annual International Meeting*, American society of agricultural and biological engineers, p. 1.
- [2] O. Das, D. Bhattacharyya, D. Hui, and K.-T. Lau, (2016) "Mechanical and flammability characterisations of biochar/polypropylene biocomposites," *Composites part B: engineering*, Vol. 106, pp. 120-128.
- [3] F. Abnisa, A. Sharuddin, S. Dayana, M. F. bin Zanil, W. Daud, W. M. Ashri, I. Mahlia, and T. Meurah, (2019) "The Yield Prediction of Synthetic Fuel Production from Pyrolysis of Plastic Waste by Levenberg–Marquardt Approach in Feedforward Neural Networks Model," *Polymers*, Vol. 11, pp. 1853.
- [4] A. Patil, A. Patel, and R. Purohit, (2017) "An overview of polymeric materials for automotive applications," *Materials today: proceedings*, Vol. 4, pp. 3807-3815.
- [5] I. Bochkov, M. Varkale, R. M. Meri, J. Zicans, P. Franciszczak, and A. Bledzki, (2018) "Selected aspects of wear and surface properties of polypropylene based wood-polymer composites," *Green tribology*, Vol. 1, pp. 5-8.
- [6] B. Marosfői, A. Szabo, G. Marosi, D. Tabuani, G. Camino, and S. Pagliari, (2006) "Thermal and spectroscopic characterization of polypropylene-carbon nanotube composites," *Journal of thermal analysis and calorimetry*, Vol. 86, pp. 669-673.
- [7] D. Bikiaris, P. Matzinos, A. Larena, V. Flaris, and C. Panayiotou, (2001) "Use of silane agents and poly (propylene-g-maleic anhydride) copolymer as adhesion promoters in glass fiber/polypropylene composites," *Journal of applied polymer science*, Vol. 81, pp. 701-709.
- [8] A. Mohanty, M. Misra, and L. T. Drzal, (2001) "Surface modifications of natural fibers and performance of the resulting biocomposites: an overview," *Composite interfaces*, Vol. 8, pp. 313-343.
- [9] N. Kim, R. Lin, and D. Bhattacharyya, (2015) "Effects of wool fibres, ammonium polyphosphate and polymer viscosity on the flammability and mechanical performance of PP/wool composites," *Polymer degradation and stability*, Vol. 119, pp. 167-177.
- [10] O. Das, A. K. Sarmah, and D. Bhattacharyya, (2015) "A sustainable and resilient approach through biochar addition in wood polymer composites," *Science of the total environment*, Vol. 512, pp. 326-336.
- [11] S. Richard, J. S. Rajadurai, and V. Manikandan, (2016) "Influence of particle size and particle loading on mechanical and dielectric properties of biochar particulate-reinforced

polymer nanocomposites," *International journal of polymer analysis and characterization*, Vol. 21, pp. 462-477.

[12] A. M. M. Amin, S. Mohd Sauid, M. S. So'aib, M. Musa, and K. H. Ku Hamid, (2017) "Mechanical and Thermal Properties of Thermoplastic Film from *Tacca leontopetaloides* Starch Reinforced with Rice Husk Biochar," in *Materials Science Forum*, Trans Tech Pub, pp. 188-191.

[13] S. C. Peterson, S. R. Chandrasekaran, and B. K. Sharma, (2016) "Birchwood biochar as partial carbon black replacement in styrene-butadiene rubber composites," *Journal of elastomers & plastics*, Vol. 48, pp. 305-316.

[14] A. M. Poulouse, A. Y. Elnour, A. Anis, H. Shaikh, S. Al-Zahrani, J. George, M. I. Al-Wabel, A. R. Usman, Y. S. Ok, and D. C. Tsang, (2018) "Date palm biochar-polymer composites: An investigation of electrical, mechanical, thermal and rheological characteristics," *Science of the total environment*, Vol. 619, pp. 311-318.

[15] T. Huber, M. Misra, and A. K. Mohanty, (2015) "The effect of particle size on the rheological properties of polyamide 6/biochar composites," in *AIP Conference Proceedings*(AIP Publishing LLC2015), pp. 150004.

[16] G. Ahmetli, S. Kocaman, I. Ozaytekin, and P. Bozkurt, (2013) "Epoxy composites based on inexpensive char filler obtained from plastic waste and natural resources," *Polymer composites*, Vol. 34, pp. 500-509.

[17] Q. Zhang, W. Yi, Z. Li, L. Wang, and H. Cai, (2018) "Mechanical properties of rice husk biochar reinforced high density polyethylene composites," *Polymers*, Vol. 10, p. 286.

[18] N. Nan, D. B. DeVallance, X. Xie, and J. Wang, (2016) "The effect of bio-carbon addition on the electrical, mechanical, and thermal properties of polyvinyl alcohol/biochar composites," *Journal of composite materials*, Vol. 50, pp. 1161-1168.

[19] O. D. Nartey, and B. Zhao, (2014) "Biochar preparation, characterization, and adsorptive capacity and its effect on bioavailability of contaminants: an overview," *Advances in materials science and engineering*, Vol. 2014.

[20] M. A. Salam, K. Ahmed, N. Akter, T. Hossain, and B. Abdullah, (2018) "A review of hydrogen production via biomass gasification and its prospect in Bangladesh," *International journal of hydrogen energy*, Vol. 43, pp. 14944-14973.

[21] K. Qian, A. Kumar, H. Zhang, D. Bellmer, and R. Huhnke, (2015) "Recent advances in utilization of biochar," *Renewable and sustainable energy reviews*, Vol. 42, pp. 1055-1064.

[22] H. S. Kambo, and A. Dutta, (2015) "A comparative review of biochar and hydrochar in terms of production, physico-chemical properties and applications," *Renewable and sustainable energy reviews*, Vol. 45, pp. 359-378.

- [23] E. Hodgson, A. Lewys-James, S. R. Ravello, S. Thomas-Jones, W. Perkins, and J. Gallagher, (2016) "Optimisation of slow-pyrolysis process conditions to maximise char yield and heavy metal adsorption of biochar produced from different feedstocks," *Bioresource technology*, Vol. 214, pp. 574-581.
- [24] S. N. Monteiro, V. Calado, R. J. Rodriguez, and F. M. Margem, (2012) "Thermogravimetric stability of polymer composites reinforced with less common lignocellulosic fibers—an Overview," *Journal of materials research and technology*, Vol. 1, pp. 117-126.
- [25] "Rice productivity." Ricepedia. Web. 26 Feb. 2020. <<http://ricepedia.org/rice-as-a-crop/rice-productivity>>
- [26] "World production volume of milled rice from 2008/2009 to 2018/2019." Statista. Web. 26 Feb. 2020. <<https://www.statista.com/statistics/271972/world-husked-rice-production-volume-since-2008/>>
- [27] Yearbook of Agricultural Statistics-2018, 30th Series. Government of the People's Republic of Bangladesh, Ministry of Planning, Bangladesh Bureau of Statistics. <http://bbs.portal.gov.bd/sites/default/files/files/bbs.portal.gov.bd/page/1b1eb817_9325_4354_a756_3d18412203e2/Agriculture1%20Year%20Book%202017-18.pdf>
- [28] S. Ong, S. Ha, P. Keng, C. Lee, and Y. Hung, (2012) "Removal of Dyes from Wastewaters," in Y. Hung, L. K. Wang, and N. K. Shamma (eds.). *Handbook of Environment and Waste Management: Air and Water Pollution Control*, chap. 21, pp. 929-970, World Scientific Publishing, Singapore.
- [29] M. Ahiduzzaman, (2007) "Rice husk energy technologies in Bangladesh," *Agricultural engineering international: CIGR Journal*, Vol. 9.
- [30] D. Pottmaier, M. r. Costa, T. Farrow, A. A. Oliveira, O. Alarcon, and C. Snape, (2013) "Comparison of rice husk and wheat straw: from slow and fast pyrolysis to char combustion," *Energy & fuels*, Vol. 27, pp. 7115-7125.
- [31] S. Xiu, A. Shahbazi, and R. Li, (2017) "Characterization, modification and application of biochar for energy storage and catalysis: a review," *Trends in renewable energy*, Vol. 3, pp. 86-101.
- [32] R. M. Irfan, F. N. Kaleri, M. Rizwan, and I. Mehmood, (2017) "Potential value of biochar as a soil amendment: A review," *Pure and applied biology (PAB)*, Vol. 6, pp. 1494-1502.
- [33] A. Bridgwater, and G. Peacocke, (2000) "Fast pyrolysis processes for biomass," *Renewable and sustainable energy reviews*, Vol. 4, pp. 1-73.
- [34] T. Xie, K. R. Reddy, C. Wang, E. Yargicoglu, and K. Spokas, (2015) "Characteristics and applications of biochar for environmental remediation: a review," *Critical reviews in environmental science and technology*, Vol. 45, pp. 939-969.

- [35] K. A. Spokas, K. B. Cantrell, J. M. Novak, D. W. Archer, J. A. Ippolito, H. P. Collins, A. A. Boateng, I. M. Lima, M. C. Lamb, and A. J. McAloon, (2012) "Biochar: a synthesis of its agronomic impact beyond carbon sequestration," *Journal of environmental quality*, Vol. 41, pp. 973-989.
- [36] A. Awad, N. Masiran, M. A. Salam, D.-V. N. Vo, and B. Abdullah, (2019) "Non-oxidative decomposition of methane/methanol mixture over mesoporous Ni-Cu/Al₂O₃ Co-doped catalysts," *International journal of hydrogen energy*, Vol. 44, pp. 20889-20899.
- [37] S. Thangalazhy-Gopakumar, W. M. A. Al-Nadheri, D. Jegarajan, J. Sahu, N. Mubarak, and S. Nizamuddin, (2015) "Utilization of palm oil sludge through pyrolysis for bio-oil and bio-char production," *Bioresource technology*, Vol. 178, pp. 65-69.
- [38] M. J. Eden, W. Bray, L. Herrera, and C. McEwan, (1984) "Terra preta soils and their archaeological context in the Caquetá basin of southeast Colombia," *American antiquity*, Vol. 49, pp. 125-140.
- [39] B. Glaser, L. Haumaier, G. Guggenberger, and W. Zech, (2001) "The Terra Preta phenomenon: a model for sustainable agriculture in the humid tropics," *Naturwissenschaften*, Vol. 88, pp. 37-41.
- [40] W. A. W. A. K. Ghani, A. Mohd, G. da Silva, R. T. Bachmann, Y. H. Taufiq-Yap, U. Rashid, and H. Ala'a, (2013) "Biochar production from waste rubber-wood-sawdust and its potential use in C sequestration: chemical and physical characterization," *Industrial crops and products*, Vol. 44, pp. 18-24.
- [41] J. Lehmann, (2009) "Biological carbon sequestration must and can be a win-win approach," *Climatic Change*, Vol. 97, p. 459.
- [42] Y. Chun, G. Sheng, C. T. Chiou, and B. Xing, (2004) "Compositions and sorptive properties of crop residue-derived chars," *Environmental science & technology*, Vol. 38, pp. 4649-4655.
- [43] Y. Feng, Y. Xu, Y. Yu, Z. Xie, and X. Lin, (2012) "Mechanisms of biochar decreasing methane emission from Chinese paddy soils," *Soil Biology and Biochemistry*, Vol. 46, pp. 80-88.
- [44] Y. Yao, B. Gao, M. Inyang, A. R. Zimmerman, X. Cao, P. Pullammanappallil, and L. Yang, (2011) "Biochar derived from anaerobically digested sugar beet tailings: characterization and phosphate removal potential," *Bioresource technology*, Vol. 102, pp. 6273-6278.
- [45] D. D. Warnock, J. Lehmann, T. W. Kuyper, and M. C. Rillig, (2007) "Mycorrhizal responses to biochar in soil—concepts and mechanisms," *Plant and soil*, Vol. 300, pp. 9-20.
- [46] M. A. Rondon, J. Lehmann, J. Ramírez, and M. Hurtado, (2007) "Biological nitrogen fixation by common beans (*Phaseolus vulgaris* L.) increases with bio-char additions," *Biology and fertility of soils*, Vol. 43, pp. 699-708.
- [47] M. I. Bird, C. M. Wurster, P. H. de Paula Silva, A. M. Bass, and R. De Nys, (2011) "Algal biochar—production and properties," *Bioresource technology*, Vol. 102, pp. 1886-1891.

- [48] T.-Y. Jiang, J. Jiang, R.-K. Xu, and Z. Li, (2012) "Adsorption of Pb (II) on variable charge soils amended with rice-straw derived biochar," *Chemosphere*, Vol. 89, pp. 249-256.
- [49] A. V. Bridgwater, (2012) "Review of fast pyrolysis of biomass and product upgrading," *Biomass and bioenergy*, Vol. 38, pp. 68-94.
- [50] M. H. Duku, S. Gu, and E. B. Hagan, (2011) "Biochar production potential in Ghana—a review," *Renewable and sustainable energy reviews*, Vol. 15, pp. 3539-3551.
- [51] M. Ahmad, S. S. Lee, X. Dou, D. Mohan, J.-K. Sung, J. E. Yang, and Y. S. Ok, (2012) "Effects of pyrolysis temperature on soybean stover-and peanut shell-derived biochar properties and TCE adsorption in water," *Bioresource technology*, Vol. 118, pp. 536-544.
- [52] Y. Yang, J. G. Brammer, A. Mahmood, and A. Hornung, (2014) "Intermediate pyrolysis of biomass energy pellets for producing sustainable liquid, gaseous and solid fuels," *Bioresource technology*, Vol. 169, pp. 794-799.
- [53] T. R. Brown, M. M. Wright, and R. C. Brown, (2011) "Estimating profitability of two biochar production scenarios: slow pyrolysis vs fast pyrolysis," *Biofuels, bioproducts and biorefining*, Vol. 5, pp. 54-68.
- [54] P. Fu, S. Hu, J. Xiang, W. Yi, X. Bai, L. Sun, and S. Su, (2012) "Evolution of char structure during steam gasification of the chars produced from rapid pyrolysis of rice husk," *Bioresource technology*, Vol. 114, pp. 691-697.
- [55] J. Mumme, L. Eckervogt, J. Pielert, M. Diakité, F. Rupp, and J. Kern, (2011) "Hydrothermal carbonization of anaerobically digested maize silage," *Bioresource technology*, Vol. 102, pp. 9255-9260.
- [56] N. Schwaiger, R. Feiner, K. Zahel, A. Pieber, V. Witek, P. Pucher, E. Ahn, P. Wilhelm, B. Chernev, and H. Schröttner, (2011) "Liquid and solid products from liquid-phase pyrolysis of softwood," *BioEnergy research*, Vol. 4, pp. 294-302.
- [57] Y. Xu, and B. Chen, (2013) "Investigation of thermodynamic parameters in the pyrolysis conversion of biomass and manure to biochars using thermogravimetric analysis," *Bioresource technology*, Vol. 146, pp. 485-493.
- [58] B. Chen, D. Zhou, and L. Zhu, (2008) "Transitional adsorption and partition of nonpolar and polar aromatic contaminants by biochars of pine needles with different pyrolytic temperatures," *Environmental science & technology*, Vol. 42, pp. 5137-5143.
- [59] X. Cao, and W. Harris, (2010) "Properties of dairy-manure-derived biochar pertinent to its potential use in remediation," *Bioresource technology*, Vol. 101, pp. 5222-5228.
- [60] S. Yorgun, and D. Yıldız, (2015) "Slow pyrolysis of paulownia wood: Effects of pyrolysis parameters on product yields and bio-oil characterization," *Journal of analytical and applied pyrolysis*, Vol. 114, pp. 68-78.
- [61] J. Akhtar, and N. S. Amin, (2012) "A review on operating parameters for optimum liquid oil yield in biomass pyrolysis," *Renewable and sustainable energy reviews*, Vol. 16, pp. 5101-5109.

- [62] T. Aysu, and M. M. Küçük, (2014) "Biomass pyrolysis in a fixed-bed reactor: effects of pyrolysis parameters on product yields and characterization of products," *Energy*, Vol. 64, pp. 1002-1025.
- [63] J. Akhtar, and N. S. Amin, (2012) "A review on operating parameters for optimum liquid oil yield in biomass pyrolysis," *Renewable and sustainable energy reviews*, Vol. 16, pp. 5101-5109.
- [64] J. Lehmann, and S. Joseph, (2009) *Biochar for environmental management: science and technology*. London: Earthscan, London.
- [65] B. Singh, B. P. Singh, and A. L. Cowie, (2010) "Characterisation and evaluation of biochars for their application as a soil amendment," *Soil Research*, Vol. 48, pp. 516-525.
- [66] W. Quayle, (2010) "Biochar potential for soil improvement and soil fertility," *IREC Farmers Newsl*, Vol. 182, pp. 4-22 .
- [67] J. Lehmann, J. P. da Silva, C. Steiner, T. Nehls, W. Zech, and B. Glaser, (2003) "Nutrient availability and leaching in an archaeological Anthrosol and a Ferralsol of the Central Amazon basin: fertilizer, manure and charcoal amendments," *Plant and soil*, Vol. 249, pp. 343-357.
- [68] S. T. Shafie, M. M. Salleh, L. L. Hang, M. Rahman, and W. Ghani, (2012) "Effect of pyrolysis temperature on the biochar nutrient and water retention capacity," *Journal of purity, utility reaction and environment*, Vol. 1, pp. 293-307.
- [69] J. Lehmann, and S. Joseph, (2015) "Biochar for environmental management: an introduction." *Biochar for environmental management*. Routledge, pp. 33-46.
- [70] I. Tsutomu, A. Takashi, K. Kuniaki, and O. Kikuo, (2004) "Comparison of removal efficiencies for ammonia and amine gases between woody charcoal and activated carbon," *Journal of health science*, Vol. 50, pp. 148-153.
- [71] M. Inyang, B. Gao, W. Ding, P. Pullammanappallil, A. R. Zimmerman, and X. Cao, (2011) "Enhanced lead sorption by biochar derived from anaerobically digested sugarcane bagasse," *Separation science and technology*, Vol. 46, pp. 1950-1956.
- [72] S. Yenisoy-Karakaş, A. Aygün, M. Güneş, and E. Tahtasakal, (2004) "Physical and chemical characteristics of polymer-based spherical activated carbon and its ability to adsorb organics," *Carbon*, Vol. 42, pp. 477-484.
- [73] X. Chen, G. Chen, L. Chen, Y. Chen, J. Lehmann, M. B. McBride, and A. G. Hay, (2011) "Adsorption of copper and zinc by biochars produced from pyrolysis of hardwood and corn straw in aqueous solution," *Bioresource technology*, Vol. 102, pp. 8877-8884.
- [74] G. C. Matteson, and B. Jenkins, (2005) "Food and processing residues in California: Resource assessment and potential for power generation," in *2005 ASAE Annual Meeting* (American society of agricultural and biological engineers, 2005), p. 1.
- [75] A. V. Bridgwater, (2003) "Renewable fuels and chemicals by thermal processing of biomass," *Chemical engineering journal*, Vol. 91, pp. 87-102.

- [76] A. Mohanty, S. Vivekanandhan, A. Anstey, and M. Misra, (2015) "Sustainable composites from renewable biochar and engineering plastic," in *Proceedings of 20th International Conference on Composite Materials*, pp. 4308-4312.
- [77] T. Väisänen, O. Das, and L. Tomppo, (2017) "A review on new bio-based constituents for natural fiber-polymer composites," *Journal of cleaner production*, Vol. 149, pp. 582-596.
- [78] P. Srinivasan, A. K. Sarmah, R. Smernik, O. Das, M. Farid, and W. Gao, (2015) "A feasibility study of agricultural and sewage biomass as biochar, bioenergy and biocomposite feedstock: production, characterization and potential applications," *Science of the total environment*, Vol. 512, pp. 495-505.
- [79] N. H. Shafie, and N. M. Esa, (2017) "The healing components of rice bran," *Functional Foods: Wonder of the World*, pp. 341-368.
- [80] W. Liu, L. Cheng, and S. Li, (2018) "Review of electrical properties for polypropylene based nanocomposite," *Composites communications*, Vol. 10, pp. 221-225.
- [81] H. Karian, (2003) *Handbook of polypropylene and polypropylene composites, revised and expanded*, CRC press, New York.
- [82] Q. T. Shubhra, A. Alam, and M. Quaiyyum, (2013) "Mechanical properties of polypropylene composites: A review," *Journal of thermoplastic composite materials*, Vol. 26, pp. 362-391.
- [83] A. Graziano, S. Jaffer, and M. Sain, (2019) "Review on modification strategies of polyethylene/polypropylene immiscible thermoplastic polymer blends for enhancing their mechanical behavior," *Journal of elastomers & plastics*, Vol. 51, pp. 291-336.
- [84] P. Galli, S. Danesi, and T. Simonazzi, (1984) "Polypropylene based polymer blends: fields of application and new trends," *Polymer engineering & science*, Vol. 24, pp. 544-554.
- [85] P. E. Moore, (1996) *Polypropylene handbook*. Hanser/Gardner Publications.
- [86] J. A. Brydson, (1999) *Plastics materials*. Reed Educational and Professional Publishing Ltd., Elsevier.
- [87] C. He, S. Costeux, P. Wood-Adams, and J. M. Dealy, (2003) "Molecular structure of high melt strength polypropylene and its application to polymer design," *Polymer*, Vol. 44, pp. 7181-7188.
- [88] M. F. Pampolino, E. V. Laureles, H. C. Gines, and R. J. Buresh, (2008) "Soil carbon and nitrogen changes in long-term continuous lowland rice cropping," *Soil Science Society of America Journal*, Vol. 72, pp. 798-807.
- [89] M. Kawasumi, N. Hasegawa, M. Kato, A. Usuki, and A. Okada, (1997) "Preparation and Mechanical Properties of Polypropylene-Clay Hybrids," *Macromolecules*, Vol. 30, pp. 6333-6338.

- [90] A. V. Karuppiyah, (2016) *Predicting the influence of weave architecture on the stress relaxation behavior of woven composite using finite element based micromechanics*, Master's Theses, Dept. of Aerospace Engineering, College of Engineering, Wichita State University.
- [91] O. M. E. S. Khayal, (2019) –Advancements in Polymer Composite Structures,” Mechanical Engineering Department, Nile Valley University, Atbara, Sudan.
- [92] P. A. Fowler, J. M. Hughes, and R. M. Elias, (2006) "Biocomposites: technology, environmental credentials and market forces," *Journal of the science of food and agriculture*, Vol. 86, pp. 1781-1789.
- [93] A. M. Díez-Pascual, M. Naffakh, C. Marco, M. A. Gómez-Fatou, and G. J. Ellis, (2014) "Multiscale fiber-reinforced thermoplastic composites incorporating carbon nanotubes: A review," *Current opinion in solid state and materials science*, Vol. 18, pp. 62-80.
- [94] G. Schmidt, and M. M. Malwitz, (2003) "Properties of polymer–nanoparticle composites," *Current opinion in colloid & interface science*, Vol. 8, pp. 103-108.
- [95] J. Agarwal, S. Sahoo, S. Mohanty, and S. K. Nayak, (2019) "Progress of novel techniques for lightweight automobile applications through innovative eco-friendly composite materials: a review," *Journal of thermoplastic composite materials*.
- [96] K. P. Kumar, and A. S. J. Sekaran, (2014) "Some natural fibers used in polymer composites and their extraction processes: A review," *Journal of reinforced plastics and composites*, Vol. 33, pp. 1879-1892.
- [97] T. Sonar, S. Patil, V. Deshmukh, and R. Acharya, (2015) "Natural Fiber Reinforced Polymer Composite Material-A Review," *IOSR Journal of mechanical and civil engineering*, pp. 2278-1684.
- [98] B.C. Suddell, and W. J. Evans, (2005) –Natural Fiber Composites in Automotive Applications in Natural Fibers in Biopolymers & Their BioComposites”, CRC Press.
- [99] I. D. Ibrahim, T. Jamiru, R. E. Sadiku, W. K. Kupolati, S. C. Agwuncha, and G. Ekundayo, (2015) "The use of polypropylene in bamboo fibre composites and their mechanical properties– A review," *Journal of reinforced plastics and composites*, Vol. 34, pp. 1347-1356.
- [100] N. Ilie, and R. Hickel, (2009) "Macro-, micro-and nano-mechanical investigations on silorane and methacrylate-based composites," *Dental materials*, Vol. 25, pp. 810-819.
- [101] A. Aruniit, J. Kers, J. Majak, A. Krumme, and K. Tall, (2012) "Influence of hollow glass microspheres on the mechanical and physical properties and cost of particle reinforced polymer composites," *Proceedings of the Estonian Academy of Sciences*, Vol. 61, pp. 160.
- [102] S. Ahmed, and F. Jones, (1990) "A review of particulate reinforcement theories for polymer composites," *Journal of materials science*, Vol. 25, pp. 4933-4942.
- [103] R. Paul, and L. Dai, (2018) "Interfacial aspects of carbon composites," *Composite interfaces*, Vol. 25, pp. 539-605.

- [104] U. Bongarde, and V. Shinde, (2014) "Review on natural fiber reinforcement polymer composites," *International journal of engineering science and innovative technology*, Vol. 3, pp. 431-436.
- [105] S. S. Kessler, S. M. Spearing, M. J. Atalla, C. E. Cesnik, and C. Soutis, (2002) "Damage detection in composite materials using frequency response methods," *Composites part B: engineering*, Vol. 33, pp. 87-95.
- [106] J. F. Patrick, K. R. Hart, B. P. Krull, C. E. Diesendruck, J. S. Moore, S. R. White, and N. R. Sottos, (2014) "Continuous self-healing life cycle in vascularized structural composites," *Advanced materials*, Vol. 26, pp. 4302-4308.
- [107] C. Gao, L. Yu, H. Liu, and L. Chen, (2012) "Development of self-reinforced polymer composites," *Progress in polymer science*, Vol. 37, pp. 767-780.
- [108] M. A. Pinto, V. B. Chalivendra, Y. K. Kim, and A. F. Lewis, (2014) "Evaluation of surface treatment and fabrication methods for jute fiber/epoxy laminar composites," *Polymer composites*, Vol. 35, pp. 310-317.
- [109] E. M. Fernandes, R. A. Pires, J. F. Mano, and R. L. Reis, (2013) "Bionanocomposites from lignocellulosic resources: Properties, applications and future trends for their use in the biomedical field," *Progress in polymer science*, Vol. 38, pp. 1415-1441.
- [110] L. Dányádi, T. Janecska, Z. Szabo, G. Nagy, J. Moczo, and B. Pukánszky, (2007) "Wood flour filled PP composites: compatibilization and adhesion," *Composites science and technology*, Vol. 67, pp. 2838-2846.
- [111] V. K. Thakur, M. K. Thakur, and R. K. Gupta, (2013) "Synthesis of lignocellulosic polymer with improved chemical resistance through free radical polymerization," *International journal of biological macromolecules*, Vol. 61, pp. 121-126.
- [112] H. Dodiuk, and S. H. Goodman, (2013) *Handbook of thermoset plastics*. William Andrew.
- [113] C. Li, and A. Strachan, (2015) "Molecular scale simulations on thermoset polymers: A review," *Journal of polymer science part B: polymer physics*, Vol. 53, pp. 103-122.
- [114] C. C. Ibeh, (2011) *Thermoplastic materials: properties, manufacturing methods, and applications*. CRC Press.
- [115] D. Clegg, and A. Collyer, (1986) *Mechanical properties of reinforced thermoplastics*. Springer.
- [116] "Thermoset Vs Thermoplastics." Modor Plastics. Web. 26 Feb. 2020. <<https://www.modorplastics.com/plastics-learning-center/thermoset-vs-thermoplastics/>>.
- [117] J. Z. Liang, (2013) "Reinforcement and quantitative description of inorganic particulate-filled polymer composites," *Composites part B: engineering*, Vol. 51, pp. 224-232.
- [118] B. Turcsanyi, B. Pukanszky, and F. Tüdös, (1988) "Composition dependence of tensile yield stress in filled polymers," *Journal of materials science letters*, Vol. 7, pp. 160-162.

- [119] A. Ariffin, Z. Ariff, and S. Jikan, (2011) "Evaluation on nonisothermal crystallization kinetics of polypropylene/kaolin composites by employing Dobreva and Kissinger methods," *Journal of thermal analysis and calorimetry*, Vol. 103, pp. 171-177.
- [120] J. Z. Liang, (2012) "Crystallization of glass fiber-reinforced poly (p-phenylene sulfide) nanocomposites," *Polymer international*, Vol. 61, pp. 511-515.
- [121] I. E. Afrooz, A. Öchsner, and M. Rahmandoust, (2012) "Effects of the carbon nanotube distribution on the macroscopic stiffness of composite materials," *Computational materials science*, Vol. 51, pp. 422-429.
- [122] J. Liang, and C. Wu, (2012) "Effects of the glass bead content and the surface treatment on the mechanical properties of polypropylene composites," *Journal of applied polymer science*, Vol. 123, pp. 3054-3063.
- [123] J. Liang, R. Li, and S. Tjong, (1998) "Morphology and tensile properties of glass bead filled low density polyethylene composites: material properties," *Polymer testing*, Vol. 16, pp. 529-548.
- [124] J. Z. Liang, (2007) "Tensile properties of hollow glass bead-filled polypropylene composites," *Journal of applied polymer science*, Vol. 104, pp. 1697-1701.
- [125] J. Liang, and A. Li, (2010) "Inorganic particle size and content effects on tensile strength of polymer composites," *Journal of reinforced plastics and composites*, Vol. 29, pp. 2744-2752.
- [126] Q. Zhang, M. U. Khan, X. Lin, H. Cai, and H. Lei, (2019) "Temperature varied biochar as a reinforcing filler for high-density polyethylene composites," *Composites part b: engineering*, Vol. 175, p. 107151.
- [127] R. Arrigo, P. Jagdale, M. Bartoli, A. Tagliaferro, and G. Malucelli, (2019) "Structure–property relationships in polyethylene-based composites filled with biochar derived from waste coffee grounds," *Polymers*, Vol. 11, p. 1336.
- [128] A. M. M. Amin, S. M. Saudid, M. S. So‘aib, M. Musa, and K. H. K Hamid, (2017) "Mechanical and Thermal Properties of Thermoplastic Film from *Tacca leontopetaloides* Starch Reinforced with Rice Husk Biochar," in *Materials Science Forum*, Trans Tech Publ, pp. 188-191.
- [129] M. Giorcelli, and M. Bartoli, (2019) "Development of coffee biochar filler for the production of electrical conductive reinforced plastic," *Polymers*, Vol. 11, pp. 1916.
- [130] M. Bartoli, M. A. Nasir, P. Jagdale, E. Passaglia, R. Spiniello, C. Rosso, M. Giorcelli, M. Rovere, and A. Tagliaferro, (2019) "Influence of pyrolytic thermal history on olive pruning biochar and related epoxy composites mechanical properties," *Journal of composite materials*.
- [131] C. Jiang, J. Bo, X. Xiao, S. Zhang, Z. Wang, G. Yan, Y. Wu, C. Wong, and H. He, (2020) "Converting waste lignin into nano-biochar as a renewable substitute of carbon black for reinforcing styrene-butadiene rubber," *Waste management*, Vol. 102, pp. 732-742.

- [132] P. Myllytie, M. Misra, and A. K. Mohanty, (2016) "Carbonized lignin as sustainable filler in biobased poly (trimethylene terephthalate) polymer for injection molding applications," *ACS sustainable chemistry & engineering*, Vol. 4, pp. 102-110.
- [133] A. Y. Elnour, A. A. Alghyamah, H. M. Shaikh, A. M. Poulouse, S. M. Al-Zahrani, A. Anis, and M. I. Al-Wabel, (2019) "Effect of pyrolysis temperature on biochar microstructural evolution, physicochemical characteristics, and its influence on biochar/polypropylene composites," *Applied Sciences*, Vol. 9, p. 1149.
- [134] O. Das, N. K. Kim, M. S. Hedenqvist, R. J. Lin, A. K. Sarmah, and D. Bhattacharyya, (2018) "An attempt to find a suitable biomass for biochar-based polypropylene biocomposites," *Environmental management*, Vol. 62, pp. 403-413.
- [135] O. Das, A. K. Sarmah, Z. Zujovic, and D. Bhattacharyya, (2016) "Characterisation of waste derived biochar added biocomposites: chemical and thermal modifications," *Science of the Total Environment*, Vol. 550, pp. 133-142.
- [136] A. Ghaffar, X. Zhu, and B. Chen, (2018) "Biochar composite membrane for high performance pollutant management: Fabrication, structural characteristics and synergistic mechanisms," *Environmental Pollution*, Vol. 233, pp. 1013-1023.
- [137] R. Sadiku, D. Ibrahim, O. Agboola, S. J. Owonubi, V. O. Fasiku, W. K. Kupolati, T. Jamiru, A. A. Eze, O. S. Adekomaya, and K. Varaprasad, (2017) "Automotive components composed of polyolefins," in *Polyolefin Fibres*, Elsevier, pp. 449-496.
- [138] S. X. Zhao, N. Ta, and X.-D. Wang, (2017) "Effect of temperature on the structural and physicochemical properties of biochar with apple tree branches as feedstock material," *Energies*, Vol. 10, p. 1293.
- [139] ASTM D3172-13, Standard Practice for Proximate Analysis of Coal and Coke, ASTM International, West Conshohocken, PA, 2013, www.astm.org
- [140] ASTM D 638 – 03, Standard Test Method for Tensile Properties of Plastics, ASTM International, West Conshohocken, PA, 2003, www.astm.org
- [141] ASTM D 790 – 03, Standard Test Methods for Flexural Properties of Unreinforced and Reinforced Plastics and Electrical Insulating Materials, ASTM International, West Conshohocken, PA, 2003, www.astm.org
- [142] ASTM D2240 – 15, Standard Test Method for Rubber Property—Durometer Hardness, ASTM International, West Conshohocken, PA, 2015, www.astm.org
- [143] N. Claoston, A. Samsuri, M. Ahmad Husni, and M. Mohd Amran, (2014) "Effects of pyrolysis temperature on the physicochemical properties of empty fruit bunch and rice husk biochars," *Waste Management & Research*, Vol. 32, pp. 331-339.
- [144] A. Demirbas, (2004) "Effects of temperature and particle size on bio-char yield from pyrolysis of agricultural residues," *Journal of analytical and applied pyrolysis*, Vol. 72, pp. 243-248.

- [145] P. A. Horne, and P. T. Williams, (1996) "Influence of temperature on the products from the flash pyrolysis of biomass," *Fuel*, Vol. 75, pp. 1051-1059.
- [146] W. T. Tsai, S. C. Liu, H. R. Chen, Y. M. Chang, and Y. L. Tsai, (2012) "Textural and chemical properties of swine-manure-derived biochar pertinent to its potential use as a soil amendment," *Chemosphere*, Vol. 89, pp. 198-203.
- [147] M. Ahiduzzaman, and A. S. Islam, (2016) "Preparation of porous bio-char and activated carbon from rice husk by leaching ash and chemical activation," *SpringerPlus*, Vol. 5, pp. 1-14.
- [148] P. Deshmukh, J. Bhatt, D. Peshwe, and S. Pathak, (2012) "Determination of silica activity index and XRD, SEM and EDS studies of amorphous SiO₂ extracted from rice husk ash," *Transactions of the Indian Institute of Metals*, Vol. 65, pp. 63-70.
- [149] J. Guo, and A. C. Lua, (1998) "Characterization of chars pyrolyzed from oil palm stones for the preparation of activated carbons," *Journal of analytical and applied pyrolysis*, Vol. 46, pp. 113-125.
- [150] Q. Zhang, H. Cai, X. Ren, L. Kong, J. Liu, and X. Jiang, (2017) "The dynamic mechanical analysis of highly filled rice husk biochar/high-density polyethylene composites," *Polymers*, Vol. 9, p. 628.
- [151] K. Jindo, H. Mizumoto, Y. Sawada, M. A. Sanchez-Monedero, and T. Sonoki, (2014) "Physical and chemical characterization of biochars derived from different agricultural residue," *Biogeosciences*, Vol. 11, pp. 6613-6621.
- [152] M. A. Salam, K. Ahmed, T. Hossain, M. S. Habib, M. S. Uddin, and N. Papri, (2019) "Prospect of Molecular Sieves Production using Rice Husk in Bangladesh: A Review," *International Journal of chemistry, mathematics and physics*, Vol. 3, pp. 105-134.
- [153] H. Abdulrazzaq, H. Jol, A. Husni, and R. Abu-Bakr, (2014) "Characterization and stabilisation of biochars obtained from empty fruit bunch, wood, and rice husk," *BioResources*, Vol. 9, pp. 2888-2898.
- [154] R. Rostamian, M. Heidarpour, S. Mousavi, and M. Afyuni, (2015) "Characterization and sodium sorption capacity of biochar and activated carbon prepared from rice husk," *Journal of agricultural science and technology*, Vol. 17, pp. 1057-1069.
- [155] A. Samsuri, F. Sadegh-Zadeh, and B. Seh-Bardan, (2014) "Characterization of biochars produced from oil palm and rice husks and their adsorption capacities for heavy metals," *International Journal of environmental science and technology*, Vol. 11, pp. 967-976.
- [156] Y. Zhang, Z. Ma, Q. Zhang, J. Wang, Q. Ma, Y. Yang, X. Luo, and W. Zhang, (2017) "Comparison of the physicochemical characteristics of bio-char pyrolyzed from moso bamboo and rice husk with different pyrolysis temperatures," *BioResources*, Vol. 12, pp. 4652-4669.
- [157] H. Weldekidan, V. Strezov, G. Town, and T. Kan, (2018) "Production and analysis of fuels and chemicals obtained from rice husk pyrolysis with concentrated solar radiation," *Fuel*, Vol. 233, pp. 396-403.

- [158] L. B. Santos, M. V. Striebeck, M. S. Crespi, C. A. Ribeiro, and M. De Julio, (2015) "Characterization of biochar of pine pellet," *Journal of thermal analysis and calorimetry*, Vol. 122, pp. 21-32.
- [159] Y. Sun, B. Gao, Y. Yao, J. Fang, M. Zhang, Y. Zhou, H. Chen, and L. Yang, (2014) "Effects of feedstock type, production method, and pyrolysis temperature on biochar and hydrochar properties," *Chemical engineering journal*, Vol. 240, pp. 574-578.
- [160] S. Wang, Q. Wang, Y. Hu, S. Xu, Z. He, and H. Ji, (2015) "Study on the synergistic co-pyrolysis behaviors of mixed rice husk and two types of seaweed by a combined TG-FTIR technique," *Journal of analytical and applied pyrolysis*, Vol. 114, pp. 109-118.
- [161] S. Kloss, F. Zehetner, A. Dellantonio, R. Hamid, F. Ottner, V. Liedtke, M. Schwanninger, M. H. Gerzabek, and G. Soja, (2012) "Characterization of slow pyrolysis biochars: effects of feedstocks and pyrolysis temperature on biochar properties," *Journal of environmental quality*, Vol. 41, pp. 990-1000.
- [162] M. Brebu, and C. Vasile, (2010) "Thermal degradation of lignin—a review," *Cellulose Chemistry & Technology*, Vol. 44, p. 353.
- [163] R. Zornoza, F. Moreno-Barriga, J. Acosta, M. Muñoz, and A. Faz, (2016) "Stability, nutrient availability and hydrophobicity of biochars derived from manure, crop residues, and municipal solid waste for their use as soil amendments," *Chemosphere*, Vol. 144, pp. 122-130.
- [164] M. P. Ho, K. T. Lau, H. Wang, and D. Hui, (2015) "Improvement on the properties of polylactic acid (PLA) using bamboo charcoal particles," *Composites part B: Engineering*, Vol. 81, pp. 14-25.
- [165] I. Ozsoy, A. Demirkol, A. Mimaroglu, H. Unal, and Z. Demir, (2015) "The influence of micro-and nano-filler content on the mechanical properties of epoxy composites," *Strojniški vestnik-Journal of mechanical engineering*, Vol. 61, pp. 601-609.
- [166] Y. Gao, J. Wu, Z. Zhang, R. Jin, X. Zhang, X. Yan, A. Umar, Z. Guo, and Q. Wang, (2013) "Synthesis of polypropylene/Mg₃Al-X (X= CO₃²⁻, NO₃³⁻, Cl⁻, SO₄²⁻) LDH nanocomposites using a solvent mixing method: thermal and melt rheological properties," *Journal of materials chemistry A*, Vol. 1, pp. 9928-9934.
- [167] O. Das, N. K. Kim, A. K. Sarmah, and D. Bhattacharyya, (2017) "Development of waste based biochar/wool hybrid biocomposites: Flammability characteristics and mechanical properties," *Journal of cleaner production*, Vol. 144, pp. 79-89.
- [168] K. S. Chun, and S. Husseinsyah, (2016) "Agrowaste-based composites from cocoa pod husk and polypropylene: effect of filler content and chemical treatment," *Journal of thermoplastic composite materials*, Vol. 29, pp. 1332-1351.
- [169] K. Yamada, M. Hikosaka, A. Toda, S. Yamazaki, and K. Tagashira, (2003) "Equilibrium melting temperature of isotactic polypropylene with high tacticity: 1. Determination by differential scanning calorimetry," *Macromolecules*, Vol. 36, pp. 4790-4801.

- [170] R. Paukkeri, and A. Lehtinen, (1993) "Thermal behaviour of polypropylene fractions: 1. Influence of tacticity and molecular weight on crystallization and melting behaviour," *Polymer*, Vol. 34, pp. 4075-4082.
- [171] D. Harper, and M. Wolcott, (2004) "Interaction between coupling agent and lubricants in wood–polypropylene composites," *Composites part A: applied science and manufacturing*, Vol. 35, pp. 385-394.
- [172] K. Radha, S. Selvasekarapandian, S. Karthikeyan, M. Hema, and C. Sanjeeviraja, (2013) "Synthesis and impedance analysis of proton-conducting polymer electrolyte PVA: NH₄F," *Ionics*, Vol. 19, pp. 1437-1447.
- [173] R. S. Gabhi, D. W. Kirk, and C. Q. Jia, (2017) "Preliminary investigation of electrical conductivity of monolithic biochar," *Carbon*, Vol. 116, pp. 435-442.

Appendix A

Table A.1: Comparison of the properties of the fabricated RHB reinforced PP composites in this study with PP and other comparable composites

Polymer and Composites	Properties				
	Tensile Strength (MPa)	Flexural Strength (MPa)	Shore Hardness (D Scale)	Melting Temperature ($^{\circ}\text{C}$)	Electrical Resistance, R ($\times 10^{07}\Omega$)
RHB Reinforced PP	26.74 - 31.41	59.07 - 70.61	78.17 - 80	172 - 175	6.24 - 3.53
Pine Wood Biochar + PP	25-28	58.26	-	~165	-
Date Palm Biochar + PP	30 - 32	-	-	163.6 – 165.6	-
RHB + HDPE	15 -20	-	-	~120	-
PP Based Car Bumpers	28 - 38	40 - 50	50 - 52	168.1 - 172.4	-
PP	34.57	64.06	75.50	~175	4.3